SÃO CARLOS INSTITUTE OF CHEMISTRY, UNIVERSITY OF SÃO PAULO
PhD SCHOOL OF THE FACULTY OF SCIENCE, UNIVERSITY OF COPENHAGEN

Aline Teixeira do Brasil Morais

Physico-chemical changes in caseins and micellar casein isolate induced by ultraviolet-C light and pulsed electrical field

This thesis has been submitted to the Institute of Chemistry, University of São Paulo and to the PhD School of The Faculty of Science, University of Copenhagen

São Carlos / Copenhagen
2022

PhD SCHOOL OF THE FACULTY OF SCIENCE, UNIVERSITY OF COPENHAGEN
SÃO CARLOS INSTITUTE OF CHEMISTRY, UNIVERSITY OF SÃO PAULO

Aline Teixeira do Brasil Morais

Physico-chemical changes in caseins and micellar casein isolate induced by ultraviolet-C light and pulsed electrical field

Dissertation presented at São Carlos Institute of Chemistry, University of São Paulo, in collaboration with the University of Copenhagen in a double degree program to obtain the Doctor of Philosophy degree in Chemistry.

Concentration Area: Biological and Organic Chemistry
Supervisors: Prof Daniel R Cardoso, São Carlos Institute of Chemistry, University of São Paulo
Profa Lilia M Ahrné, Department of Food Science, University of Copenhagen.

São Carlos / Copenhagen

2022

Assinatura: Aline T. B. Morais

Data: 09.02.2023

Ficha Catalográfica elaborada pela Seção de Referência e Atendimento ao Usuário do SBI/IQSC

Morais, Aline Teixeira do Brasil
Physico-chemical changes in caseins and micellar casein isolate induced by ultraviolet-C light and pulsed electrical field / Aline Teixeira do Brasil Morais. — São Carlos, 2022.
120 f.

Tese (Doutorado em Química Orgânica e Biológica) — Instituto de Química de São Carlos / Universidade de São Paulo, 2022.
Edição revisada

Orientador: Prof. Dr. Daniel Rodrigues Cardoso
Coorientadora: Profa. Dra. Lilia Maria Ahrné

1. Dairy products. 2. Nonthermal processing. 3. UV-C light. 4. Pulsed electric field. 5. Título. I. Título.

Sonia Alves - CRB: 4280/8

To Mom and dad (in memoriam), Mara Jainy and Jefferson

who did not dismiss the effort to give the best they could,

to my personal and professional education.

To my husband who always gives me

the support during my Ph.D.

ACKNOWLEDGMENTS

First, I would like to express my gratitude to God for giving me the strength, health, and knowledge to undertake this study successfully. I am thankful for the remarkable experiences throughout my research, even with all the challenges.

I am extremely grateful to my mother and dad (*in memoriam*), Mara Jainy and Jefferson, for all the love and support given to me throughout these years, pushing me to do my best. To my siblings, Sinara and Jefferson Júnior, to motivate and encourage my decisions. I would also like to express my special thanks to my husband, Henrique, who cheers me every step of my academic life. Thank you for your confidence, love, and care at all moments. None of these would be possible without your motivating words; love you all!

I express my sincere thanks to Prof. Daniel Cardoso for his expertise, guidance, and support. Thank you for supervising and pushing me to explore many paths in this doctorate. Thank you for always believing that I could do more. Your wisdom inspires me to achieve my professional aspiration.

The warmest thanks go to Profa. Lilia Ahrné, from the University of Copenhagen-KU, for supervising me even at long distances and for the great opportunity of working with you. Thank you for the wise words and for putting me in touch with brilliant minds at the Department of Food Science. Your participation and scientific vision inspired me.

I would like to thank my coworkers and friends at Analytical and Inorganic Group at USP: Felipe, Jéssica, Jenifer, Juliana Barreiro, Keila, Priscila, Rodrigo, Silmara, Silvinha, Sinara. Thank you for your friendship, your pleasant moments, and for sharing your life experiences. To Dr. Willy Glen, for teaching me the flash photolysis experiments and for all the productive discussions.

I wish also to thank the Lilia lab for welcoming me so well around the lab during my days at KU. The amazing technicians: Ösp, Henriette, and Bente for your support. To all my coworkers at the Lilia lab: Anne Katrine, Emilie, Gabriele, and Mikkel. A very special thanks to my Chinese friends who shared the office with me in the Department of Food Science/KU, Ran and Wenbo, for the friendship, great lunches, and nice atmosphere. Prof. Franciscus Winfried for helping with FT-IR analysis. I also express my thanks to Dr. Markus Ribeiro for always being prompt to assist me with the PEF experiments, patience, guidance, and great conversations in the daily lab.

I would like to express the deepest thanks to IQSC/USP for the support and to all professors here who extensively taught me science from different perspectives during my 10 years at the institute. Also, we thank all the secretaries, especially Andreia, Danielle, and Gislei,

who were always prompt to advise me. I am thankful to Dr. Antonio Roveda for the Raman analysis, Ph.D. Lucas Catunda at Group of Electrochemical Materials and Electroanalytical Methods for the AFM analysis, Ph.D. Keila, and Dra. Sinara for helping with the peptidomic analyses.

I wish to particularly thank the Department of Food Science at the University of Copenhagen for the support and the opportunity to enhance my knowledge at one of the most recognized universities around the world surrounded by gentle and excellent academic professionals.

Foremost, I would to acknowledge CNPq - Conselho Nacional de Desenvolvimento Científico e Tecnológico, for the 4 years of financial support under the grant 168720/2018-3. This study was also financed by FAPESP in the thematic project 2017/01189-0 and, in part by the Coordenação de Aperfeiçoamento de Pessoal de Nível Superior - Brasil (CAPES) - Finance Code 001"; CAPES (grant: 88887.570813/2020-00) during my internship at the University of Copenhagen within the PrInt program – Programa Institucional de Internacionalização.

We should always explore the things that we are afraid of.

Andrea Ghez

RESUMO

Os produtos lácteos são denominados alimentos funcionais por conterem proteínas, gorduras, açúcares, vitaminas e minerais como cálcio e fosfato. Embora, estejam presentes na dieta da maioria da população, crianças menores de 2 anos e idosos desenvolvem respostas alérgicas as proteínas do leite o que resulta na redução da absorção de nutrientes como proteínas que são essenciais para a manutenção da saúde mental e óssea, além de serem importantes no desenvolvimento da massa muscular. As caseínas compreendem 80% do conteúdo total de proteínas do leite e apresentam maior alergenicidade devido a sequência dos epítopos IgE e do tipo de processamento que são submetidos na indústria alimentícia. Durante a digestão, a hidrólise das caseínas libera peptídeos bioativos, especialmente as β-casomorfinas, peptídeos com atividade opioide que são responsáveis por desencadear processos alérgicos causando inflamação no intestino. Com isso, este estudo teve como objetivo investigar modificações físico-químicas nas caseínas após o processamento não térmico, por luz contínua na região do UV-C e pulso de campo elétrico-PEF. Também, foram avaliados o impacto no perfil dos peptídeos liberados, pela simulação *in vitro* da digestão gástrica de idosos, e a absorção dos peptídeos por células do tipo caco-2, como um modelo de absorção em células epiteliais intestinais. A exposição da caseína micelar na luz UV-C por 15 minutos levou a redução no tamanho da micela de caseína de 138.1 para 96.0 nm ($p<0.05$). Como modelo de tratamento térmico, a pasteurização lenta, promoveu a formação de agregados micelares observados pelas imagens de AFM. As modificações estruturais foram observadas nas micelas expostas à luz pela diminuição da intensidade de espalhamento Raman de aminoácidos como tirosina e triptofano que são importantes para manter a conformação das proteínas, o que não afetou na produção e absorção dos peptídeos. O tratamento com PEF resultou em diferentes efeitos, na condição RT notou-se um efeito térmico devido à formação de agregados micelares. Na condição CT, o efeito elétrico foi observado pela redução do tamanho das partículas, e as pequenas modificações na estrutura da micela observadas por espalhamento Raman sugerem uma reorganização espacial na conformação da micela. Além disso, o tratamento por PEF na condição de CT apresentou aumento no número de peptídeos liberados na digestão gástrica, mas com baixa absorção mesmo após 90 minutos de transporte. Ambos tratamentos, UV-C e PEF, mostraram-se promissores como alternativas não térmicas para melhorar as propriedades nutricionais em produtos lácteos, pela liberação de peptídeos bioativos que podem suprir o comprometimento da absorção de nutrientes pela população idosa.

ABSTRACT

Dairy products are defined as functional foods that contain proteins, fats, sugars, vitamins, and minerals such as calcium and phosphate. Although they are present in the daily diet of most of the population, children under 2 years of age and older adults commonly develop an allergic response to milk proteins, reducing the uptake of important nutrients such as proteins essential for maintaining mental and bone health and important for building muscle mass. Caseins comprise 80% of total milk protein and are the most allergenic protein due to the sequence of IgE epitopes and the type of processing in the food industry. During digestion, casein hydrolysis releases bioactive peptides, specially β-casomorphins, peptides with opioid activity that trigger allergic processes causing inflammation in the intestine. From this perspective, this work aimed to investigate the physico-chemical modifications in caseins and micellar casein isolate after nonthermal treatments, by UV-C light and pulsed electric field, PEF. Furthermore, evaluate the peptides of released impact on the peptide profile, by simulating *in vitro* gastric digestion and the uptake through caco-2 cells, as a model of intestine epithelium cells. Micellar casein showed a reduction in particle size ($p<0.05$), after 15 minutes of light exposure, from 138.1 to 96.0 nm. In the opposite direction, thermal treatment, LTLT, generated large micellar aggregates, as seen with increasing particle size to 159.8 nm ($p<0.05$) and micelle surface in AFM images. Structural modifications were observed in samples pretreated with UV-C light by decreasing the intensity of aromatic amino acids such as tyrosine and tryptophan, which are important in maintaining the conformation of the proteins. The slight modifications induced in micellar caseins by exposure to light did not affect the production of peptides or the absorption experiments. The treatment with PEF resulted in different effects; under the RT condition, there was a thermal effect due to the formation of micelle aggregates by increasing the roughness of the micelle surface. Under CT conditions, the electrical effect was observed by a reduction in the particle size, and the slight modifications in the micelle structure at Raman scattering suggest spatial reorganization in the micelle conformation. Furthermore, micellar casein PEF treated with CT showed an improvement in the number of peptides released from gastric digestion, but with lower uptake even after 90 minutes of transport assay. In conclusion, both treatments, UV-C and PEF, have proven promising as nonthermal alternatives to enhance nutritional properties in dairy products in the food industry by promoting the release of bioactive peptides that could provide the uptake of impaired nutrients in the elderly population.

ABSTRAKT

Mejeriprodukter er defineret som funktionelle fødevarer, der indeholder proteiner, fedtstoffer, sukkerarter, vitaminer og mineraler såsom calcium og fosfat. Selvom de er til stede i den daglige kost for det meste af befolkningen, udvikler børn under 2 år og ældre voksne almindeligvis en allergisk reaktion på mælkeproteiner, hvilket reducerer optagelsen af vigtige næringsstoffer såsom proteiner. Disse er afgørende for at opretholde mental og knoglesundhed og vigtige til opbygning af muskelmasse. Kaseiner udgør 80 % af det samlede mælkeprotein og er det mest allergifremkaldende protein på grund af sekvensen af IgE-epitoper, samt typen af forarbejdning i fødevareindustrien. Under fordøjelsen frigiver kaseinhydrolyse bioaktive peptider, især β-casomorfiner, peptider med opioidaktivitet, der udløser allergiske processer, der forårsager betændelse i tarmen. Fra dette perspektiv har dette arbejde til formål at undersøge de fysisk-kemiske modifikationer i kaseiner og micellære kaseinisolater efter ikke-termiske behandlinger ved hjælp af UV-C lys og pulsed electric field, PEF. Evaluer desuden peptiderne med frigivet indvirkning på peptidprofilen ved at simulere in vitro gastrisk fordøjelse og optagelsen gennem caco-2-celler, som en model af tarmepitelceller. Micellært kasein viste en reduktion i partikelstørrelse ($p<0,05$), efter 15 minutters lyseksponering, fra 138,1 til 96,0 nm. Modsat genererede termisk behandling, LTLT, store micellære aggregater, som det ses med stigende partikelstørrelse til 159,8 nm ($p<0,05$) og micelleoverflade i AFM-billeder. Strukturelle modifikationer blev observeret i prøver forbehandlet med UV-C lys ved at reducere intensiteten af aromatiske aminosyrer såsom tyrosin og tryptophan, som er vigtige for at opretholde konformationen af proteinerne. De små modifikationer induceret i micellære kaseiner ved eksponering for lys påvirkede ikke produktionen af peptider eller absorptionsforsøgene. Behandlingen med PEF resulterede i forskellige effekter; under RT-tilstanden var der en termisk effekt på grund af aggregatedannelse af miceller ved at øge ruheden af micelleoverfladen. Under CT-forhold blev den elektriske effekt observeret ved en reduktion i partikelstørrelsen, og de små modifikationer i micellestrukturen ved Raman-spektroskopi tyder på rumlig reorganisering i micellekonformationen. Endvidere viste PEF behandlet micellært kasein med CT, en forbedring i antallet af peptider frigivet fra gastrisk fordøjelse, men med lavere optagelse selv efter 90 minutters transport assay. Som konklusion har begge behandlinger, UV-C og PEF, vist sig lovende som ikke-termiske alternativer til at forbedre ernæringsmæssige egenskaber i mejeriprodukter i fødevareindustrien ved at frigive bioaktive peptider, der kunne give optagelsen af svækkede næringsstoffer i den ældre voksne befolkning.

LIST OF FIGURES

LIST OF TABLES

ABREVIATION LIST

AFM – Atomic force microscopy

Asp – Aspartic acid

BCM – β-casomorphin

CT – Cold temperature

CN – Casein

DLS – Dynamic light scattering

FTIR- ATR – Fourier transform infrared spectroscopy – attenuated total reflectance

Glu- Glutamic acid

IBGE – Instituto Brasileiro de Geografia e Estatística

LFP – Laser flash photolysis

LC-MS/QqQ – Liquid chromatography triple quadrupole mass spectrometry

LTLT – Low-temperature long time

Lys – Lysine

MALDI-TOF – Matrix-assisted laser desorption – time of flight

MBPDB – Milk bioactive peptide data base

PEF – Pulsed electric field

PEP – Prolyl-endopeptidase

RT – Room temperature

SGF – Simulated gastric fluid

SMUF – Simulated Milk Ultra-filtrate

SSF – Simulated salivary fluid

Tyr – Tyrosine

Trp - Tryptophan

UHT – Ultra-high temperature

WHO – World Health Organization

TABLE OF CONTENTS

1. Introduction

1.1. Dairy products as functional food

The term "functional" food was introduced in the 1980s for the first time to specify products enriched with bioactive components, i.e. products that have beneficial physiological effects.

Unlike nutraceuticals, functional food is a product that includes bioactive compounds such as probiotics, antioxidants, soluble fibers, polyunsaturated fatty acids, vitamins and minerals, proteins and functional peptides, and phospholipids (Bath and Bath, 2011). There are several definitions for the term “functional food”, however, it can best be defined as a food that beneficially affects metabolic functions, improves health and well-being, and/or reduces the risk of chronic diseases (Bath and Bath, 2011; Guimarães et al., 2018).

Dairy products are functional foods with high added value and, from a nutritional point of view, are rich in nutrients because they contain proteins, fats, sugars, vitamins, and minerals such as calcium and phosphate. These components are essential to maintain mental and bone health and build muscle mass. The presence of a variety of micro- and macronutrients shows the potential of dairy products in terms of taste, texture, and nutritional values to meet the needs of the elderly population (Kanekanian, 2014).

Some studies have shown that dairy products play an important role in maintaining bone health, both during the childhood period by stimulating growth hormone synthesis and preserving bone density in the prevention of osteoporosis in seniors. (Rizzoli, 2014; Houchins et al., 2017). Furthermore, dairy products act as modulators of digestive and gastrointestinal functions that control the growth of the microbiota in the digestive system and as regulators of the immune system (Bath and Bath, 2011).

Although milk and its derivatives are nutritionally rich foods and are important for maintaining health, children under 2 years of age and elderly people commonly develop allergic responses to milk, or more precisely to milk proteins. Caseins are among the proteins that promote greater allergenicity to milk, followed by the whey protein β-lactoglobulin. The allergenic activity of milk proteins is related to the structural properties of caseins, the sequence of IgE epitopes and the type of processing in which dairy products are submitted (Hu et al., 2016; Hu et al., 2017).

Ingestion of milk proteins, caseins, β-lactoglobulin, α-lactoalbumin, immunoglobulin, lactoferrin, and serum albumin shows direct biological activity since the peptides released from enzyme hydrolysis may affect the immune, digestive, cardiovascular, and nervous systems (Bath

and Bath, 2011). During digestion, casein hydrolysis releases compounds essential for body function, such as phosphopeptides and bioactive peptides, which can have opioid, antioxidant, antihypertensive, and anti-inflammatory activities (Hu et al., 2017; Srinivas and Prakash, 2010). Phosphopeptides are composed of phosphorylated serines in their monoester form that act as carriers of calcium ions in the intestinal mucosa and inhibit caries formation through the process of recalcification of dental enamel (Wang and Li, 2018; Bath and Bath, 2018; Bath and Bath, 2011). Among bioactive peptides with opioid activity, β-casomorphins are responsible for triggering allergic processes, that is, reactions in the body of the immune system against the substance detected as 'invasive' (Bath and Bath, 2011; Hu et al., 2017).

Increasingly, dairy products have been included in the diet of many consumers, especially older people, not only to address the lack of nutrients but also to improve physical and mental well-being. Currently, new methodologies have been developed in the processing of dairy products in search of convenience, nutritional quality, and improvement of the sensory properties of the product (Rizzoli, 2014; Bath and Bath, 2011; Guimarães et al., 2018).

The WHO- World Health Organization estimates that by 2050 the world population will have a greater number of elderly people, aged 60 years and over (Beard and Chatterji (2015)). According to IBGE (Instituto Brasileiro de Geografia e Estatística) data, Brazil's aging index, which measures the ratio of the percentage of elderly and young people, is expected to increase from 43.19% in 2018 to 173.47% in 2060. This change in the demographic profile of the Brazilian population follows a worldwide trend of narrowing the base of the age pyramid (Figure 1) and is related to an increase in life expectancy and a decrease in the fertility rate (Perissé et al., 2019).

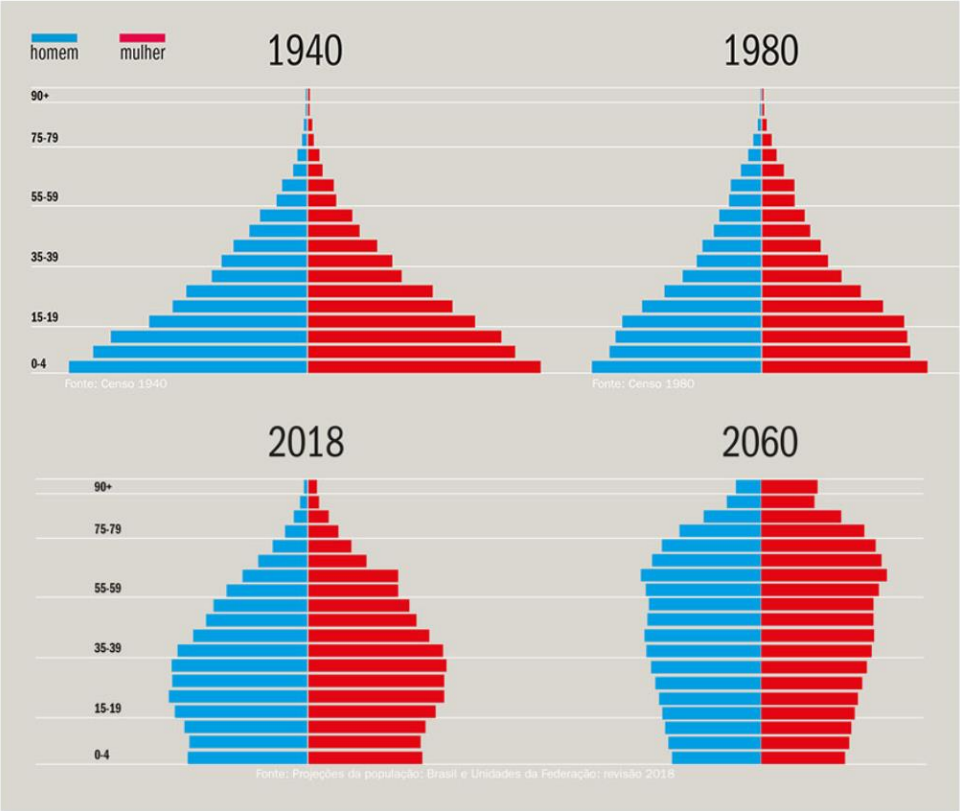

Figure 1 – Distribution of the Brazilian population by age group for the years 1940, 1980, and 2018. Also, a projection for 2060 years. Source: Adapted from Perissé et al., 2019.

It is evident that aging is accompanied by changes in quality of life in the majority of people. Some of these changes are observed by decreased muscle mass, inadequate food intake, reduced appetite, increased chronic diseases, and altered metabolic functions in the organism such as the digestion of certain foods (Beard e Chatterji (2015); Levi et al., 2017).

Malnutrition in older people is caused by limited absorption of vitamin B_{12} into the gastrointestinal tract, as well as reduced protein digestibility, resulting in sensory impairment such as loss of vision, taste, and smell (Houchins et al., 2017 Douaud *et al.*, 2013, Cooper *et al.*, 2016). Deficiency in vitamin $B_{12,}$ cobalamins, in seniors has as a consequence anemia and neurologic disorders such as memory impairment, dementia, and depression (Vogiatzoglou et al., 2009). The decline in nutrient intake and uptake in seniors leads to several aging-related pathologies, such as sarcopenia, osteoporosis, and fatigue. Sarcopenia is defined by the decrease in skeletal muscle mass with age, observed from the age of 50 years. The loss of skeletal mass can reduce mobility and

quality of life for older people, increasing healthcare costs (Houchins et al., 2017; Beard e Chatterji (2015); Rizzoli, 2014).

In this sense, several alternatives have emerged with the interest of improving the processing of milk and its derivatives to reduce their allergic potential without alterations in the quality of nutritional and organoleptic properties of the product, resulting in a functionalized food product.

1.2. Caseins

Among the proteins found in milk, caseins are the majority and account for 80% of the total protein content and 20% corresponds to whey protein (β-lactoglobulin and α-lactoalbumin). Four different types of caseins compose the structure of the casein micelle: α_{s1}, α_{s2}, β and κ-casein. Caseins are highly negatively charged in phosphorylated serine residues found in groups of 4, 3, and 2 units along their primary sequence, as represented in Figure 2 (Dalgleish e Corredig, 2012; Kamigaki et al., 2018; Horne, 2006).

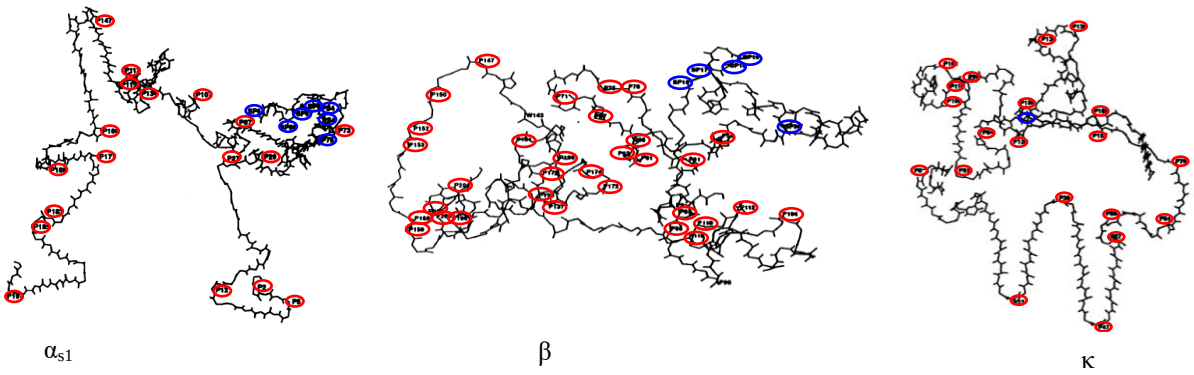

Figure 2 – α_{s1}, β and κ-casein structures, respectively, highlighting the proline residues in red and phosphoserines in blue. Source: Adapted from Farrel et al., 2003.

Unlike whey proteins, caseins have a flexible and open conformation and are slowly digested by the organism since they are retained in acid environments, as in the stomach, favoring the formation of a clot. (Hu et al., 2017). Susceptibility to protein hydrolysis depends both on the proteolytic enzyme and the flexibility of the protein chain, consequently, it depends on the physicochemical changes induced by processing technologies (Hu et al., 2017; Fox e McSweeney, 2003).

The hydrophobic characteristics of caseins are reflected in the high content of proline residues in their structures, and then they organize themselves into a micellar heterogeneous network stabilized by calcium phosphate bridges and hydrophobic interactions. Caseins are present in milk as colloidal particles with diameters between 20 and 600 nm (Dalgleish e Correding, 2012; Kamigaki et al., 2018).

Figure 3 represents a model of a casein micelle in which each casein is color-enhanced. α and β-caseins (orange and blue, respectively), calcium sensitive, are found inside the micelle attached by hydrophobic interactions, and both are linked by nanoclusters of inorganic calcium phosphate (gray spheres). On the hydrophilic surface, from the colloidal particle, there is κ-casein (green) that extends from the micellar surface to most of the solution, a glycopeptide (black hair) linked to the C-terminal portion of the protein (residues 106-169) (Horne, 2006; Dalgleish e Correding, 2012; Horne, 2006).

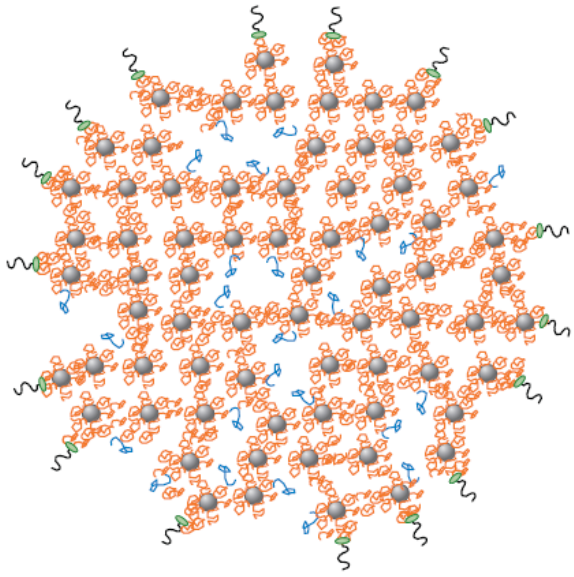

Figure 3 – Micellar casein structure model. Adapted from Dalgleish e Corredig, 2012.

Exposure of macro-glycopeptides to the bulk of the solution creates a layer estimated to be 5–10 nm thick that provides steric stabilization against micelle aggregation (Dalgleish e Corredig, 2012).

α-casein comprise 50% of the total content of caseins, exhibit a higher allergic response compared to whey proteins, due to the release of bioactive peptides, called casomorphins, during

digestion and dairy processing (Hu et al., 2016; Srinivas and Prakash, 2010). β-casomorphins (BCMs) are generated by hydrolysis of β-casein from cows with genetic variance A^1 and B. The primary sequence of proteins is subject to genetic variations that may occur with the substitution of some amino acid, as in the case of β-casein.

The sequence of BCM-7 (60-67), illustrated in Figure 4, of cows with genetic variance A^1 and B, is observed to have the presence of histidine amino acid while in cows with genetic variance A^2, histidine was evolutionarily replaced by proline amino acid. This genetic replacement has been reported to prevent hydrolysis of the peptide bond between residues 66 and 67 of β-casein from cows with genetic variance A^2, thus preventing the production of β-casomorphin7, which manifests inflammation in the intestinal tract, intensifying the symptoms of lactose intolerance (Fontes, 2019; Pal et al., 2015).

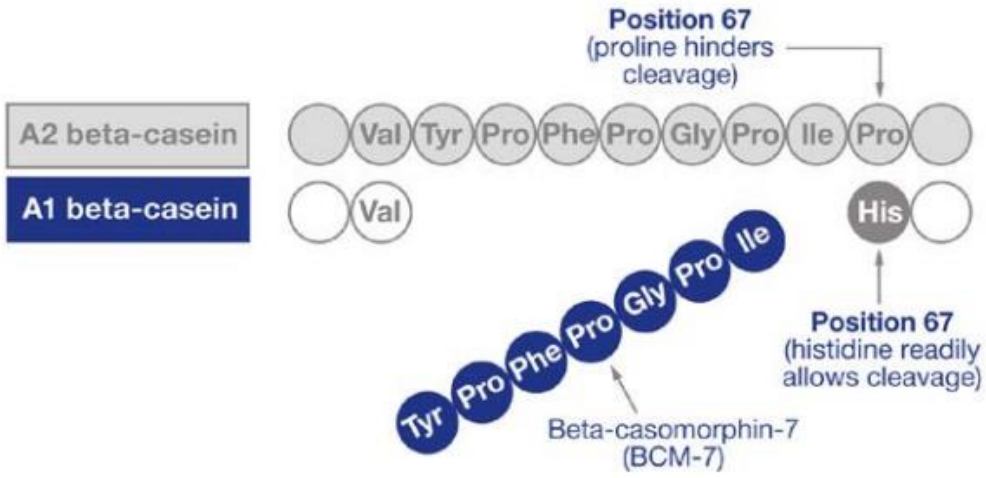

Figure 4 - The formation of β-casomorphin7 in variant A^1 and the genotypic difference in variant A^2 of β-casein. Adapted from Pal et al., 2015.

The other three epitopes from β-casein 19-30, 86-103, and 141-150 were located in hydrophobic regions of the protein that were inaccessible to antibody interaction, resulting in an allergic response for some people. The most immunoreactive peptide was the sequence 86-103 (Wal, 2001).

β-casomorphins are considered by the dairy industry the main contributor to allergic responses to milk. Furthermore, they have addressed the development of new technologies for the production of cow milk dairy products with the genetic variant A^2 (Noni *et al.*, 2009; Fontes, 2019).

The allergenic activity of some peptides is related to the food source and its genetic variances, the structural properties of the protein, and the processing of food in the industry. Caseins are important protein sources in the diet of most of the population, and are available in a variety of dairy products. In view of this, emerging technologies of food processing have been developed in search of reducing or even eliminating the production of allergen peptides, guaranteeing nutritional and organoleptic qualities in the final product. (Hu et al., 2016; Xu et al., 2020; Wang et al., 2020).

1.3. Processing in the food industry

Thermal processing in the food industry, such as sterilization by ultra-high temperature (UHT) and pasteurization, is commonly used to inactivate the growth of pathogen microorganisms and inactivate proteolytic enzymes, increasing the shelf life of the final product. Thermal processing in foods may cause alterations in primary, secondary, and tertiary protein structures that affect the interactions between casein micelles and whey proteins and the association of caseins within the micellar network (Awuah et al., 2007).

Structural modifications induced by thermal processing can influence the digestibility of proteolytic enzymes, making the active site more or less accessible to the enzyme. In addition to this, thermal treatment can alter food quality, as changes in the physical-chemical properties of proteins lead to the development of allergic reactions and undesirable sensorial and nutritional alterations resulting in consumer rejection (Awuah et al., 2007; Calvano et al., 2013).

Another important aspect of thermal processing in foods is the Maillard reaction, or nonenzymatic browning. The reaction takes place between amino acids, such as Lys, and the carbonyl group from reduction of the presence of carbohydrate and heat. The Maillard reaction is responsible for the production of compounds, such as melanoidins, that give flavor, odor, and color characteristics to thermally processed foods. However, nonenzymatic browning reactions result in the loss of essential amino acids, reduced protein digestibility, and formation of potentially toxic products such as acrolein, aromatic heterocyclic amines, and dicarbonyl compounds from the oxidation of lipids and sugars, the latter increasing the level of glucose in the bloodstream. Some of them are highly reactive compounds that directly affect the intake of adequate amounts of protein by people with restrictive diets (Dutson et al., 1984; Delorme et al., 2020).

Recently, researchers have used nonthermal technologies such as high pressure, pulsed electric field, PEF, and UV-C photolysis as alternatives to reduce the allergenicity of milk protein, improving nutritional digestibility, intake, and uptake (Orlien et al., 2006; Sharma et al., 2014; Hu et al., 2017; Xu et al., 2020; Cadesky et al., 2016).

1.3.1. UV-C light treatment

Our research group, Analytical and Inorganic Chemistry, has investigated the application of continuous light in the UV-C region, λ = 266 nm, as an alternative to non-thermal processing in dairy proteins. Silva (2019) reported alterations in the structure of β-lactoglobulin and the profile of the released peptides after simulating gastric conditions *in vitro* digestion for adults and seniors.

Ultraviolet light is non-ionizing and is located in the electromagnetic spectral region between visible light and the x-ray region. UV radiation can be classified into four types located in the range of 100 to 400 nm; they are UV-A ((315-400 nm), UV-B (280-315 nm) UV-C (200-280 nm) and far-UV (100-200 nm) (Hawkins e Davies, 2019; Delorme et al., 2020). UV-C radiation has been used as a promising nonthermal technique to increase the digestibility of dairy proteins without alterations. As a benefit, this nonthermal technology presents a low investment and maintenance and is considered safe, nontoxic, and harmless to the environment (Delorme et al., 2020).

Light radiation in the UV-C region is a technological process used to inactivate pathogenic microorganisms to preserve fluid foods and has been proposed for application in the processing of dairy foods, because it does not promote adverse effects compromising the nutritional values of the product (Manzocco, 2015; Delorme et al., 2020). The microorganism inactivation mechanism of UV-C radiation consists to damage of DNA bases leading to the formation of pyrimidine dimers that inhibit the synthesis of DNA in cells, so microorganisms can not reproduce, resulting in cell death. In this sense, the European Food Safety Authority (EFSA) approved the use of UV-C as a technique that can inactivate pathogens in pasteurized milk (EFSA Panel on Dietetic Products, 2016; Liu et al., 2022). However, several factors such as turbidity, the geometry of the device, and light power should be addressed to be efficient for the microbial inactivation process (Delorme et al., 2020; Liu et al., 2022).

However, light radiation, in the UV-C region, is capable of causing oxidative modifications in protein structures due to the presence of chromophores groups of amino acids in the polypeptide

chain, such as tryptophan, tyrosine, phenylalanine, and cysteine. In the presence of light, these amino acids may react with reactive oxygen, nitrogen, or sulfur species, as illustrated in Figure 5, where R is the amino acid side chain in the protein structure.

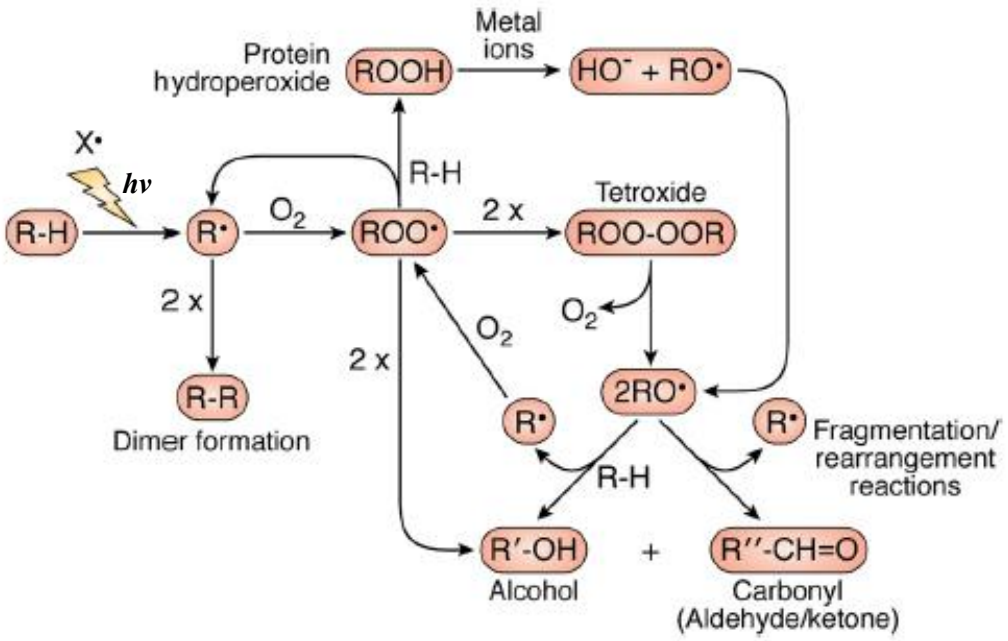

Figure 5 – Potential protein oxidative modifications during UV-C light exposure. Source: Adapted from Hawkins and Davies, 2019.

Such reactions lead to the formation of secondary products such as aldehydes, hydroperoxides, carbonyl compounds, tryptophan dimers, and/or tyrosine, resulting in a variety of post-translational modifications in the primary structure of the protein. Consequently, post-translational modifications could alter the secondary structure, charge, folding, and exposition of hydrophilic / hydrophobic regions, compromising protein function (Hawkins et al., 2019).

Protein radical reactions occur through the abstraction of hydrogen atoms from C-H, S-H, N-H, or O-H bonds and the electronic abstraction from electron donor sites such as aromatic amino acids (tryptophan, tyrosine, phenylalanine) and R-SS-R disulfide bridges (Cardoso et al., 2012; Hawkins and Davies, 2019).

Photochemical reactions generally take place by direct oxidation, from the absorption of radiation by the protein (type II reaction), or by indirect reaction (photosensitization), in which the mechanism is mediated by radical species (type I reaction) (Cardoso et al., 2012; Hawkins and Davies, 2019). Proportionally, light radiation compromises protein function due to changes in

secondary and tertiary protein structures that provide individual allergic responses without significantly altering the sensory quality of the dairy product (Silva, 2019; Manzocco, 2015; Andrés et al., 2018).

1.3.2. Treatment with pulsed electric field (PEF)

Another emerging technology that has been used as a nonthermal treatment is the pulsed electric field (PEF). Processing consists of the application of short electric pulses (1−100 μs), at a high electric field (0.5-50 kV/cm) applied between two electrodes, and short residence times (lower than 1 s). The design of the treatment chamber, specifically the insulator shape, is an important factor that contributes to the distribution of the electric field strength and therefore affects the process performance (Meneses et al., 2010).

The insulator designs in Figure 6 illustrate the real distribution of the electric field within the treatment zone. For the rounded edges, geometry (Figure 6A) is expected to have a less homogeneous electric field due to the distance between the high voltage and the grounded electrode, therefore, to improve the inactivation process, it is interesting to increase the pulse frequency. On the other hand, the convex geometry (Figure 6B) provides a higher average of the electric field strength due to the low difference between the maximum and minimum field intensities, calculated from the central line of the treatment zone. Lastly, parallel geometry provides the most homogeneous electric field, where the electric field intensity is directly proportional to the insulator area.

However, other parameters must be taken into account to achieve a homogeneous electric field for a specific system, such as the medium conductivity and the flow rate of the fluid to avoid overprocessing and electrical arcing in the treatment chamber (Meneses et al., 2010; Reineke et al., 2015).

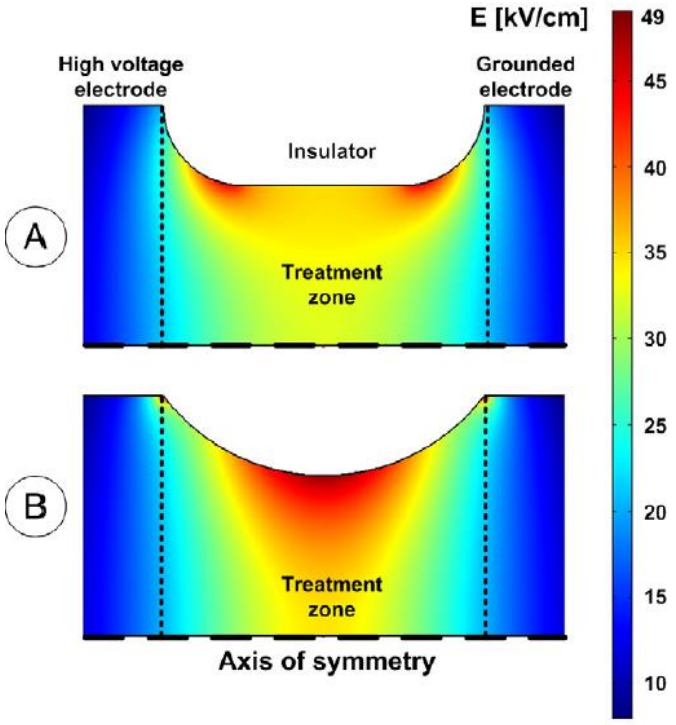

Figure 6 - Distribution of electric field strength for different insulator geometry: A – rounded edges and B – convex. Adapted from Meneses et al., 2010.

Food processing by applying electrical discharges began to be explored in the early 1900s. At this time, the researchers demonstrated lethal effects on microorganisms due to the applied electric intensity (Sharma et al., 2014). The principle which involves the death of microorganisms by applying high-voltage pulses is called electroporation and is based on charge polarization on the cell membrane. When microorganisms are exposed to high voltages, pulses induce a mechanical stress on the cell membrane. The accumulation of charge causes the formation of hydrophilic pores in the membrane, disrupting its integrity and inactivating the growth of the microorganism (Figure 7) (Middendorf et al., 2021). Modifications in the membrane are irreversible, which means that it ceases to act as a semi-permeable barrier, leading to cell death (Guimarães et al., 2018; Bendicho et al., 2002; Sharma et al., 2014).

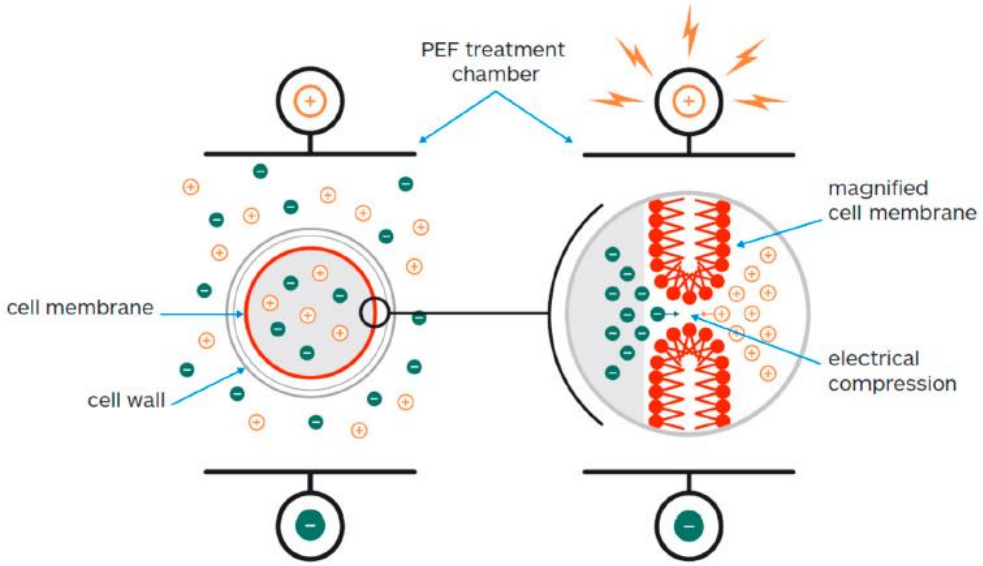

Figure 7 – Illustration of the electroporation phenomenon in biological cells. Adapted from Middendorf et al., 2021.

The same phenomenon occurs in different matrices and its application has been explored in the food industry based on the consumer's demand for fresh and safe ingredients to preserve the sensorial aspects of the food product (Reineke et al., 2015; Fauster et al., 2021; Marsellés-Fontanet et al., 2012). However, the effectiveness of the aspects of process depends on the ionic strength, pH, and treatment chamber. The pulsed electric field can induce physicochemical changes in protein structures that affect proteolytic extension and the profile of released peptides after digestion (Mikhaylin et al., 2017; Guimarães et al., 2018; Bendicho et al., 2002).

Processing of PEF in dairy proteins has shown an efficient nonthermal technology for the inactivation of pathogens in addition to inducing protein structural modifications of proteins without compromising the composition and organoleptic properties of dairy products (Bendicho et al., 2002; Sharma et al., 2014). Researchers have reported the potential of PEF in whey protein that promotes structural modifications by exposing hydrophobic regions in the protein that facilitate the access of proteolytic enzymes to cleavage sites (Mikhaylin et al., 2017; Xiang et al., 2011).

Middendorf et al. (2021) reported the use of PEF processing as a tool to prepare the micellar casein structure to encapsulate lipophilic organic compounds, such as β-carotene, in a procedure to disintegrate/integrate the micelle structure. In this regard, PEF can be a suitable technique for

producing micellar caseins binding to other organic compounds, such as fat-soluble bioactive substances that act as carriers and supplying the low consumption of vitamins in overweight and obese people.

In raw milk, the applied moderate electric field (9-16 $kV.cm^{-1}$) resulted in the phenomenon of electroporation in milk fat globules. The pronounced effect of PEF showed an interaction of milk fat globules with whey proteins such as β-lactoglobulin and α-lactalbumin, and changes in enzyme activity that led to the liberation of fatty acids due to changes in pH and exposure of some triglycerides to lipase (Yang et al., 2021).

For micellar casein, the double layer of negative charge of carboxyl groups from glyco-macropeptide, present in κ-casein, and calcium ions can act as a lipophilic membrane, therefore, the application of the electric field induces charge disturbance that results in micelle disintegration. Few studies are exploring the modifications generated on the micelle structures, however, some authors reported that the micelles can reorganize even after overnight storage (Sharma et al., 2014; Soltanzadeh et al., 2020).

2. Objectives

The present study aimed to assess the potential of emerging nonthermal technologies, such as UV-C light at 255 nm and PEF in modifying the structure of caseins and micellar casein from bovine milk, in a synthetic milk ultrafiltrate, and consequently the peptides from their digestion, which may have reduced protein allergenicity. Specific sub-objectives were:

I. Investigate physicochemical changes in micellar casein structure induced by UV-C light at 255 ± 4 nm and PEF treatments.
II. Evaluate the impact of the modifications caused by UV-C light and PEF on the digestibility of caseins by the peptide profile;
III. Evaluate the uptake of peptides by caco-2 cells as a model of intestinal epithelial cells.

3. Materials and Methods

3.1. Chemicals

α-casein (≥70%), β-casein (≥98%), κ-casein (≥70%), and micellar casein isolate from bovine milk were acquired from Sigma-Aldrich. Potassium citrate ($K_3.C_6H_5O_7$) from Pantofarma Ltda; sodium citrate dihydrate ($Na_3.C_6H_5O_7.2H_2O$) purchased from Baker's Analyzed; anhydrous

potassium sulfate (K_2SO_4 ≥99%); calcium chloride dihydrate ($CaCl_2.2H_2O$ 99-105%) purchased from Vetec; magnesium chloride hexahydrate ($MgCl_2.6H_2O$ ≥99%), potassium carbonate (K_2CO_3 99%), potassium chloride (KCl ≥99%) and potassium phosphate monobasic (KH_2PO_4 ≥98%) were obtained from Sigma-Aldrich. The water used in the experiments was previously deionized in a Milli-Q system (18.2 MΩ cm^{-1} at 25 ºC, Millipore Co., Eschborn, Germany).

Micellar casein isolated used for PEF treatments was provided by Arla Foods Ingredients.

3.2. UV-C light and thermal treatment

UV-C light treatment was performed on a photochemical bench equipped with a LED255W, center emission in 255 ± 4 nm, and a high power controller (200 – 1200 mA) from Thor Labs. Caseins were prepared in a pH 6.5 phosphate buffer, ionic strength of 0.16 M NaCl to a protein concentration of 3 mg mL^{-1} in ultrapure water. The caseins were separately exposed to light in cuvettes (1 cm x 1 cm quartz cuvettes, Hellma Analytics, Mülheim, Germany) for 15 and 30 minutes. The temperature was maintained at 25 ± 0.5 ° C using a circulating water bath, under continuous agitation. The casein micelle was prepared at a concentration of 0.25% w/v in synthetic milk ultrafiltrate (SMUF), lactose-free, containing 1,58 g L^{-1} of KH_2PO_4; 1,2 g L^{-1} of K_3.citrato.H_2O; 1,79 g L^{-1} of Na_3.citrato.$2H_2O$; 0,18 g L^{-1} of K_2SO_4; 1,32 g L^{-1} of $CaCl_2.2H_2O$; 0,65 g L^{-1} of $MgCl_2.6H_2O$; 0,30 g L^{-1} of K_2CO_3 and 0,60 g L^{-1} of KCl in ultrapure water, pH 6.5.

The intensity of light was measured by chemical actinometry using Parker salt according to Kuhn et al., 1989, and the dose of light in the cuvettes was of 3 W m^{-2}.

For the slow pasteurization, low temperature long time (LTLT), caseins were placed in sealed ampoules and heated at 63 ± 2°C for 30 minutes (Grappin & Beuvier, 1997; Viazis et al., 2008).

3.3. Pulsed electric field - PEF treatment

The PEF experiments were performed in a colinear treatment chamber, equipped with one central high voltage electrode and two outer grounded electrodes (all stainless steel, inner diameter of 6 mm) separated by a distance of 4 mm using two polyoxymethylene insulators with an inner diameter of 4 mm. Actual voltage and current signals in the treatment chamber were measured using a high-voltage probe (Tektronix, P6015A, Wilsonwille, OR, USA) and a current probe connected to a 350 MHz digital oscilloscope (RIGOL, MSO5354, UK).

The samples were pre-equilibrated at room temperature (RT) ± 23 ° C and cold temperature (CT) ± 4 ° C in the ice bath and guided through the PEF unit using a peristaltic pump with two flow rates of 1 L h^{-1} and 5 L h^{-1}, under both temperature conditions. The capacitive power supply (CPPS voltage) was set at 0.6 kV in the computer control system; with a pulse width of 2 µs, 100 Hz in monopolar mode. The E-strength and treatment time (t) were calculated based on the shape, flow speed, monopolar pulse frequency and width as described by Meneses et al., (2011). The E-strength was 16 kV cm^{-1} for both treatments, 1 and 5 L h^{-1}, and the total sample treatment time were 31 and 6 µs, respectively. Inlet and outlet temperatures were measured immediately using a thermometer. Control samples were passed through PEF without voltage at a flow of 1 L h^{-1}.

The flow for PEF processing was established by passing deionized water through the PEF system without voltage.

3.4. Spectroscopic analyses

3.4.1. Fluorescence spectroscopy

Fluorescence emission, for the UV-C treated samples, was recorded in a Hitachi F - 4500 spectrofluorometer (Hitachi High-Technologies Corporation, Tokyo, Japan). Measurements were made in a quartz cuvette (Hellma Analytics, Müllheim, Alemanha) of 1.0 cm x 1.0 cm pathlength. For micellar casein, treated with PEF, fluorescence was recorded in Spectramax® i3x (Molecular Device). The sample measurements were performed on a 96-well quartz plate.

The excitation band of tyrosine was set at 275 nm and recorded between 290 and 500 nm. For tryptophan, the excitation wavelength was set at 299 nm, and the emission spectra were recorded between 330 and 500 nm, both using a 2.5 mm slit width for excitation and emission. Spectra were processed using the Origin academic 2020 version (OriginLab Corporation, Northampton, MA, USA) and calculated by the spectral center of mass, where F_i is the fluorescence intensity and λ_i its respective wavelength:

$$< \lambda > = \Sigma(F_i \times \lambda_i) / \Sigma F_i$$

3.4.2. Raman spectroscopy

The spectra were recorded on a confocal Raman microscopy spectrometer model LabRam HR evolution, equipped with Edge grating 1800 grooves/mm at 500 nm. The spectra were collected

in the range of 500-4000 cm^{-1} using a 100x objective, with a 785 nm laser excitation and power of 180 mW. Raman spectra were acquired by performing 16 scans and an integration time of 64.2 s. The sample was spotted onto a gold surface and air dried at room temperature. Spectra were acquired from multiple regions of the sample. All of them were compared to confirm the profile of spectra, and one with a better signal-to-noise ratio was chosen to attribute the bands for the secondary structure.

3.4.3. Transient absorption laser flash photolysis spectroscopy (LFP)

The experiments were carried out with a flash photolysis spectrometer, LFP-112 ns (Luzchem, Ottawa, Canada). The second harmonic at 266 nm of a pulsed Q-switched Nd:YAG laser (Brilliant-B, LesUlis, France) was used to pump a dye laser (Quantel). The intensity was 1.4 mJ cm^{-2}, with a duration of 8 ns. A Hamamatsu photomultiplier tube and a monochromator were used to detect transient absorption (300-800 nm) in an oscilloscope (Tektronix TDS 2012 digitizer, Beaverton, OR, USA).

The experimental parameters of the kinetic curve and the transient absorption spectrum were set in Luzchem software (Luzchem, Ottawa, Canada). Kinetics was acquired after 4 shots and the rate constant was adjusted to the exponential decay function. Tyrosine and tryptophan were acquired in a water solution and, for caseins, excited in buffer phosphate, pH 6.5 (I = 160 mM), in fluorescence cuvettes of 1.0 cm × 0.5 cm (Hellma Analytics). All measurements were made with fresh solutions and purged with Ar for at least 15 minutes prior to the experiment.

3.4.4. Electron paramagnetic resonance (SSEPR) spectroscopy

X-band (~9.5 GHz) EPR measurements were performed using a Bruker EMXplus spectrometer at 298 K in a Suprasil quartz capillary tube with 100 kHz magnetic field modulation, modulation amplitude of 0.1 or 1.0 G, time constant of 163.8 ms conversion time of 128 ms and 1024 data points. In a typical experiment, a protein solution 8.4 x 10-5 mol L-1 was prepared in an oxygen-free environment in the presence of TMPO (4 x 10-1 mol L-1). Irradiation of the solution samples (15 min) was performed with the fourth harmonic of a pulsed Nd:YAG laser source (266 nm, power ~of 1.5 mJ cm-2, and repetition rate of 10 Hz, and pulse width of 6 ns).

3.4.5. Fourier transform infrared with attenuated total reflectance (FTIR – ATR)

The analysis of the secondary structure of α and β-casein was recorded in a Vertex 70v Bruker FT-IR spectrometer model equipped with an accessory of attenuated total reflection with diamond crystal and MCT detector. The spectrometer was purged with $N_{2(l)}$ to reduce the contribution of water steam during the acquisition of the spectra. For micellar caseins, PEF treated analyses were carried out in infrared spectroscopy (ABB Bomem Inc., MB100) equipped with the ZnSe accessory of attenuated total reflection.

The spectra were acquired with a resolution of 4 cm^{-1}, a speed of 20 kHz, and 128 scans. The data obtained were processed and the absorption bands were deconvoluted to their secondary structure using the Origin academic 2020 version. Assignment and relative quantification of the frequency secondary structure in the region of the amide I frequency ($\nu \sim 1600 – 1700$ cm^{-1}) was carried out using the area of the deconvoluted bands according to Yang et al., 2015 and Hu et al., 2016.

3.5. Dynamic light scattering (DLS)

The size distribution of the samples was recorded on Mastersizer equipment (Malvern Instrument Ltd). The analysis was recorded in triplicate of untreated and treated MCI in quartz cuvettes (Hellma Analytics, Müllheim, Alemanha) 1.0 cm x 1.0 cm pathlength. The solutions of untreated and pretreated micelle casein were diluted to a protein concentration of 0.5 mg mL^{-1}.

3.6. Atomic force microscopy (AFM)

Analysis of the surface topography of micellar casein was carried out using Nanosurf Easyscan 2 (Nanosurf) equipment. 10 µL of micellar casein at a concentration of 0.05 mg mL^{-1} were deposited on the surface of the mica plate (1.5 cm x 1.5 cm) spread and dried at room temperature before image acquisition. AFM images were recorded in tapping mode with a Tap190Al-G tip (Budget Sensors).

Data were processed using the Gwyddion 2.59 software to determine the height and width of each sample untreated, irradiated and pasteurized. Images were collected in triplicate for each sample.

3.7. Liquid chromatography triple quadrupole mass spectrometry (LC-ESI-MS/MS)

Qualitative analysis was performed in LC-ESI-MS/MS (Thermo Scientific) equipped with a quaternary pump, Accela 1250, Accela autosampler, TSQ Quantum Access, column C18 (2,7 µm, 15 x 3,0 mm, Supelco), for caseins treated with UV-C light. Conditions used were: oven temperature 25 °C; injection volume: 10 µL; mobile phase: water (phase A) and methanol (phase B) both with 0.5% formic acid. A linear gradient from 5 to 95% B in 40 minutes with a flow rate of 0.400 mL min^{-1}, analytical column equilibration time of 5 minutes. The samples were filtered through a cellulose acetate filter for aqueous/polar media (Chromafil® XTra CA-20/25), with a pore size of 0.20 µm and a diameter of 25 mm. The ionization source was electrospray (ESI) and the parameters were: capillary temperature 350°C; spray voltage 3500 V; nebulizer gas pressure 45 psi; auxiliary gas pressure 10 psi. Data acquisition and processing were performed using the Xcalibur™ software (Thermo Scientific). The spectra for the analysis of di-tyrosine synthesis were acquired in positive mode, product ion scan, in the range of m/z 120 – 400 to read the ion mass m/z 361. For hydrolyzed caseins, spectra were acquired in positive full scan mode, in the m/z range 120 – 400.

The synthesis of di-tyrosine was performed following the methodology proposed by Kato et al., 2009, with some adaptations. 30 mg of L-tyrosine, 1 mg of horseradish peroxidase (HRP) and 5 µL of H_2O_2 (30%, v/ v) in 0.1 M sodium tetraborate buffer ($Na_2B_4O_7.10H_2O$) at pH 9.0. The reaction mixture was kept under magnetic stirring for 1 hour at 35 ° C. The reaction was stopped by adding 500 µL of 6M HCl and 100 µL of formic acid. The solution was filtered through an aqueous/polar cellulose acetate filter (Chromafil® XTra CA-20/25) and applied to a solid phase extraction (SPE) column (Waters, C18, 2g).

Hydrolysis of caseins was performed as described by Dalsgaard et al. (2007). The native and UV-C light pretreated protein solutions were precipitated with 10% trifluoroacetic acid (TFA) and centrifuged at 3,000 rpm for 25 minutes. The precipitate was washed with 1.33 mL of 1 M HCl and centrifuged at 3,000 rpm for 20 minutes. The precipitates were dissolved in 0.33 mL of 6M HCl and purged with argon for 5 minutes. The solutions were kept in a dry bath at 105 ° C overnight. After hydrolysis, the samples were neutralized with 6M NaOH and analyzed by LC-ESI-MS/MS.

3.8. *In vitro* gastric digestion *model*

To evaluate the profile of peptides released after nonthermal treatments, an experiment was performed that simulates gastric conditions for the elderly. Fluids such as Simulated Salivary Fluid (SSF) and Simulated Gastric Fluid (SGF) for *in vitro* gastric digestion for the elderly were made following the method described by Minekus et al., 2014.

The oral bolus was prepared by mixing 1 mL of casein solution with 1 mL of SSF in a Falcon tube (n = 3) and stirred at 200 rpm inside an incubator at 37 ° C. The oral bolus was mixed with 1.5 mL of SGF, 1 µL of $CaCl_2$, and 0.179 mL of water, and the pH was set at 3.0. After adjustment of pH, 0.280 mL of porcine pepsin stock solution (1400 U mL^{-1}) was added to the solution and placed in an incubator at 37 °C, 200 rpm for 3 h. The reaction was interrupted by adding sodium bicarbonate ($NaHCO_3$) until pH 7.

3.9. Transepithelial transport of peptides across caco-2 cell monolayers

Transepithelial transport across caco-2 cell monolayers was carried out using Transwell permeable supports (polycarbonate/ polyester membrane pore size 0.4 mm, diameter 6.5 mm, 24-well cat. no. 3396, Corning Costar). Caco-2 cells (ATCC HTB-37) were seeded in permeable supports in passage 54 and a concentration of 6.10^5 cell mL^{-1}. The medium (DMEM - Dulbecco's modified Eagle Medium High glucose, with L-glutamine, 10% fetal bovine serum (FBS), 1% 100x nonessential amino acids and 1% PEST 100x (penicillin 10,000 U mL^{-1} streptomycin, 10,000 µg mL^{-1}) was exchanged every other day. Cells were allowed to differentiate on supports for 21 days for further transport analysis. Cell monolayer integrity was determined by diffusion of phenol red (paracellular marker) (10 µmol L^{-1}) and by the use of cell trackers to monitor the monolayer formation. DAPI (4′,6-diamidino-2-phenylindole) dye was used to monitor cell nuclei, while ZO-1 (Zonula Occludens 1) dye was used to track tight junction formation. Counterstaining guarantees an image of the entire monolayer with the formation of the essential structures for the transport of nutrients. The fluorescent dyes were tracked using a Zeiss LSM 780 confocal microscope with a 488 nm argon ion laser and a Coherent Chameleon laser (Ti:sapphire) as a source for two-photon excitation at the wavelength of 800 nm. For peptide transport, all digested caseins were lyophilized, resuspended in HBSS (Hanks balanced salt solution) at a protein concentration of 12 mg mL^{-1}, and filtered (0.2 µm) for further contact with cells. The transport of peptides was carried out for 90 minutes at 37 ° C with mild agitation. Aliquots were collected every 30 minutes from

the basal chamber, while the same volume of HBSS was replaced as described by (Hubatsch et al., 2007). Final and initial apical aliquots were also collected for further MALDI-TOF/TOF-MS analyses.

3.10. Peptidomic by MALDI-TOF/TOF-MS

To identify peptides in the basolateral chamber, the samples were mixed 1:1 (v/v) with matrix solution (4-chloro-a-hydroxycinnamic acid, 5 mg mL^{-1} in 66% acetonitrile, 0.1% TFA). The mixture (1 μL) was spotted directly on a ground steel MALDI target, air dried at room temperature. The mass spectra were acquired in the AutoFlex Max (TOF/TOF) MS (Bruker Daltonics, Bremen, Germany) in the positive ion reflector mode over the mass range of 500-3000 Da. External calibration was performed by employing a peptide mixture (Peptide Calibration Standard II, Bruker). All spectra processing and peptidomics analyses were performed using FlexAnalysis and *Biotools* software (Bruker Daltonics, Bremen, Germany).

For relative semi-quantification, 1,25 μL of 4 μM aqueous angiotensin I solution (Sigma Aldrich) was mixed with 3,75 μL of each sample and mixed 1:1 with matrix solution as described above. The intensity of the angiotensin I signal in the spectra was set at 100%.

3.11. Statiscal analyses

The statistical differences between the pretreated and control samples were analyzed using Paired Sample t-test with significance at $p < 0.05$ using Origin Academic 2020 version. For the AFM surface images the samples were determined as statiscally different from controls by one-way ANOVA with Tukey's test using Origin Academic 2020 version (OriginLab Corporation, Northampton, MA, USA).

4. Results and Discussion

4.1. UV-C light treatment

4.1.1. Fluorescence spectroscopy of the UV-C light pretreated casein micelle

The fluorescence of aromatic amino acids is a well-established method to investigate conformational protein structures, connection of protein subunits, substrate binding, and even denaturation (Chakraborty et al., 2020; Manzocco et al., 2015).

The slight decrease in tryptophan and tyrosine fluorescence emission for α and β-casein (Appendix) may be attributed to a quenching due to the approximation of amino acids such as histidine to tryptophan and tyrosine in the structure of casein (Xu et al., 2020; Lakowics, 2006).

For micellar casein isolate, the intrinsic fluorescence of tyrosine and tryptophan moieties showed a significant decrease after 30 min of exposure to UV-C light, $p<0.05$ (Figure 8). These data suggest that UV-C light treatment promotes changes in the chemical environment of the aromatic amino acids that lead to changes in the configuration of the micelle.

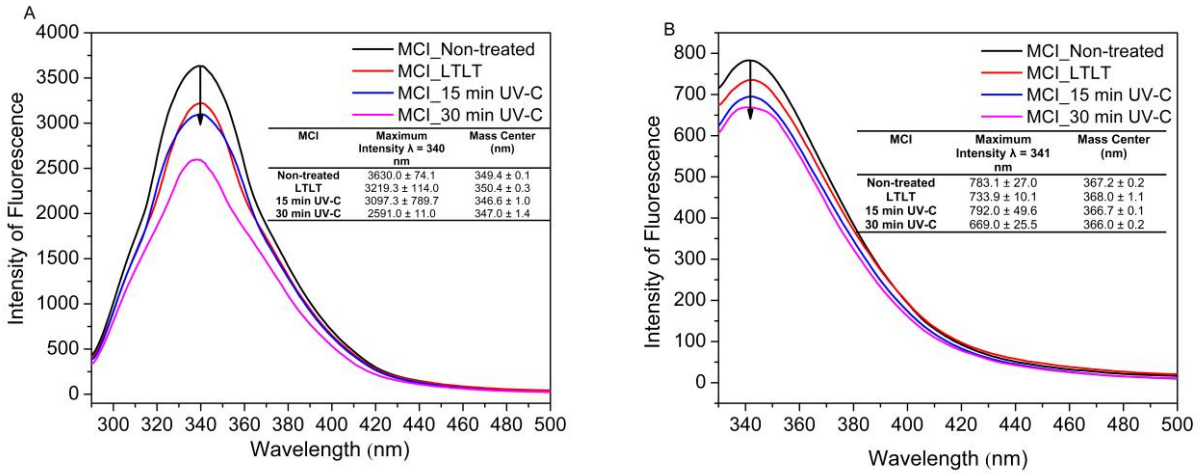

Figure 8 - Fluorescence emission of tyrosine (A) and tryptophan (B) obtained for untreated, ultraviolet light irradiated (UV-C; 3 W m^{-2} for 15 and 30 min), and low-temperature long-time pasteurized low temperature micellar casein (62-64 ° C for 30 min) in simulated milk ultrafiltrate (SMUF).

4.1.2. Assignment of the secondary structure of UV-C light pretreated casein micelle

The light exposure of caseins showed an increase in the absorption band in the amide I region that can be attributed to changes in the secondary structure from the deconvoluted bands (Appendix). Table 1 shows the attribution of the secondary structure of caseins in the region of the amide I band (1600 – 1700 cm^{-1}).

Table 1 - Assignment of secondary structure under native conditions and irradiated with ultraviolet light (UV-C; 3 W m^{-2} for 15 and 30 min), and corresponding to the region of the amide I bands ($\nu \sim 1600 - 1700$ cm^{-1}) for α and β-casein ($n = 3$), in phosphate buffer pD 6.8, I = 160 mM.

Secondary Structure (cm^{-1})	**% of contribution α-casein**			**% of contribution β-casein**		
	Untreated (n = 3)	**UV-C light pretreated 15min (n = 3)**	**UV-C light pretreated 30min (n = 3)**	**Untreated (n = 3)**	**UV-C light pretreated 15min (n = 3)**	**UV-C light pretreated 30min (n = 3)**
β-sheet (1620 ± 20)	44.1 ± 0.4	42.8 ± 2.8	43.1 ± 1.5	37.9 ± 0.7	45.5 ± 1.8*	41.1 ± 0.6*
α-helix (1654 ± 4)	19.5 ± 0.4	14.2 ± 2.6	12.8 ± 0.6*	11.4 ± 2.2	7.7 ± 0.9	31.6 ± 8.2
β-turn (1680 ± 20)	26.7 ± 2.5	31.1 ± 1.3	31.8 ± 0.3	31.3 ± 3.2	32.6 ± 4.2	36.0 ± 4.6
random (1645 ± 5)	27.2 ± 0.7	11.9 ± 1.4*	11.6 ± 1.7*	14.9 ± 0.4	6.8 ± 0.7*	7.6 ± 4.1

*$p<0.05$

α and β-caseins are calcium sensitive and present significant quantities of ordered structures, approximately 50% of residues in β-sheet, α-helix, and β-turn (Hu et al., 2016; Fox and McSweeney, 2003). β-sheet bands are centered around 1620 cm^{-1}. The vibrational bands centered on 1645 and 1654 cm^{-1} are ascribed to random and α-helix secondary structures, respectively. The frequencies centered in 1680 cm^{-1} are associated with β-turn vibrations (Hu et al., 2016). The attribution of secondary structures for light-exposed caseins was obtained by the deconvoluted area of the ATR-FTIR spectra as shown in Table 1.

Exposure to UV-C light induced a significant loss of α-helix and random structure for α-casein 30 min UV-C pretreated. For β-casein an increase in the contribution of β-sheet structure, $p<0.05$, and a significant reduction in the contribution of the random structure was observed for 15 min of β-casein irradiated to UV-C light (Table 1). Furthermore, it was noted a shift in the maximum absorbance of 8 cm^{-1} from native to light exposed for α and β-caseins. The maximum intensity in ATR-FTIR and the shift of wave numbers for α and β-caseins light exposed presented a significant difference compared to native caseins ($p<0.05$) which confirms the secondary structure was modified by UV-C light.

4.1.3. Evaluation of UV-C light pretreated micelle size

Figure 9 shows the average size distribution of micellar casein after 15 and 30 minutes of exposition to UV-C light and for the slow pasteurization process.

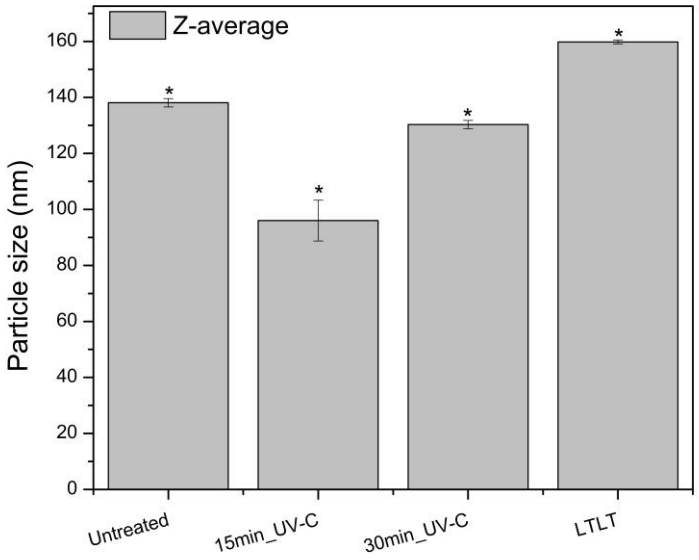

Figure 9 - Particle size distribution obtained for untreated. ultraviolet light irradiated (UV-C; 3 W m^{-2} for 15 and 30 min), and low-temperature long-time pasteurized (62-64 °C for 30 min) micellar casein in simulated milk ultrafiltrate (SMUF).

A significant decrease ($p<0.05$) in the average size of the hydrodynamic diameter of the micellar casein particles is observed from 138.1 to 96.01 and 130.3 nm after 15 and 30 minutes of exposure to UV-C light (Figure 9). The association among caseins is controlled by interactions between hydrophobic regions and electrostatic repulsive interactions that are found in domains of caseins α, β, and κ that define micelle growth (Horne, 1998; Dalgleish et al., 2012). Accordingly, it can be inferred that the solution of micellar casein showed an unbalance in repulsive and electrostatic interactions as a result of modifications in the bond strength of proteins and among caseins. The micelle pretreated with UV-C light showed a decrease in colloidal particle size, as can be observed in Figure 9 (Orlien et al., 2006; Manzocco et al., 2015). The average particle size of the pasteurized micelle increased significantly to 159.8 nm. This can be attributed to the formation of micellar aggregates as a result of the thermal process.

4.1.4. Surface topography of the UV-C light pretreated casein micelle

AFM analyses were conducted to observe the morphology of the micellar casein surface. Figure 10 shows the topography of the micelle after UV-C light exposure.

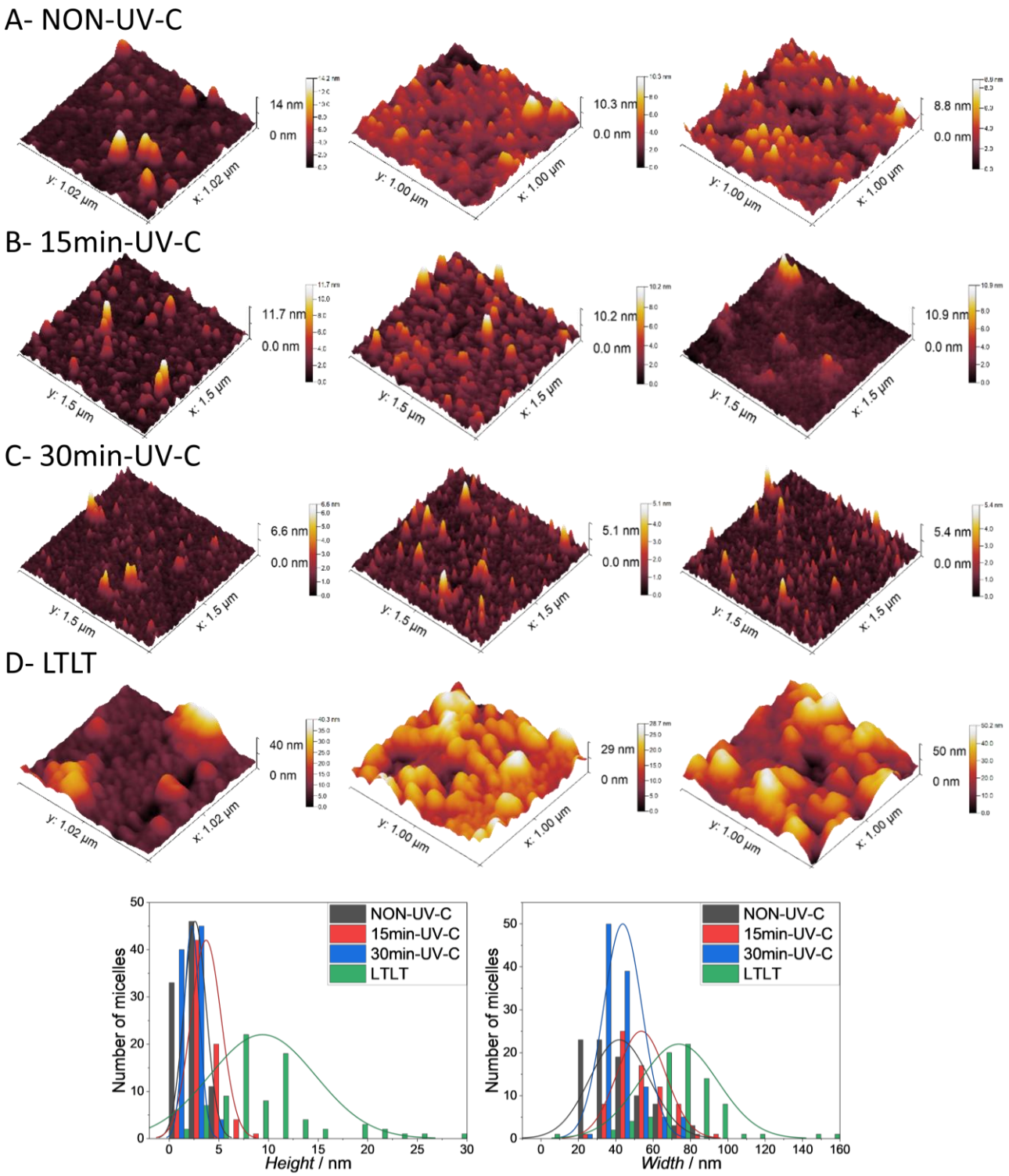

Figure 10 – AFM images of micellar casein isolate in simulated milk ultrafiltrate (SMUF) solutions for untreated (A) UV-C pretreated for 15 min (B), 30 min (C) (light dose of 3 W m^{-2}) and low-temperature long-time pasteurized (62-64 °C for 30 min). The white scale bar is 0.1 µm.

It is observed that the heterogeneous surface of a nontreated micelle agrees with the particle size distribution. Also, the non-irradiated micelle is observed in regions with large aggregates of the micelle.

After 15 and 30 minutes of light exposure, the height and width of the aggregates decrease considerably (Figures 10B and 10C). For micellar casein isolate light exposed can be observed on a rough surface with different sizes of the height and width sizes of aggregates. The descriptive statistical analysis by ANOVA test presented a significant difference in the average width between the non-irradiated micelle and the 15 min irradiated micelle, ($p<0.05$). However, it is easily seen as an uneven surface in Figure 10C has few aggregation regions compared to the untreated micelle 10A. Figure 10D shows the image of micellar casein isolate after the slow pasteurization process. The increase in particle size evaluated by DLS (Figure 10) is observed in the AFM images of the micellar casein isolate (Figure 10D), where there are several regions of micellar aggregates.

The distribution graphs (Figure 10) show exactly what is seen in the AFM images. The micelle treated with ultraviolet-visible (UV-C) light showed small differences in height and width. Only the micelle exposed to 15 minutes of UV-C presented a significant increase in width. The pasteurization distribution graph shows a significant increase in particle size, 9.4 ± 5.3 nm in height and 73.8 ± 20.9 nm of width, compared to untreated micelle, 2.6 ± 1.1 nm of height and 42.0 ± 16.0 nm of width. This increase is due to the temperature used during pasteurization, which allows a rise in the number of collisions between micelles, leading to the formation of aggregates seen in Figure 10D.

4.1.5. Raman spectroscopy of UV-C light pretreated casein micelle

Raman spectroscopy was employed to investigate the structure of the micelle after it was exposed to light. It is a powerful technique for identifying Raman scattering of some regions and for characterizing the secondary structures of proteins. Typical wave numbers are correlated to the secondary structure of proteins for the amide I and amide III regions: tryptophan indole ring at 950 – 990 cm^{-1}, Raman scattering of the phenylalanine ring at 1000 cm^{-1}, β-sheet and α-helix structure are centered at 1270 and 1320 – 1340 cm^{-1} in the amide III bands, respectively, CH_2 bending at 1450 cm^{-1}, Raman scattering of tyrosine at 1614 cm^{-1} and the amide I band is located at 1650 – 1670 cm^{-1} (Rygula et al., 2013, Alinovi et al., 2020).

The bands at 618 and 640 cm^{-1} correspond to Raman scattering of phenylalanine and tyrosine amino acids, respectively (Fig. 11). These resolved peaks for the irradiated micelle indicated changes in the configuration of the casein micelle after exposure to UV-C light. At 850 cm^{-1} is the Raman scattering of the hydroxyl bonding of tyrosine amino acid. The irradiated casein showed a decrease in this region that could be due to a strong hydrogen bond between the OH tyrosyl and negatively charged acceptor as carboxylate ions located near Tyr groups in the primary sequence of caseins as Glu and Asp residues (Navarra et al., 2014).

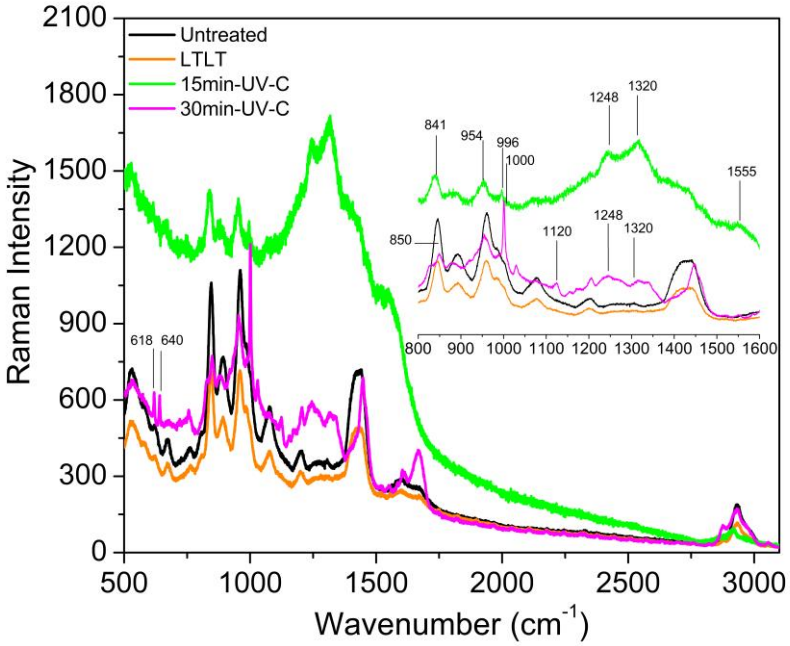

Figure 11 - Raman spectra of micellar casein isolate. UV-C light pretreated solutions in green (3 W m^{-2} for 15 min) and pink (3 W m^{-2} for 30 min), and long-term pasteurized (62-64 °C for 30 min) in simulated milk ultrafiltrate (SMUF) in orange line.

There is a decrease in the intensity of vibrations of tryptophan indole at 950 cm^{-1} for UV-C light pretreated micelle, which suggests the exposition of the aromatic amino acid to solvent. It is observed that a resolved peak at 1000 cm^{-1} corresponds to the breathing of the benzene ring of phenylalanine for the irradiated micelle (green and pink lines), and it is not noted for the nonirradiated micelle (black line).

The bands centered in 1450 and 1663 cm^{-1} are from the binding of CH_2 and α-helix structure of the amide I band. The band at 1120 cm^{-1} is attributed to a C-N bond. The other two bands

centered at 1248 and 1320 cm^{-1} are from β-sheet and α-helix structures, respectively, both from the amide III region. The resolved bands at 1600 and 1668 cm^{-1} correspond to Amide I which shows the exposition to UV-C light led changes in the configuration of casein micelle.

The pasteurized micelle (orange line) did not show changes in the peaks assigned to the micelle structural conformation. However, an increase in the dimensions of particle size was observed after the slow pasteurization process (Figure 9).

4.1.6. Transient absorption spectroscopy of caseins

We first observed that UV-C light irradiation of caseins and micellar casein isolate promotes structural changes in the protein and micelles. The absorption of UV-C light at 255 ± 4 nm of caseins is due to the absorptivity of different amino acids such as tryptophan (Trp), tyrosine (Tyr), phenylalanine (Phe), histidine (His), cysteine (Cys) and cystine (CysCys). Although caseins are chemically composed of more Phe and Tyr than Trp, the contribution of Trp for the fraction of light absorbed by α-casein and β-casein at 255 nm is estimated to be around 0.55, followed by Tyr with approximately 0.33 (Hilario et al., 2017). While for κ-casein, Trp accounts for around 0.23 of the fractions of light absorbed at 255 nm and Tyr for 0.48. Therefore, we could assume that the photochemistry of α-casein and β-casein is primarily related to the photochemistry of the Trp and Tyr residues (Hilario et al., 2017).

Upon light excitation of α-casein, β-casein, and κ-casein at 266 nm (laser power ~ 1.5 mJ cm^{-2} and pulse width 6 ns), a transient electronic absorption spectrum is observed on the microsecond time scale after the laser pulse, Figure 12. For both α-casein, β-casein, and κ-casein, the transient spectrum recorded 0.5 μs after the laser pulse was qualitatively similar and showed an absorption band centered at 340 and 620 nm with a lifetime of 2.9 μs which is typically the absorption spectra for the triplet state of tyrosine, ^{3}Tyr (Figure 12) (Bent and Hayon, 1974). This band can be seen as a result of the relatively low laser power applied for light excitation and the pH of the medium, which does not favor the monophotonic ionization of Tyr through the singlet channel (Clancy and Fobres, 1998). At 535 nm, a typical absorption of the neutral radical, Trp•, originating from monophotonic photoionization of tryptophan can also be observed (t = 2.8 μs) (Müller et al., 2018; Joshi et al., 2002; Tsentalovich et al., 2004). The other expected absorption band centered at 350 nm for Trp• is not clearly seen, as it overlaps with the triplet Tyr band centered at 340 nm. In addition, a broad band centered around 700-720 nm appears and is assigned to the

hydrated electron generated from Trp photoionization (Stevenson et al., 2000; Sherin et al., 2004). This assignment was corroborated with an experiment employing a saturated N_2O solution, which causes the disappearance of this band without affecting the other featured bands since N_2O is a well-known solvated electron. The formation of the hydrated electron was further probed by electron paramagnetic resonance spin trapping experiments using TMPO as the spin-trap. Figure 12 shows the typical EPR spectra recorded for argon-saturated aqueous solutions of α-casein irradiated for 15 min with 266 nm laser pulses of 1.5 mJ cm^{-2} (pulse width 6 ns and repetition rate of 10 Hz) in the presence of TMPO. The EPR spectra (Figure 12) of photoexcitation of caseins in the presence of TMPO are characterized mainly by a nine-line EPR signal with relative intensities of 1:1:2:1:2:1:2:1:1 and Hamiltonian parameters a_N = 1.66 mT and $a_{H\_(2xH\ nucleus)}$ = 2.18 mT, representing the adduct of the hydrated electron with TMPO (Murakami et al., 1989).

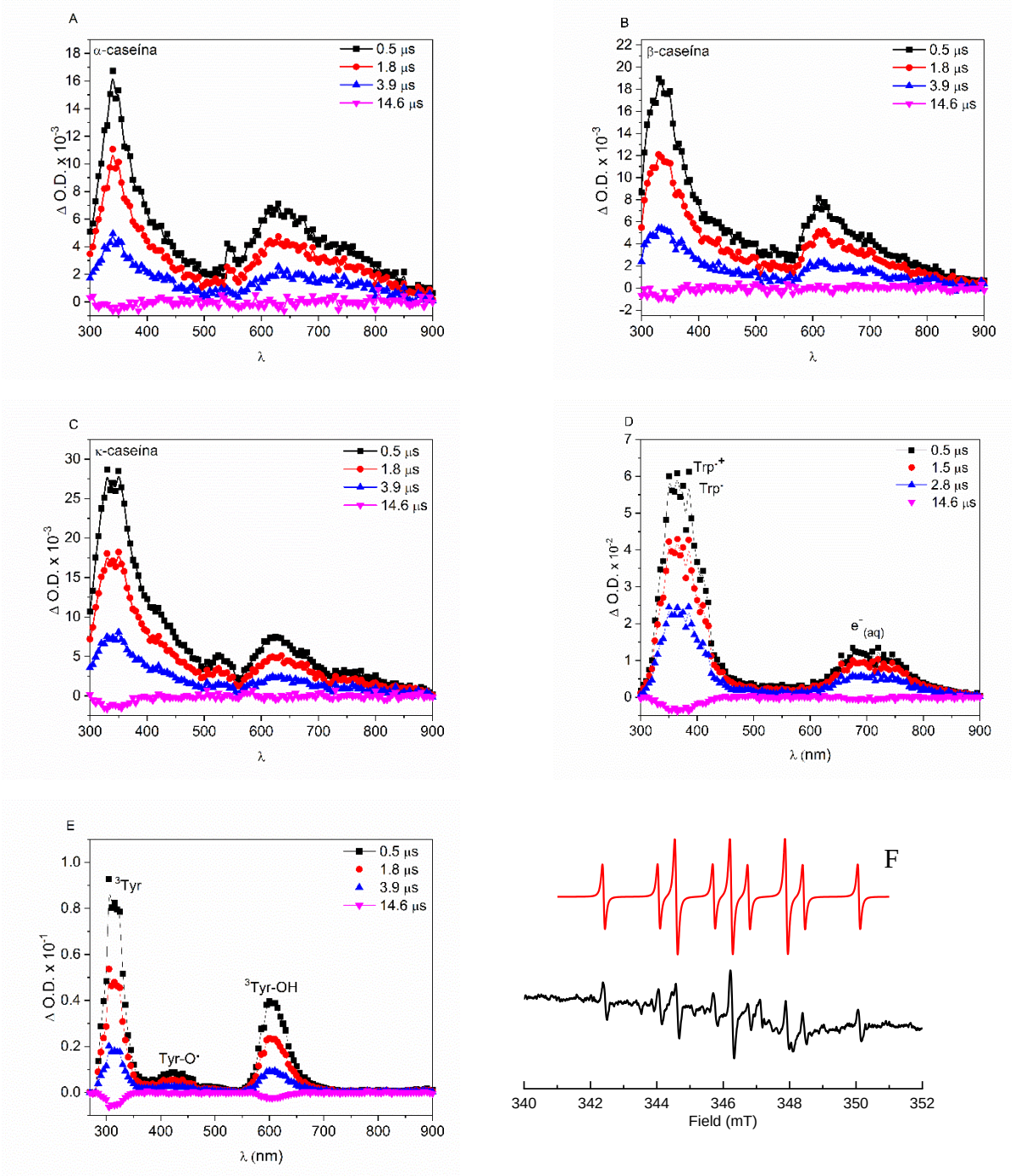

Figure 12 - Transient electronic absorption spectra in phosphate buffer, pH 6.5, I = 160 mM NaCl recorded at different delay times after 266 nm laser pulses of 1.5 mJ cm^{-2} for: A) [α-casein] = 11.8 10^{-6} mol L^{-1}, B) [β-casein] = 29 10^{-6} mol L^{-1}, C) [κ-casein] = 17.0 x 10^{-6} mol L^{-1}, D) [Trp] = 7.1 x 10^{-5} mol L^{-1} and E) [Tyr] = 3.7 x 10^{-4} mol L^{-1}. F) EPR spin-trapping spectrum recorded for argon-saturated aqueous solutions of α-casein irradiated for 15 min with 266 nm laser pulses of 1.5 mJ cm^{-2} (pulse width 6 ns and repetition rate of 10 Hz) in the presence of TMPO (4 10^{-1} mol L^{-1}).

In proteins, electron transfer reactions depend on the proximity of the acceptor and donor group of electrons, the reducing potential for each species, the microenvironment, and the flexibility of the protein structure (Prütz et al., 1982). For caseins, the debate of redox reactions becomes difficult in terms of distance between amino acid moieties, because they do not have a defined tridimensional structure. However, the flexibility of caseins and the presence of tryptophan and tyrosine close in the primary sequence can facilitate the occurrence of electron transfer reactions (Joshi et al., 2002; Jovanovic et al., 1986). In the case of α-casein, the presence of two tryptophan residues in the polypeptide chain, one of them located adjacent to the tyrosine moieties (Trp_{164} - Tyr_{165} - Tyr_{166}) could favor charge transfer (scheme 1) and lead to the formation of the neutral tyrosine radical, $Tyr^{\bullet}$, as observed at 415 nm (Figure 12). Direct electron transfer between the $Trp^{\bullet}$ radical and Tyr-OH has a low bimolecular rate constant due to the small thermodynamic driving force under neutral pH conditions, DG^{o} = -8 kJ mol^{-1} Harriman (1987). However, proton-coupled electron transfer may be facilitated by the interaction of the spatially close amino acid moieties in the polypeptide chain and would pull the overall redox reaction forward. Proton transfer as illustrated in Step I (scheme 1) can greatly favor the redox potential between the tryptophan cation radical and phenoxide ions, in fact, increasing the rate of the redox reaction (Cardoso et al., 2012; Jovanovic et al., 1986; Joshi et al., 2002).

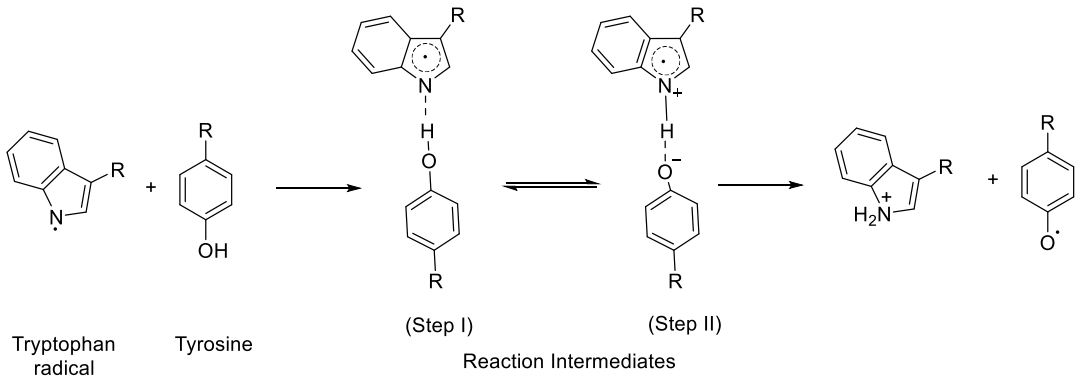

Scheme 1. Illustration of the proton-coupled electron transfer (PCET) mechanism involving electron transfer from the Tyr to Trp moiety in the backbone chain of caseins.

β-casein has one tryptophan residue (Trp_{143}) that is not close to the tyrosine moieties (Tyr_{193}, Tyr_{180}, Tyr_{114}, Tyr80, and Tyr_{60}) in the primary sequence of the protein. This fact may justify the weak band of photoexcited tryptophan, $Trp^{\bullet}$, at 535 nm (Figure 12). In the case of κ-casein, one

tryptophan residue, Trp_{76}, is located near the tyrosine moieties in the primary sequence (Tyr_{61}, Tyr_{60}, and Tyr_{58}).

Tyrosine can also photoeject electrons in a biphotonic process that involves the absorption of a second photon by Tyr in the triplet state leading to the formation of Tyr cation radicals, $Tyr\text{-}OH^{+\bullet}$. However, the triplet channel for photoionization of Tyr is not favored in neutral to acid conditions and at low light intensity, as employed in the present study (Clancy and Fobres, 1998). As for Trp, photoionization may also occur by a biphotonic process; however, at the low laser power employed in our experiments, photoionization of Trp and the triplet-excited-state population is hampered. In this way, on our experimental data and the conditions employed, we may propose the following predominant photoinduced reactions (eq. 1-7) to be occurring during UV-C light treatment of micellar casein isolate. It is important to note that, under aerobic conditions, the fate of the reactive species generated during UV-C light treatment can contribute to induce oxidative stress in the medium, as illustrated by eq. 8-11 and contribute to the oxidative degradation of sensitive amino acids and components.

$$Trp + hv \rightarrow {}^1Trp^* \quad (1)$$

$${}^1Trp^* \rightarrow Trp^{+\bullet} + e^-_{aq} \quad (2)$$

$$Trp^{+\bullet} + Tyr \rightarrow Trp^{+\bullet} + Tyr^{+\bullet} \quad (3)$$

$$Tyr + hv \rightarrow {}^1Tyr^* \quad (4)$$

$${}^1Tyr^* \rightarrow {}^3Tyr^* \quad (5)$$

$${}^3Tyr^* + Trp \rightarrow Tyr + {}^3Trp^* \quad (6)$$

$${}^3Trp^* + hv \rightarrow Trp^{+\bullet} + e^-_{aq} \quad (7)$$

$$Trp^{+\bullet} + O_2 \rightarrow TrpOO^{\bullet} \quad (8)$$

$${}^3Tyr^* + O_2 \rightarrow Tyr + O_2^{-\bullet} \quad (9)$$

$$e^-_{aq} + O_2 \rightarrow O_2^{-\bullet} \quad (10)$$

$$2O_2^{-\bullet} \rightarrow H_2O_2 \quad (11)$$

4.1.7. Qualitative analysis of di-tyrosine in UV-C light pretreated caseins

The random folding and lack of tertiary structure defined in caseins make these proteins more susceptible to oxidative processes. The oxidation reactions in proteins can occur in several ways, like thermal, enzymatic, and photo-oxidation mediated by transition metals in Fenton

reactions. These reactions may lead to cross-linking intramolecular or intermolecular, breaking of covalent bonds, and modifications in amino acids that are easily oxidized, such as methionine, histidine, tryptophan, and tyrosine. The main modifications are the introduction of carbonyl groups and the formation of di-tyrosine from hydroxyl radicals (OH•), peroxyl (ROO•), and tyrosil (TyrO•). (Dalsgaard et al., 2007; Fenaille et al., 2004)

The oxidative process in dairy proteins is an investigative subject among researches, once milk contains macromolecules such as lipids, carbohydrates, and vitamins. The presence of oxygen and light could be a perfect scenario for the investigation of oxidative reactions. Processing and storage of dairy products can result in the formation of carbonyl intermediates from Maillard reactions. The amino acids are oxidized and promote modifications in protein as glycooxidation products (Fenaille et al., 2004). Oxidative damage can affect organoleptic properties and the nutritional value of the products. In addition, damage can affect the digestibility of proteins with adverse health consequences (Lemus et al., 2018).

Qualitative analysis using triple quadrupole mass spectrometry was performed to detect the formation of di-tyrosine in caseins after exposure to light. The synthesis yielded 21% di-tyrosine. It monitored the molecular ion m/z 361.15 and the fragment m/z 315.09 in ion product scan mode (Appendix).

4.1.8. *In vitro* gastric digestion of UV-C light pretreated caseins

When caseins are in an acidic environment, they form a curd. The formation of this curd was observed in our simulated *in vitro* gastric digestion experiments for the elderly, at pH 3.0. Caseins make these curds or aggregations as a result of the attraction of hydrophobic groups near the isoelectric point. During digestion, pepsin cut some of these hydrophobic segments to make the solution clear. (Ono et al., 1998).

Exposure to UV-C light did not promote a significant impact on the structure of caseins. This is reflected in the production of peptides during *in vitro* digestion simulated for the elderly.

However, α-casein exposed to UV-C light released 46 peptides from gastric digestion in comparison to the control and pasteurized process (30 and 36 peptides released, respectively), ($p<0.05$). The peptides were detected and quantified by high-resolution mass spectrometry using angiotensin I as an internal standard. Peptidomics analyses were performed using Biotools software. Among the fragments generated from α-casein RYLGY, RYLGYL and TTMPLW were

identified as bioactive peptides by MBPDB (Milk bioactive peptides data base – Nielsen et al., 2015), both in control and irradiated casein. TTMPLW was identified with oxidative modifications in tryptophan and methionine amino acids as post-translational modifications. RYLGYL is known to be an opioid, antioxidant, antihypertensive, and ACE inhibitor (Rivera et al., 2020). The presence of tyrosine at the end of the N-terminal or in the third position is well defined to characterize RYLGY-derived, RYLGY and RYLGYL, as an opioid peptide (Meisel et al., 1989; Rivera et al., 2020). The antimicrobial activity of the TTMPLW sequence TTMPLW f(209-214) which could be beneficial to control pathogens in the gastrointestinal tract or used as a preservative in the food industry (McClean et al., 2014).

β-casein produced 48 peptides from nonphotolyzed compared to 50 and 45 from photolyzed and pasteurized samples. The IHPFAQTQ sequence released from β-casein was identified in both control and nonirradiated samples. IHPFAQTQ is known to be an inhibitor of prolyl endopeptidase (PEP). The hydrophobic properties of this fragment could facilitate access to the active site of PEP which is associated with psychological disturbances (Meisel et al., 1989; Asano et al., 1992). For micellar casein, 73 peptides were produced from untreated micelle. The photolyzed and pasteurized micelle produced 61 and 66 peptides, respectively. All bioactive peptides identified for β-casein were detected in hydrolyzed micellar casein isolate.

4.1.9. Transport of peptides from UV-C light pretreated casein micelle across caco-2 monolayer using Transwell

The transport of peptides was simulated using a transwell assay in which a monolayer of caco-2 cells is grown for 21 days and the transport experiment takes place. On the 21st day, the epithelial cells are expected to exhibit several properties, such as the formation of tight junction formation, polarity, presence of enzymes and proteins acting as receptors and transport carriers (Ding et al., 2018). Some properties of peptides can influence the type of transport of molecules through epithelial cells, such as hydrophobicity, polarity, and molecular weight. There are several different processes of peptide absorption into the intestine, including active and passive transport. Transcytosis and carrier-mediated transport are the active ones, while transcellular diffusion and the paracellular route are the passive ones. The most common process for permeation of peptides through epithelial cells is the paracellular route. (Ding et al., 2018; Szłapka et al., 2009).

Exposure of caseins to UV-C light did not significantly impact the composition of the amino acid and the number of peptides absorbed by the control and irradiated casein ($p>0.05$). From peptides released from α-casein during digestion, 4 were identified as bioactive peptides, RYLGY, RYLGYL, TTMPLW (W and M oxidation) and TTMPLW (W(2) and M oxidation). The fragment TTMPLW (oxidation of W and M) was only detected in α-casein light exposed, as ACE inhibitor activity (Table 2).

Table 2 - Values of the apparent permeability coefficient of the caco-2 cell monolayer for bioactive peptides released from caseins and micellar casein isolate for 90 min of the transwell bioavailability assay.

m/z	**Sequence**		**Apparent Permeability (cm s^{-1})**		
			C	**I**	**T**
671.270	RYLGY	α-casein	9.4 E-3	5.8 E-2	N.D.
780.0	TTMPLW (M) and (W) oxidation	α-casein	N.D.	2.2 E-1	N.D.
784.368	RYLGYL	α-casein	1.6 E-2	9.1 E-2	N.D.
796.293	TTMPLW (M) and O2(W) oxidation	α-casein	2.4 E-2	9.7 E-2	N.D.
941.524	IHPFAQTQ	β-casein	7.2 E-3	3.7 E-2	N.D.
*From Micellar casein					
671.324	RYLGY	α-casein	1.1 E-2	2.4E-03	N.D.
772.366	SRYPSY	κ-casein	3.8 E-2	N.D.	N.D.
784.440	RYLGYL	α-casein	6.4 E-3	3.2E-03	N.D.
941.524	IHPFAQTQ	β-casein	2.8E-03	N.D.	1.7E-03

Control (C), UV-C light (I), and thermal treatment (T); Non detected (N.D.).

*Peptides produced from the digestion of micellar casein.

The bioactive peptides released after digestion of micellar casein were the same identified from α-casein, RYLGY, RYLGYL, and the fragment IHPFAQTQ from β-casein. In addition, it was detected a peptide with opioid activity from κ-casein, SRYPSY in untreated micellar casein isolate. It is interesting to note that opioid activity, RYLGY, and RYLGYL from α-casein UV-C pretreated were detected in lower concentration than the untreated casein micelle and the peptide SRYPSY from κ-casein was not detected in micellar casein exposed to UV-C light (Table 2). These results may be promising considering the benefits of dairy products as a product with high nutritional value and a lower potential to induce allergic reactions during digestion.

Although the same bioactive peptides identified in the untreated sample were detected in samples of gastric digestion from pasteurized micelle, only the IHPFAQTQ fragment from β-casein was detected after the transport assay. This may be due to the low concentration of production of these peptides, which makes it difficult to be detected in the transport assay.

4.2. Pulsed electric field treatment

4.2.1. Fluorescence of micellar casein PEF-treated

Aromatic amino acid residues present in the structure of the protein, such as tyrosine (Tyr) and tryptophan (Trp), can provide information on changes in the tertiary structure of caseins as a result of the sensitivity to variation of the microenvironment, namely, 10 Tyr and 2 Trp residues in α-casein, 4 Tyr and 1 Trp residues in β-casein, and 9 Tyr and 1 Trp residues in κ-casein.

Caseins lack an ordered structure due to the high content of proline residues that interrupt the formation of α-helix and β-turn structures blocking the protein from reaching a defined tertiary structure (Kumosinski et al., 1991a, 1991b, 1993). Thus, they can position in different conformations depending on the surrounding conditions, such as temperature, pH, and polarity of the solvent.

At RT condition for both 1 and 5 L h^{-1}, a slight decrease in the intensity of emission of tryptophan and tyrosine was observed (Figure 13). This indicates that the temperature led to the unfolding of the micelle structure, exposing the hydrophobic regions to the solvent.

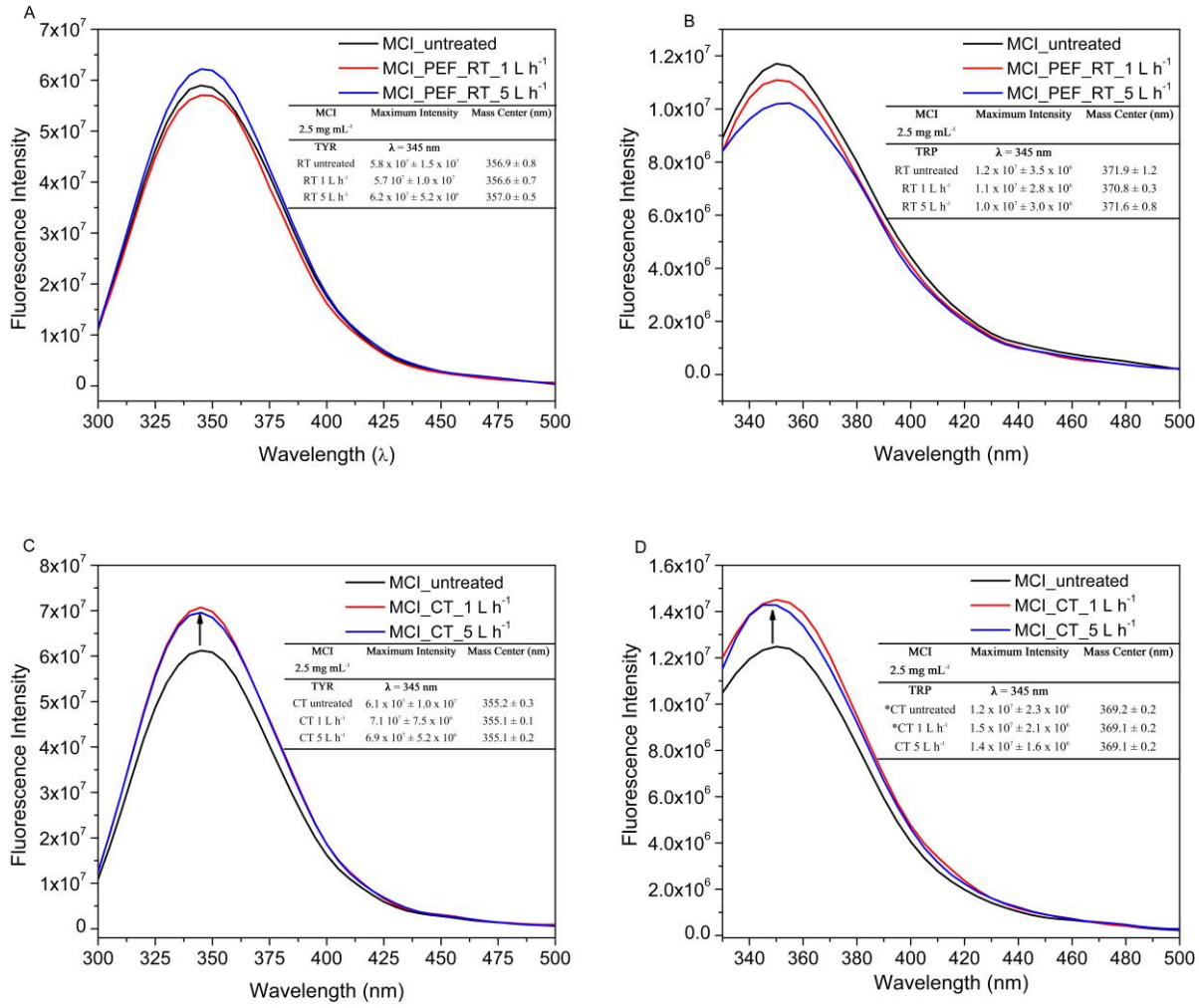

Figure 13 – Fluorescence emission of tyrosine and tryptophan obtained for untreated and micellar casein isolate PEF-treated (16 kV cm^{-1}) at room temperature (RT) A and B, for 31 and 6 µs of residence time at 1 and 5 L h^{-1} corresponding to 84 and 24 kJ L^{-1} and, cold temperature (CT) C and D for 31 and 6 µs of residence time at 1 and 5 L h^{-1} corresponding to 100 and 92 kJ L^{-1}.
*$p < 0.05$ at the confidence level.

For CT samples, an increase in tyrosine and tryptophan emission were observed with a significant difference ($p<0.05$). The increase in the fluorescence emission is characterized by reducing the Trp polarity in the protein microenvironment causing the molecular folding of the micelle structure that may be attributed to the changes induced by the treatment. The same behavior was reported by Xu et al., 2020 from the observation of changes in spatial conformation of caseins due to the application of different ultrasound frequencies (20/40/60 kHz mode).

4.2.2. Assignment of the secondary structure of PEF-treated casein micelle

The mode of action for the electroporation of cellular membranes by PEF has been researched over several decades. The most widely accepted explanation is, that high voltage currents applied to the cell membrane induce polarization of the inner and outer surfaces of the membrane due to charge accumulation (Jeyamkondan et al., 1999; Soltanzadeh et al., 2020). The latter exerts electrocompressive forces on the membrane until the transmembrane potential is exceeded, so that electropermeabilization takes place, leading to pore formation in the stressed and thinned cell membrane. In the case of irreversible electroporation increased cell membrane permeability then causes the death of microorganisms (Jeyamkondan et al., 1999; Middendorf et al., 2021; Soltanzadeh et al., 2020).

Once the micelle is an amphiphilic system, composed of κ-casein in the external layer holding the structure of the micelle, the same principles, i.e., the accumulation of charges, may occur. Thus, there is a possibility that PEF affects the configuration of the micelle, even more, if the short pulses and the voltages applied may modify the structure of caseins.

In Table 3 are the contribution of the secondary structure within the micelle presented for both PEF processing intensities and processing temperature levels. For MCI samples PEF-treated at CT no significant changes with regard to carboxyl group stretching as well as the β-sheet, and β-turn contents were found ($p \geq 0.05$). These changes may be attributed to a small difference in the energy input 100 and 92 kJ L^{-1} in comparison to the untreated MCI sample. However, for RT condition the more pulses applied, 31 and 6 µs, the higher is the temperature gradient as noted by the specific energy input, corresponding to 84 and 24 kJ L^{-1}, which may lead to considerable changes in the MCI structure as observed by the contribution of the secondary structure.

Table 3 – Attribution of the secondary structure of the untreated and PEF-treated casein micelle isolate at room temperature (RT) for 31 and 6 µs of residence time at 1 and 5 L h^{-1} corresponding to 84 and 24 kJ L^{-1} and, cold temperature (CT) for 31 and 6 µs of residence time at 1 and 5 L h^{-1} corresponding to 100 and 92 kJ L^{-1}.

Secondary Structure (cm^{-1})	**% of Contribution**					
	CT_untreated	**CT_1 L h^{-1}**	**CT_5 L h^{-1}**	**RT_untreated**	**RT_1 L h^{-1}**	**RT_5 L h^{-1}**
O-C-O stretching of carboxyl groups (1560-1585±10)	36.7 ± 3.1	39.8 ± 2.9	44.8 ± 4.9	45.8 ± 1.2	34.2 ± 1.8*	42.8 ± 1.1*
β-sheet (1630 ±10)	58.6 ± 0.9	54.2 ± 5.3	52.1 ± 4.6	48.5 ± 2.6	46.8 ± 2.6	54.2 ± 1.2
α-Helix (1650±5)	3.7 ± 3.7	5.0 ± 4.9	1.5 ± 1.5	3.1 ± 3.1	13.6 ± 0.7	4.9 ± 4.9
β-turn (1690±20)	1.0 ± 0.5	1.0 ± 0.5	1.6 ± 0.2	2.6 ± 1.0	2.9 ± 0.5	1.7 ± 0.1

*$p < 0.05$ at the confidence level.

At RT a shift in the secondary structure was indicated for the intense PEF treatment with a 11.6 and 3% smaller contribution in the carboxyl group stretching ($p<0.05$) for 31 and 6 µs treatment time in comparison to the untreated MCI samples. It is noteworthy, that thermal effects occurred in the treatment chamber, that was at its processing limit when the more intense treatment conditions were applied, leading to the formation of aggregates. Floury et al., 2006 observed a reduction in the hydrodynamic volume of the casein micelle PEF-processed (45-55 kV cm^{-1} for 2.1-3.5 µs) that enhanced the coagulation properties of caseins. Another study, Xu et al., 2020 reported remarkable changes on the casein structure also noted by significant differences in the morphology and topography surface of the micelle pretreated by different frequencies power ultrasound (20/40/60 kHz mode). The authors concluded that the alterations on the caseins structure may be a result of the unfolding process due to the modification of the hydrophobic and ionic interactions after the external electric field applied.

4.2.3. Raman spectroscopy of PEF-treated casein micelle

Utilizing several spectroscopic techniques can contribute to in-depth investigation of structural properties in proteins. This approach - including powerful analysis by Raman spectroscopy - allows for improved correlation of the results and to better understand the behavior of proteins subjected to different treatment conditions.

The results of the PEF-treated MCI structure analysis by Raman spectroscopy are summarized in Figure 14. At RT it can be seen, that some regions were affected by PEF, for instance, a loss in resolution of the band centered at 945 cm^{-1} due to the stretching of tryptophan. This may indicate a disorder in the micelle configuration, as presented in the infrared spectroscopy data (Table 3). Furthermore, the decrease in intensity and broadening of the bands centered at 1427 and 1437 cm^{-1} observed in PEF treatments at both intensities which could be attributed to a loss in micelle structure due to the thermal effect during the processing of PEF (Navarra et al., 2014) .

Other important bands attributed to the structure of proteins are centered at 988 and 1001 cm^{-1}, from the spectra of the 31 μs PEF treatment (Figure 14) and correspond to the stretching of tryptophan and the breathing motions of the phenylalanine ring, respectively. These bands also showed an intensity decrease and resolution loss, suggesting that the thermal effect associated with the electric field may induce changes in the micelle configuration, destabilizing the hydrophobic interactions that hold the structure together.

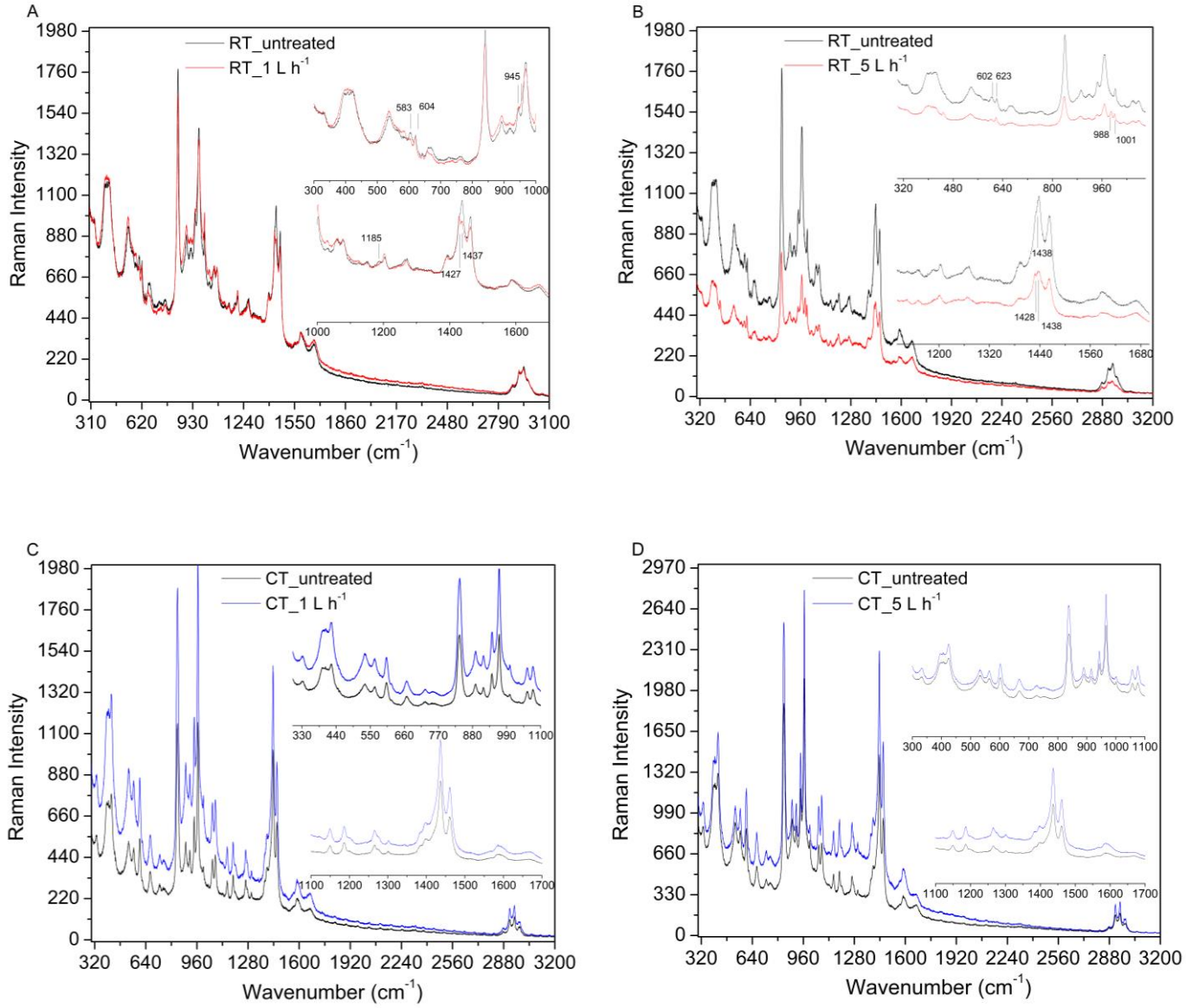

Figure 14 – Raman spectra of the micellar casein isolate obtained after treatment with PEF (16 kV cm^{-1}) at room temperature (RT) for 31 and 6 µs of residence time at 1 and 5 L h^{-1} corresponding to 84 and 24 kJ L^{-1} – A and B and, cold temperature (CT) for 31 and 6 µs of residence time at 1 and 5 L h^{-1} corresponding to 100 and 92 kJ L^{-1} – C and D.

Under CT conditions, the spectra for more (1 L h^{-1}) and less (5 L h^{-1}) intense PEF treatments were observed to be similar in all regions ($p \geq 0.05$). The spectra of the treated micelle show an increase in intensity that can be attributed to the polarization of the aromatic amino acid, stabilizing the structure of the micelle, as seen in the fluorescence spectra (Figure 13). It is known to assume different behavior depending on the pH. With regard to the latter it was reported (Ouanezar et al.,

2012; Rojas-Candelas et al., 2022), that near the net isoelectric point the charge of the micelle approximated zero, the repulsive forces decreased, and large micelle aggregates precicpitated. This is in line with the findings obtained in the presented as the micellar casein exhibited a stable structure even after treatment with PEF. Based on these coinciding results it can be reasoned, that casein micelles reorganize after PEF processing by means of electrostatic/attractive forces, maintaining the micelle configuration at the native pH (6.5).

4.2.4. Evaluation of the size of PEF-treated casein micelle

Heat gradients, that occur in the PEF treatment chamber based on the processing conditions applied, were used to evaluate possible temperature effects on the structure of the micelle. Thus, for the RT condition, a difference in temperature in and outflow of the treatment chamber of 13.6 °C at 1 L h^{-1} and 6.6 °C at 5 L h^{-1}. Figure 15 shows a slight increase in particle size in strong treatment, which may be due to the increase in the temperature outlet of the PEF chamber.

As indicated in Figure 15 no significant differences in particle size distribution between untreated MCI samples and those treated at different PEF intensities at either CT or RT, suggesting that the structure of the micellar casein remained unaffected following PEF treatment. Moreover, this also suggests that the raised processing temperature had no impact on the micellar structure due to the higher heat gradients obtained during processing for the more intense PEF treatments, accounting for 9.4 and 7.0 °C higher temperatures than for samples subjecting to milder PEF conditions at CT and RT, respectively.

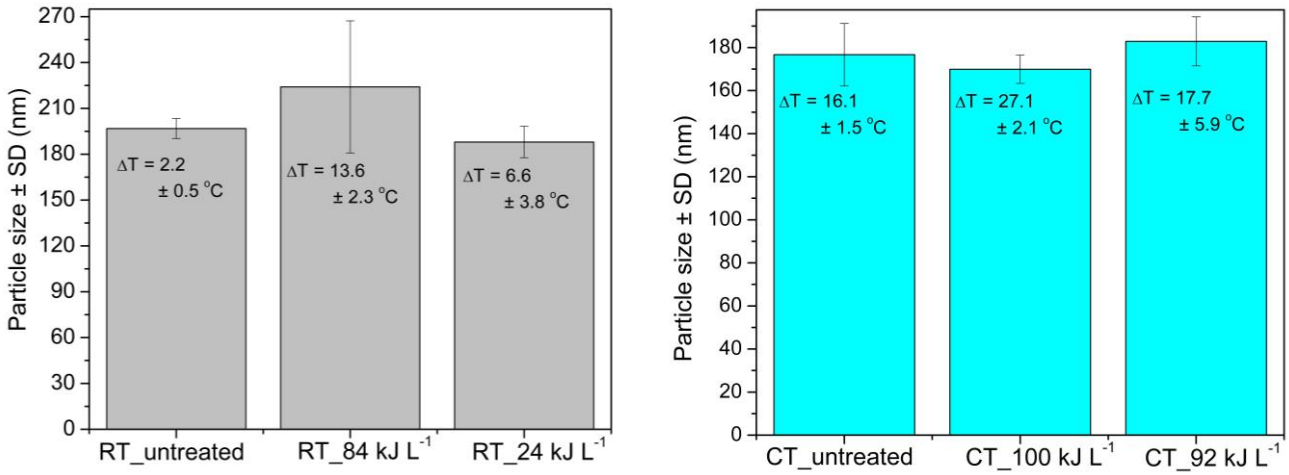

Figure 15 - Particle size of the micellar casein isolate obtained after treatment with PEF (16 kV cm^{-1}) at room temperature (RT) for 31 and 6 µs of residence time at 1 and 5 L h^{-1} corresponding to 84 and 24 kJ L^{-1} and, cold temperature (CT) for 31 and 6 µs of residence time at 1 and 5 L h^{-1} corresponding to 100 and 92 kJ L^{-1}.

However, an occasional formation of aggregates was observed at the intense PEF settings, where the system was operated at its limit for the given product and treatment chamber, causing blockages in the treatment chamber and consequently, interrupting the process, and exiting the treatment chamber particularly during cleaning cycles. The high standard deviations at the most challenging PEF processing conditions (RT, 84 kJ L^{-1}) can be attributed to the formation of clotted particles inside the treatment chamber, which affected the sample analysis by dynamic light scattering adversely, and that, otherwise, could have indicated a PEF-based effect on the micellar structure. While there is no statistical evidence, in addition to the much larger standard deviations, the elevated mean compared to the other means, visible clot formation, and the much higher product temperature of 44°C at the chamber outlet should also be taken into account, which all point to a heat- and PEF-based effect on the structure of MCI.

Albeit a higher increase in the temperature gradient was detected following MCI treatment with PEF under CT conditions, the product temperature at the chamber exit remained below 30°C in contrast to that under RT conditions also processed at 16 kV cm^{-1} for 31 µs. A possible explanation could be, that a certain temperature level needs to be reached in order to initiate these reactions which lead to the formation of aggregates and thus, this could be valuable information

with regard to industrial application of PEF for casein-based food products. Changes in micelle particle size were already described as a reversible process after overnight storage at 4°C (Sharma, et al., 2014; Hemar et al., 2011). In contrast, Shamsi (2008), reported was not observed significant differences in micelle size, $p>0.05$, even employing a relatively high electric field of 35 kV cm^{-1} (30 °C) and 38 kV cm^{-1} (60 °C), in 19.2 µs treatment time and the total specific energy input for both treatments as 154 kJ L^{-1}.

4.2.5. Evaluation of the degree of hydrolysis of PEF-treated casein micelle

The investigation of the extent of hydrolysis showed an increase for MCI samples PEF-treated at milder RT conditions, suggesting that the heat dissipation into the product during PEF led to the exposure of cleavage sites that promote digestion (Figure 16). These results are consistent with FTIR spectroscopy data, exhibiting a loss in stretching of carboxyl groups (as previously presented in Figure 13 and Table 3). Furthermore, it can be speculated that the afore-mentioned thermal effect occurring during PEF treatment at RT and indicating a higher reactivity, in addition to its charge accumulation effect, may explain changes in the spatial configuration of the micelle (Figure 14), disrupting hydrophobic interactions, and enlarging the surface area for the cleaving of peptide bonds (Xu et al., 2020).

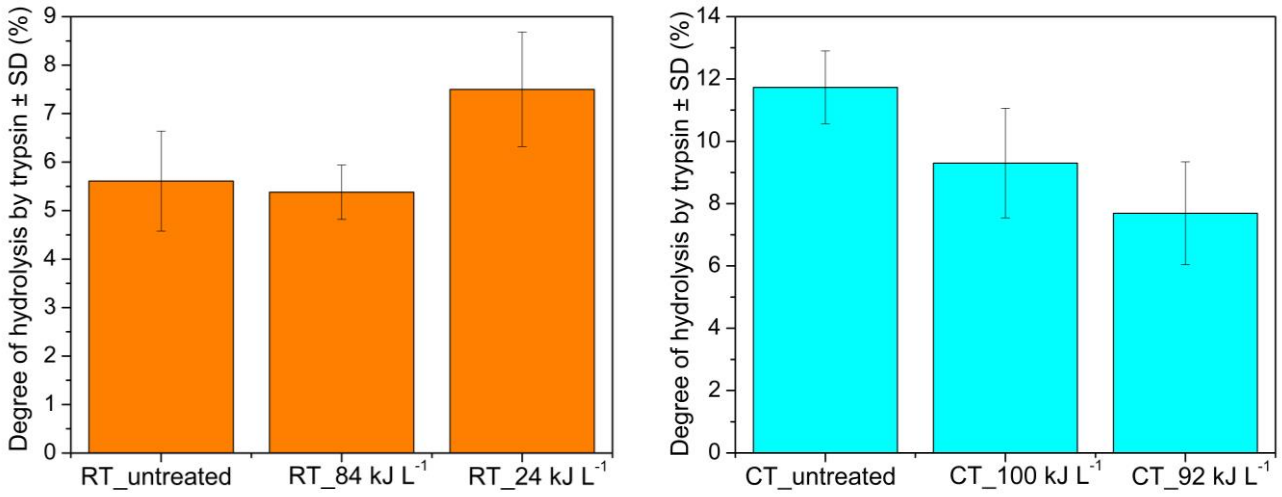

Figure 16 – Degree of hydrolysis of the micellar casein isolate obtained after treatment with PEF (16 kV cm^{-1}) at room temperature (RT) for 31 and 6 µs of residence time at 1 and 5 L h^{-1} corresponding to 84 and 24 kJ L^{-1} and, cold temperature (CT) for 31 and 6 µs of residence time at 1 and 5 L h^{-1} corresponding to 100 and 92 kJ L^{-1}.

However, the decrease in the degree of hydrolysis at CT from the untreated to the mildly PEF-treated MCI samples might be associated with the difficulty of the enzyme to reach the cleavage sites after PEF treatment (Figure 16). These findings are in agreement with the previously discussed fluorescence data for tryptophan and tyrosine, suggesting a micelle folding process. At CT the micelle was subjected to an electric effect, because small changes in the configuration occurred.

4.2.6. Topography of the surface of the PEF-treated casein micelle

Few works in the literature use the versatility of image techniques to characterize the micelle at the nano and molecular levels. In this work, the AFM technique was used to investigate the nanostructure and the topography of untreated micelles and those of PEF-treated micelles at both RT and CT levels, shown in Figure 17.

At RT solitary peaks of large aggregates between 8.2 and 14 nm were detected in native casein micelles (Figure 17A). By contrast, a less uniform and consequently uneven surface, characterized by the appearance of smaller aggregate peaks over a larger area, was observed after MCI samples were exposed to PEF. Possible explanations for these changes, that were registered for the both PEF treatment intensities, might be the occurrence of a structure-altering forces or a reconfiguration of the different casein's fractions within the micelle due to possible charge effects brought by PEF in combination with heating effects. It is worth mentioning though, that a less uneven surface formation with fewer peaks was obtained after more intense processing with PEF.

Due to the occurrence of protein aggregation and clotting at the more intense PEF treatment conditions, a possible loss of micelle content may have taken place based on protein build-up and blockage in the PEF treatment chamber and, thus, not present in samples analyzed by AFM subsequently. This could explain the overall lower spread of peaks than for the milder PEF treatment, whereas it is also a possibility that a higher heat gradient and temperature level may have allowed for enough reactivity and conformational changes to create a more uniform surface profile. Both reasonings could explain the more than doubled number relatively small 3 nm micellar structures after more intense exposure to PEF and heating in comparison to the native and mildly PEF-treated samples, and the more than 50% higher content of 6 nm micellar structures for the mildly PEF-treated samples than for native and intensely PEF-treated samples. The absence of taller than 9 nm structures for the latter and above 12 nm for the untreated samples also

demonstrates that the surface topography between the native and the two PEF-treated MCI samples differed significantly from each other at RT. In a similar manner for the width of the micellar structures in the lower range between 20 and 60 nm structures of the more intensely PEF-processed MCI dominated and were overall spread from 20 to 200 nm, while the MCI samples subjected to milder PEF extended only in the range from 60 to 180 nm and showed the highest number in micellar structures between 100 and 140 nm of width. In addition, the range of untreated MCI samples was from 20 to 160 nm with consistenly lower numbers than either the more intensely or the milder PEF-treated MCI samples, also emphasizing the structural differences in the surface profiles. With a more pronounced roughness level of the surface more contact between the enzyme and the substrates is enabled, also expressed by the degree of hydrolysis (Figure 16) and differences in the extent of loose structures (Table 3 and Figure 14) (Xu et al., 2020).

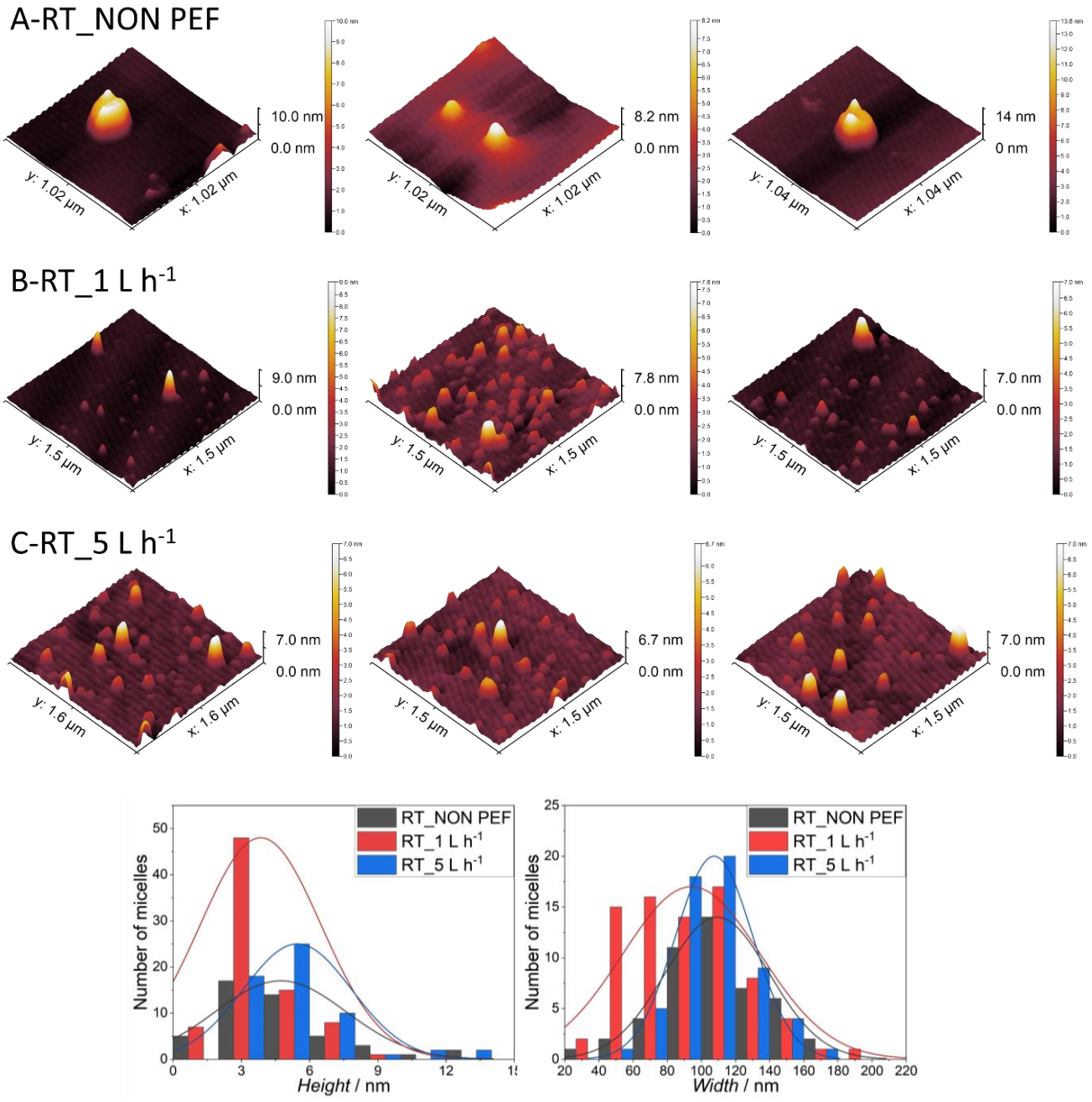

Figure 17 - AFM images of micellar casein at room temperature (RT) for 31 and 6 µs of residence time at 1 and 5 L h^{-1} corresponding to 84 and 24 kJ L^{-1}.

At CT less volatility in the peak formation and spreading area on the surface as well as structures height and width were observed (Figure 18) in comparison to the MCI samples untreated or processed with PEF at RT (Figure 17). Unlike the findings obtained for RT, PEF induced little formation of small peaks at CT, thus, making it more difficult to spot significant differences

between the three-dimensional topographic diagrams of untreated as well as milder and more intense PEF processing of the MCI samples.

The more overlapping maximum height ranges for peaks between 7.3 and 13.0 nm for untreated and more intensely PEF-processed samples contrast with those of the mildy PEF-processed MCI ranging from 4.2 to 7.6 nm, with the latter barely overlapping with the maximum peak range of untreated PEF-treated samples. A possible reason for this could be the smaller temperature gradients and overall lower PEF chamber exit temperatures when processing at CT. However, the micellar structure distribution graphs also showed differences depending on the PEF treatment intensity in height and width at CT. While around 3 to 4 nm height the number of milder PEF-treated micelle structures had a maximum, both the untreated (to a slightly higher number) and intensely PEF-treated had their maxima in the number of casein micelle structures at around 6nm height. However, with regard to width distribution the maxima of all samples were closer together between 110 and 125 nm, indicating more structural similarities between native and PEF-processed MCI. This faster climb and more rapid decline in height, resulting in a smaller spread for the milder PEF-treated MCI samples contrasts those of the untreated and intensely PEF-treated samples, both offering wider distribution curves and height spreads.

These larger differences for the milder PEF-treated coincided with the above-mentioned findings at RT, representing a more reactive environment that led noticeable discrepancies in distributions of both height and width. Overall, these surface topography data and distribution graphs are in agreement with the micelle folding process discussed earlier in this work for the fluorescence data (Figure 13), suggesting that the micelle at colder processing conditions were affected by the electric field, which induced a lower spread in height and width distribution and small differences for number of micellar structures. As a consequence of hydrophobic groups were hidden, resulting in the formation of more compacted micelle aggregates (Figure 18).

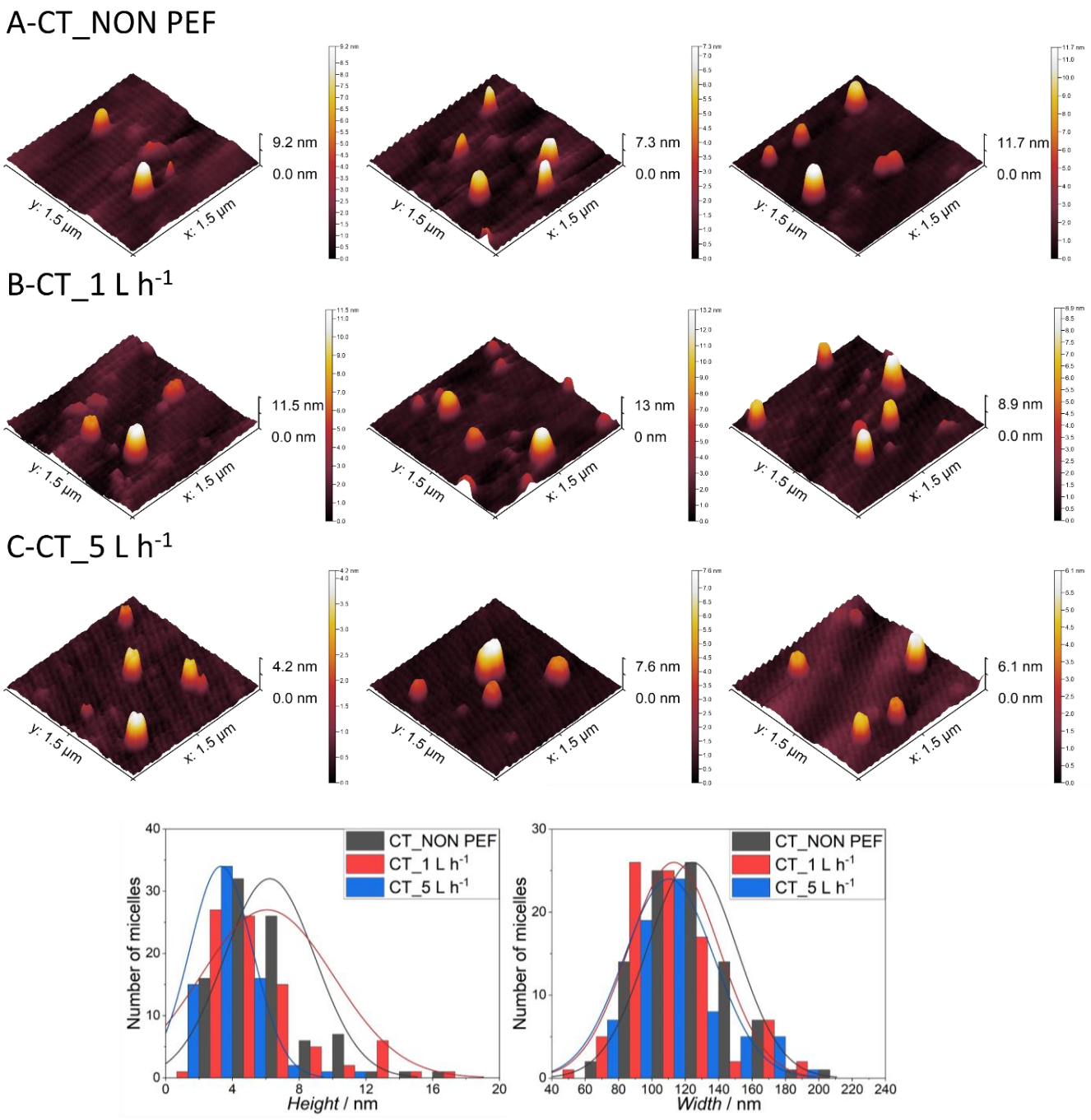

Figure 18 - AFM images of micellar casein at cold temperature (CT) for 31 and 6 µs of residence time at 1 and 5 L h^{-1} corresponding to 100 and 92 kJ L^{-1}.

4.2.7. *In vitro* gastric digestion followed the transport of peptides from PEF-treated casein micelle across caco-2 monolayer using Transwell.

Aging is accompanied by many alterations in metabolic processes in the organism that directly affect the quality of life of the majority of the population. Sarcopenia, which may be the result of inadequate nutrient intake characterized by loss of muscle mass and strength, is one of the challenges in older adults and is also related to reduced appetite and other alterations in metabolic function (Aalaei et al., 2021). In this study we adopted a model of transepithelial transport to mimic the structure and functions of the human intestinal epithelium. All peptides released from gastric digestion were sequenced, and their sequence and permeability through the transport assay can be accessed in the appendix.

The number of peptides generated from the processing of PEF at room temperature did not show significant differences from those of untreated micellar casein (untreated: 72 vs. mildly PEF-treated: 85 vs. intensely PEF-treated: 77; $p \geq 0.05$). However, the bioactive peptide $RELEEL_{f(16-21)}$ from β-casein, at m/z 787.418, was detected particularly in micellar casein PEF processed at both intensities and the concentration of f (16-21) in gastric digestion and the amount transported by the transport assay is presented in Figure 19. The presence of three aromatic amino acids in $RELEEL_{f\ (16-21)}$ contributes to antioxidant activity due to the proton in the carboxyl group on the side chain of glutamic acid (Liu et al., 2020).

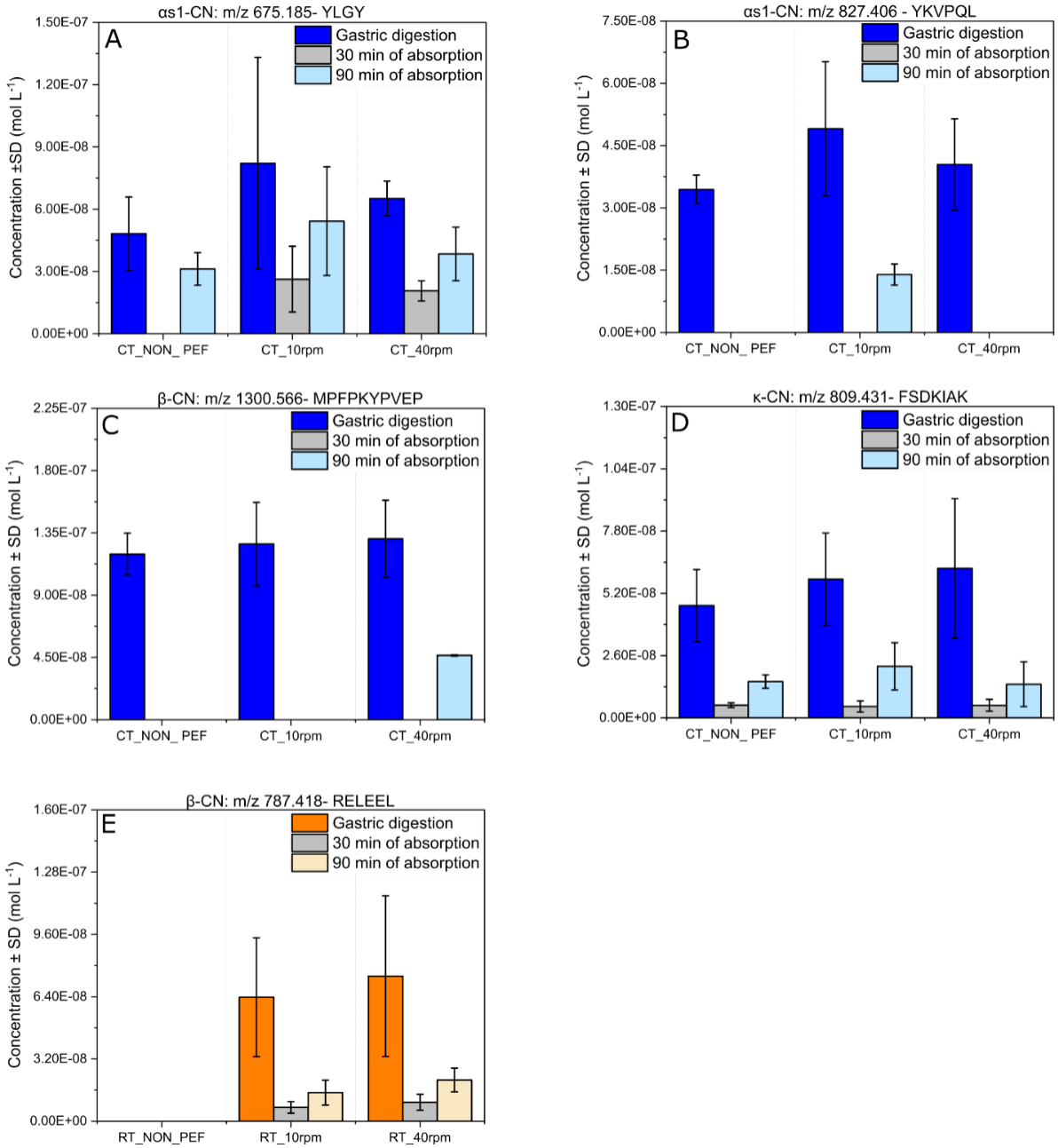

Figure 19 – Relative concentration for the bioactive peptides generated from micellar casein isolate pretreated PEF from gastric digestion and followed by caco-2 cell uptake; cold temperature (A-D): A- α_{s1}-CN YLGY; B- α_{s1}-CN YKVPQL; C- β-CN MPFPKYPVEP; D- κ-CN FSDKIAK ; room temperature E- β-CN RELEEL.

Previous studies reported that the characteristics of bioactive peptides, such as molecular weight, hydrophobicity, and charge property, determine transepithelial transport (Wang and Li, 2018; Yang et al., 2019). (Wang and Li, 2018) reported that positively charged and more hydrophobic casein peptides are preferably transported by an active process mediated by PepT1, a

proton-coupled membrane transporter, and the paracellular route, the passive route. As indicated in Figure 6E, the relatively low bioavailability of RELEEL$_{f\ (16-21)}$ after 90 min for cell uptake that did not differ significantly in PEF-treated samples at RT, may have occured due to the active process involved in the caco-2 monolayer, which was not monitored in these assays.

At cold processing conditions, PEF produced a larger amount of peptides compared to the untreated samples (untreated: 104 vs. mild PEF: 99- vs. intense PEF: 99). Among the samples investigated four bioactive peptides were detected (Figure 19A-D). Regarding the four bioactive peptides detected, f(106-109) and f(119-124) originated from α_{s1}-casein, f(124-133) created from β-casein, and f (31-45) formed from κ-casein, all of them was ascribed to ACE-inhibitory activity (Amigo et al., 2020; Hayes et al., 2007; López-Expósito et al., 2007). YLGY$_{f(106-109)}$ was identified with phosphorylated tyrosine and is described as a RYLGY-derived peptide that presents antioxidant activity and is known as an opioid peptide (Amigo et al., 2020; Sánchez-Rivera et al., 2020). The sequence FSDKIAK$_{f\ (31-45)}$ from κ-casein was also reported (López-Expósito et al., 2007) to exhibit antimicrobial activity. Large quantities of the YLGY sequence, originating from α_{s1}-casein, were observed in samples processed with PEF and transported to the monolayer of caco2 cells for both PEF processing intensities ($p \geq 0.05$) within 90 min of absorption time.

On the contrary, the sequences YKVPQL$_{f(119-124)}$ from α_{s1}-casein, MPFPKYPVEP$_{f(124-133)}$ from β-casein and FSDKIAK$_{f(31-45)}$ from κ-casein were detected in high concentrations in gastric digestion, but showed lower peptide uptake by caco-2 cells after 90 minutes of transport from the apical site to the basolateral chamber. In the case of YKVPQL$_{f\ (119-124)}$ production from α_{s1}-casein following similar concentrations obtained after gastric digestion only for the higher intensity PEF a transport that led to a noticeable adsorption within a 90 min time period was obtained, while for untreated and lower intensity PEF no uptake was registered under the same adsorption conditions most likely due to longer transportation times. The reversed trend was determined for MPFPKYPVEP$_{f(124-133)}$, where lower intensity PEF led to a noticeable uptake in contrast to that of untreated and higher intensity PEF samples within 90 min of absorption time. For FSDKIAK$_{f(31-45)}$ no significant differences were found between the untreated and both PEF-treated MCI samples for gastric digestion and subsequent peptide transport. The peptides from α- and β-casein were identified with post-translational modification of phosphorylation in residues of tyrosine and oxidation in methionine for MPFPKYPVEP.

5. Conclusion

Emerging technologies such as UV-C light and PEF showed their potential to be used as nonthermal treatments to modify proteins in dairy products, in the food industry. α, β and κ-casein presented slightly changes in the protein structure after light exposition. α-casein showed significant decrease in the contribution of α-helix and random structure, both after 30 min of exposure to light and, a significant increase in the random structure for β-casein after 15 and 30 min of UV-C light treatment. In addition, a significant difference ($p<0.05$) in the wave number shift of the maximum absorbance, 8 and 7 cm^{-1} for α and β-casein light exposed indicated structural modifications induced by light exposure. Micellar casein presented a significant reduction in particle size ($p<0.05$), after 15 minutes of exposure to UV-C light, from 138.1 to 96.0 nm. Unlikely, thermal treatment, LTLT, generated large micellar aggregates, increasing the particle size to 159.8 nm ($p<0.05$), which is under the topography of the micelle surface in the AFM images.

Raman spectroscopy showed spectral differences only for the micellar casein light exposed suggesting modifications in the structure of the casein micelle. The transient absorption indicated that the photochemical reaction can occur through electron transfer coupled with a proton transfer from tyrosine to tryptophan. In this sense, no significant impact on the production of peptides for micellar casein that simulates *in vitro* gastric digestion for older adults. The transport of peptides by caco-2 cells did not change significantly in the number of peptides absorbed. However, the opioid peptides RYLGY and RYLGYL released from α-casein UV-C pretreated were detected in lower concentration than native casein micelle and, SRYPSY released from κ-casein UV-C pretreated was not detected after the transportation across caco-2 cell monolayer.

For PEF treatments, fluorescence spectroscopy at RT condition presented a slightly decrease in the tryptophan and tyrosine emission. In contrast at CT condition, the fluorescence of both amino acids showed a reduction in the polarity that may be attributed to the higher specific energy input in comparison to untreated MCI. The findings for the contribution of the secondary structure, at CT condition, did not show significant changes for the mildly and intensely PEF-treated MCI sample. However, for the intense PEF-treated at RT condition a smaller contribution in the carboxyl group stretching was obtained in comparison to untreated MCI sample.

Raman spectroscopy indicated similar changes in MCI regardless of PEF intensity compared to untreated samples at CT, while untreated and intensely PEF-treated MCI showed no significance difference in contrast to mildly PEF-treated MCI for which the data differed

considerably form that of untreated MCI and emphasizing the higher reactivity in a higher temperature environment.

Moreover, particle size distribution was not found to change between native, and PEF-treated MCI at either intensity. However, an impact of PEF was determined the degree of trypsin hydrolysis, which was highest for untreated MCI and the lowest for the milder PEF processing conditions at CT, whereas at RT the opposite trend was observed. The topography of the surface of micellar casein structures was modified by the use of PEF more substantially when applied at RT than at CT, with again PEF at lower intensity altering the structure of micelles with a greater impact that led to a rougher surface profile than at higher intensity.

Analysis of gastric digestion and peptide transport showed, that milder PEF generally improved the uptake of bioactive peptides over untreated MCI, especially, absorption of $FSDKIAK_{f(31-45)}$ and $MPFPKYPVEP_{f(124-133)}$ using lower and higher processing intensities at CT, respectively. Application of PEF led to a concurrent heating gradient and a thermal effect that also affected the findings.

Based on the findings obtained in this study, it can be concluded that UV-C light was efficient to induce modifications in the structure of micellar casein and, promote peptides with lower potential to induce allergic reactions during digestion for older adults. Also, PEF treatments in combination with heat dissipation affected the structure of micelles substantially, which should be taken into account in order to tailor PEF for processing of casein-based products at commercial scale. Modifications caused in micellar casein were shown to be efficient in generating bioactive peptides and suggesting great potential of PEF to contribute in the production of casein-based food with enhanced nutritional value for elderly suffering from impaired uptake.,

6. Final Remarks

The main objective of this work was to investigate physicochemical modifications in the micellar structure after both UV-C light, and PEF. Furthermore, the released evaluation of the peptide profile was carried out after *in vitro* digestion that simulates the gastric conditions of older adults and the uptake of peptide were monitored by transport assay using caco-2 cells as a model of intestine epithelium cell absorption.

Although UV-C light and PEF showed their potential to improve nutritional properties in micellar casein, more information and experimentation are still needed to ensure the efficacy of both technologies to be applied on a large scale.

For UV-C treatment, several parameters should be taken into account, such as the light geometry, treatment area, and the turbidity level of the milk could influence the treatment efficiency. Additionally, experiments such as microbial count it is an interesting factor to study to guarantee the safe and the shelf-life of the product.

Lastly, for PEF treatment, parameters such as the solid composition of milk could influence the treatment, leading to arcing formation in the PEF chamber interrupting the process. In addition, the temperature should be monitored to avoid undesirable thermal effects during the process, and the insulator geometry is an important aspect to study to provide the best homogeneous electric field that assurance equal treatment for the whole sample.

Both treatments, UV-C light, and PEF have proven to be great alternatives to thermal processing in the food industry due to the slight modifications induced in the micellar structure that were precisely described in this dissertation. Moreover, the bioactive peptides detected in the treated micelles from UV-C light and PEF treatments, indicated the potential of these techniques to raise the nutritional properties of dairy products in the food industry.

7. References

AALAEI, K., KHAKIMOV, B., DE GOBBA, C. AHRNÉ, L. Digestion patterns of proteins in pasteurized and ultra-high temperature milk using in vitro gastric models of adult and elderly. **J. Food Eng.**, Oxon, v. 292, p. 110305, 2021.

AGOUA, R. S., BAZINET, L., THIBODEAU, J., VOROBIEV, E., GRIMI, N., MYKHAYLIN, S. High voltage electrical treatments can eco-efficiently promote the production of high added value peptides during chymotyptic hydrolysis of β-lactoglobulin. **Food Biosci.**, Amsterdam, v. 47, 2022.

ALINOVI, M., MUCCHETI, G., ANDERSEN, E., ROVERS, T. A. M., MIKKELSEN, B., WIKING, L., CORREDIG, M. Applicability of confocal Raman microscopy to observe microstructural modifications of cream cheeses as influenced by freezing. **Foods**, Basel, v. 9, p. 679, 2020.

AMIGO, L., MARTÍNEZ-MAQUEDA, D., HERNÁNDEZ-LEDESMA, B. In sílico and *in vitro* analysis of multifunctionality of animal food-derived peptides. **Foods**, Basel, v.9, p.991, 2020.

ASANO, M., NIO, N., ARIYOSHI, Y. Inhibition of prolyl endopeptidase by synthetic β-casein and their derivatives with a C-terminal prolinol or prolinal. **Biosci. Biotechnol. Biochem.**, Oxford, v. 56, p. 976-977, 1992.

AWUAH, G. B., RAMASWAMY, H. S., ECONOMIDES, A. Thermal processing and quality: principles and overview. **Chem. Eng. Process.**, Lausanne, v. 46, p. 584-602, 2007.

BENDICHO, S., CÁNOVAS, G. V. B., MARTÍN, O. Milk processing by high intensity pulsed electric fields. **Trends Food Sci. Technol.**, London, v. 13 p. 195–204, 2002.

BENT, D. V., HAYON, E. Excited state chemistry of aromatic amino acids and related peptides. I. Tyrosine. **J. Am. Chem. Soc.**, Washington, v. 97, p. 2599-2606, 1975.

CADESKY, L., WALKLING-RIBEIRO, M., KRINER, K. T., KARWE, M. V., MORARU, C. Structural changes induced by high-pressure processing in micellar casein and milk concentrates. **J. Dairy. Sci.**, New York, v. 100, p. 7055-7070, 2016.

CALVANO, C. D., MONOPOLI, A., LOIZZO, P., FACCIA, M., ZAMBONIN, C. Proteomic approach based on MALDI-TOF MS to detect powerdered milk in fresh cow's milk. **J. Agric. Food Chem.**, Washington, v. 61, p. 1609-1617, 2013.

CARDOSO, D. R., LIBARDI, S. H., SKIBSTED, L. H. Riboflavin as a photosensitizer. effects on human health and food quality. **Food Funct.**, Cambridge, v.5, p. 1-10, 2012.

CLANCY, C. M. R. and FORBES, M. D. Time-resolved electron paramagnetic resonance study of photoionization of tyrosine anion in aqueous solution. **Photochem. and Photobiol.**, Hoboken, v.69, p. 16-21, 1998

DALGLEISH, D. G. and CORREDIG, M. The structure of the casein micelle of milk and its changes during processing. **Annu. Rev. Food Sci. Technol.**, Palo Alto, v. 3, p. 449-467, 2012.

DELORME, M. M., GUIMARÃES, J. T., COUTINHO, N. M., BALTHAZAR, C. F., ROCHA, R. S., SILVA, R., MARGALHO, L. P., PIMENTEL, T. C., SILVA, M. C., FREITAS, M. Q., GRANATO, D., SANT'ANA, A. S., DUART, M. C. K. H., CRUZ, A. G. Ultraviolet radiation: an interesting technology to preserve quality and safety of milk and dairy foods. **Trends Food Sci. Technol.**, London, v. 102, p. 146-154, 2020

DING, L., WANG, L., ZHANG, T., YU, Z., LIU, J. Hydrolysis and transepithelial transport of two corn gluten derived bioactive peptides in human caco-2 cell monolayers. **Food Res. Int.**, Amsterdam, v. 106, p. 475-480, 2018.

EFSA Panel on Dietetic Products. Safety of UV-treated milk as a novel food pursuant to regulation (EC) No. 258/97. **EFSA Journal**, Hoboken, v.14(1), 4370, 2016.

FAUSTER, T.; OSTERMEIER, R.; SCHEIBELBERGER, R.; JÄGER, H. Pulsed electric field (PEF) application in the potato industry. **Innov. Food Process. Technol.**, New York, p. 253–270, 2021.

FLOURY, J., GROSSET, N., LECONTE, N., PASCO, M., MADEC, M. N., JEANTET, R. Continuous raw skim milk processing by pulsed electric field at non-lethal temperature: effect on microbial inactivation and functional properties. **Lait**, Paris, v. 86, p. 43-57, 2006.

GRAPPIN, R., BEUVIER, E. Possible implications of milk pasteurization on the manufacture and sensory quality of ripened cheese. **Int. Dairy Journal**, Oxford, v. 7, p. 751-761, 1997.

HAYES, M., STANTON, C., SLATTERY, H., O'SULLIVAN, O., HILL, C., FITZGERALD, G. F., ROSS, R. P. Casein fermentate of *Lactobacillus animalis* DPC6134 contains a range of novel propeptide angiotensin-converting enzyme inhbitors. **Appl. and Environ. Microbiol.**, Washington v.73, p. 4658-4667, 2007.

HARRIMAN, A. Further comments on the redox potentials of tryptophan and tyrosine. **J. Phys. Chem.**, Washington, v.91, p. 6102-6104, 1987.

HEMAR, Y.; AUGUSTIN, M.; CHENG, L. J.; SANGUANSRI, P.; SWIERGON, P.; WAN, J. The effect of pulsed electric field processing on particle size and viscosity of milk and milk concentrates. **Milchwissenschaft-Milk Sci. Int.**, Kempten, v. 66, p. 126, 2011.

HILARIO, E. C., Stern, A., WANG, C. H., VARGAS, Y. W., MORGAN, C. J., SWARTZ, T. E., PATAPOFF, T. W. An improved method of predicting extinction coefficients for the determination of protein concentration. ***PDA J Pharm Sci Technol***., Bethesda, v. 71, p. 127-135, 2017.

HORNE, D. S. Casein micelle structure: models and muddles. **Curr. Opi. Colloid & Interface Sci.**, London, v. 11, p. 148 – 153, 2006.

HU, G., ZHENG, Y., LIU, Z., DENG, Y., ZHAO, Y. Structure and IgE-binding properties of α-casein treated by high hydrostatic pressure, UV-C, and far-IR radiations. **Food Chem.**, Oxford, v. 204, p. 46-55, 2016.

HUBATSCH, I., RAGNARSSON, E. ARTURSSON, P. Determination of drug permeability and prediction of drug absorption in caco-2 monolayers. **Nat. Protoc.,** Berlin, v. 2, p. 2111–2119, 2007.

HU, G., ZHENG, Y., LIU, Z., XIAO, Y., DENG, Y., ZHAO, Y. Effects of high hydrostatic pressure, ultraviolet light-C, and far-infrared treatments on the digestibility, antioxidant and antihypertensive activity of α-casein. **Food Chem.**, Oxford, v. 22, p. 1860-1866, 2017.

JEYAMKONDAN, S., JAYAS, D. S., HOLLEY, R. A. Pulsed electric field processing of foods: A review. **J. Food Prot.**, Des Moines, v. 62, p. 1088-1096, 1999.

JOSHI, R., MUKHERJEE, T. Charge transfer between tryptophan and tyrosine in casein: a pulse radiolysis study. **Biophys. Chem.**, Amsterdam, v. 96, p. 15-19, 2002.

JOVANOVIC, S. V., HARRIMAN, A., SIMIC, M. G. Electron-transfer reactions of tryptophan and tyrosine derivatives. **J. Phys. Chem.**, Washington, v. 90, p. 1935-1939, 1986.

JOSHI, R., Mukherjee, T. Charge transfer between tryptophan and tyrosine in casein: a pulse radiolysis study. **Biophys. Chem.**, Amsterdam, v. 96, p. 15-19, 2002.

KUHN, H. J., BRASLAVSKY, S. E., SCHMIDT, R. Chemical actinometry. **Pure Appl. Chem.**, Berlin, v. 61, p. 187-210, 1989.

KUMOSINSKI, T. F., BROWN, E. M., FARREL, H. M. JR., Three-dimensional molecular modeling of bovine caseins: α_{s1}-casein. **J. Dairy Sci.**, New York, v. 74, p. 2889-2895, 1991a.

KUMOSINSKI, T. F., BROWN, E. M., FARREL, H. M. JR., Three-dimensional molecular modeling of bovine caseins: an energy-minimized β-casein structure. **J. Dairy Sci.**, New York, v. 76, p. 931-945, 1993.

KUMOSINSKI, T. F., BROWN, E. M., FARREL, H. M. JR., Three-dimensional molecular modeling of bovine caseins: κ-casein. **J. Dairy Sci.**, New York, v. 74, p. 2879-2887, 1991b.

LEVI, C. S., GOLDSTEIN, N., PORTMANN, R., LESMES, U. Emulsion and protein degradation in the elderly: qualitative insights from a study coupling a dynamic in vitro digestion model with proteomic analyses. **Food Hydrocoll.** Oxford, v. 69, p. 393-401, 2017.

LIU, Q., YANG, M., ZHAO, B., YANG, F. Isolation of antioxidant peptides from yak casein hydrolysate. **RSC Adv**., Cambridge, v.10, p. 19844, 2020.

LÓPES-EXPÓSITO, I., MINERVINI, F., AMIGO, L., RECIO, I. Identification of antibacterial peptides from bovine κ-casein. **J. Food Prot.**, Des Moines, v. 69, p. 2992-2997, 2006.

LÓPES-EXPÓSITO, I., QUIRÓS, A., AMIGO, L., RECIO, I. Casein hydrolysates as a source of antimicrobial, antioxidant and antihypertensive peptides. **Lait**, Paris, p.241-249, 2007.

MARSELLÉS-FONTANET, A.R.; ELEZ-MARTÍNEZ, P.; MARTÍN-BELLOSO, O. Juice preservation by pulsed electric fields. **Stewart Postharvest Rev.**, London, v. 8, p. 1–4, 2012.

MCCLEAN, S., BEGGS, L. B., WELCH, R. W. Antimicrobial activity of antihypertensive food-derived peptides and selected alanine analogues. **Food Chem.**, Oxford, v.146, p. 443-447, 2014.

MEISEL, H., FRISTER, H., SCHLIMME, E. Biologically active peptides in milk proteins. **J. Nutr. Sci.**, New York, v. 28, p.267-278, 1989.

MENESES, N., JAEGER, H., MORITZ, J., KNORR, D. Impact of insulator shape, flow rate and electrical parameters on inactivation of E. coli using a continuous co-linear PEF system. **Innov. Food Sci. Emerg. Technol.**, Oxford, v.12, p. 6-12, 2011.

MIDDENDORF, D., BINDRICH, U., SIEMER, C., TÖPFL, S., HEINZ, V. Affecting casein micelles by pulsed electrical field (PEF) for inclusion of lipophilic organic compounds. **Appl. Sci**., Basel, v. 11, p.4611, 2021.

MIKHAYLIN, S., BOUSSETTA, N., VOROBIEV, E., BAZINET, L. High voltage electrical treatments to improve the protein susceptibility to enzymatic hydrolysis. **ACS Sustain. Chem. Eng.**, Washington, v. 5, p. 11706-11714, 2017.

MINEKUS, M., ALMINGER, M., ALVITO, P., BALANCE, S., BOHN, T., BOURLIEU, C., CARRIÈRE, F., BOUTROU, R., CORREDIG, M., DUPONT,D., DUFOUR, C., EGGER, L., GOLDING, M., KARAKAYA, S., KIRKHUS, B., LE FEUNTEUN, S., LESMES, U., MACIERZANKA, A., MACKIE, A., MARZE, S., McCLEMENTS, D. J., MÉNARD, O., RECIO, I., SANTOS, C. N., SINGH, R. P., VEGARUD, G. E., WICKHAM, M. S. J., WEITSCHIES, W., BRODKORB, A. A standardized static *in vitro* digestion method suitable for food – an international consensus, **Food Funct.**, Cambridge, v.5, p. 1113-1124, 2014.

NAVARRA, G., TINTI, A., DI FOGGIA, M., LEONE, M., MILITELLO, V., TORREGGIANI, A. Metal ions modulate termal aggregation of beta-lactoglobulin: A joint chemical and physical characterization. **J. Inorg. Biochem**., New York, v. 137, p. 64-73, 2014.

MÜLLER, P., IGNATZ, E., KIONTKE, S., BRETTEL, K., ESSEN, L. O. Sub-nanosecond tryptophan radical deprotonation mediated by a protein-bound water cluster in class II DNA photolyases. **Chem. Sci.**, Cambridge, v.9, p. 1200-1212, 2018.

MURAKAMI, J., OKAZAKI, M., SHIGA, T. Near Uv-induced free radicals in ocular lens, studied by ESR and spin trapping. **Photochem. and Photobiol.**, Hoboken, v. 49, p. 465-473, 1989.

NIELSEN, DRUD, S., BEVERLY, R. L., QU, Y., DALLAS, D. C. Milk Bioactive Peptide Database: A Comprehensive Database of Milk Protein-Derived Bioactive Peptides and Novel Visualization. **Food Chem.**, Oxford, v.232, p. 673–82, 2017.

OUANEZAR, M., GUYOMARC'H, F., BOUCHOUX, A. AFM Imaging of milk casein micelles: evidence for structural rearrangement upon acidification. **Langmuir**, Washington, v. 28, p. 4915-4919, 2012.

ONO, T., TAKAGI, Y., KUNISHI, I. Casein phosphopetides from casein micelles by successive digestion with pepsin and trypsin. **Biosci. Biotechnol. Biochem.**, Oxford, v. 62, p. 16-21, 1998.

PRÜTZ, W. A., SIEBERT, F., BUTLER, J., LAND, E. J., MENEZ, A., GARESTIER, T., M. Charge transfer in peptides, intramolecular radical transformations involving methionine, tryptophan and tyrosine. **Biochim. et Biophyis. Acta**, Amsterdam, v.7-5, p. 139-149, 1982.

REINEKE, K., SCHTTROFF, F., MENESES, N., KNORR, D. Sterilization of liquid foods by pulsed electric fields-an innovative ultra-high temperature process. **Front. Microbiol.**, Lausanne, v.6, 2015.

RIVERA-SÁNCHEZ, L., SANTOS, P. F., SEVILLA, M. A., MONTERO, M. J., RECIO, I., MIRALLES, B. Implication of opioid receptors in the antihypertensive effect of a bovine casein hydrolysate and α_{s1}-casein-derived peptides. **J. Agric. Food Chem.**, Washington, v.68, p.1877-1883, 2020.

ROJAS-CANDELAS, L. E., CHANONA-PÉREZ, J. J., MÉNDEZ, J. V. M. Characterization of structural changes of casein micelles at different pH using microscopy and spectroscopy techniques. **Microsc. Microanal.**, New York, v. 28, p. 527-536, 2022.

RYGULA, A., MAJZNER, K., MARZEC, K. M., KACZOR, A., PILARCZYK, M., BARANSKA, M. Raman spectroscopy of proteins: a review. **J. Raman Spectrosc.**, Hoboken, v. 44, p. 1061-1076, 2013.

SHAMSI, K.; VERSTEEG, C.; SHERKAT, F.; WAN, J. Alkaline phosphatase and microbial inactivation by pulsed electric field in bovine milk. **Innov. Food Sci. Emerg. Technol**, Oxford, v. 9, p. 217–223, 2008.

SHARMA, P., OEY, I., EVERETT, D. W. Effect of pulsed electric field processing on the functional properties of bovine milk. **Trends Food Sci. Technol.**, London, v. 35 p. 87-101, 2014.

SHERIN, P. S., SNYTNIKOVA, O. A., TSENTALOVICH, Y. P. Tryptophan photoionization from prefluorescent and fluorescent states. **Chem. Phys. Lett.**, Netherlands, v. 391, p. 44-49, 2004.

SOLTANZADEH, M., PEIGHAMBARDOUST, S. H., GULLON, P., HESARI, J., GULLÓN, B., ALIREZALU, K., LORENZO, J. Quality aspects and safety of pulsed electric field (PEF) processing on dairy products: a comprehensive review. **Food Rev. Int.**, Philadelphia, v. 2020.

STEVENSON, K. L., PAPADANTONAKIS, G. A., LeBreton, P. R. Nanosecond UV laser photoionization of aqueous tryptophan: temperature dependence of quantum yield, mechanism, and kinetics of hydrated electron decay. **J. Photochem. Photobiol. A: Chem.**, Lausanne, v. 133, p. 159-167, 2000.

SZŁAPKA, E. S., JARMOŁOWSKAM B., KRAWCZUK, S., KOSTYRA, E., KOSTYRA, H., BIELIKOWICZ, K. Transport of bovine milk-derived opioid peptides across a caco-2 monolayer**. Int. Dairy J.**, Oxford, v. 19, p. 252-257, 2009.

TSENTALOVICH, Y. P., SNYTNIKOVA, O. A., Sagdeev, R. Z. Properties of excited states of aqueous tryptophan. **J. Photochem. Photobiol. A: Chem.**, Lausanne, v. 162, p. 371-379, 2004.

VIAZIS, S., FARKAS, B. E., JAYKUS, L. A. Inactivation of bacterial pathogens in human milk by high-pressure processing. **J. Food Prot.**, Des Moines, v. 71, p.109-118, 2008.

XIANG, B. Y., NGADI, M. O., OCHOA-MARTINEZ, L. A., SIMPSON, M. V. Pulsed electric field-induced structural modification of whey protein isolate. **Food Bioprocess Technol**., New York, v. 4, p. 1341-1348, 2011.

XU, B., YUAN, J., WANG, L., LU, F., WEI, B., AZAM, R. S. M., REN, X., ZHOU, C., MA, H., BHANDARI, B. Effect of multi-frequency power ultrasound (MFPU) treatment on enzyme hydrolysis of casein. **Ultrason. Sonochem.**, Amsterdam, v. 63, p. 104930, 2020.

YANG, H., YANG, S., KONG, J., DONG, A., YU, S. Obtaining information about protein secondary structures in aqueous solution using fourier transform IR spectroscopy. **Nat. Protoc.**, Berlin, v. 10, p. 382-394, 2015.

YANG, Y., WANG, B., LI, B. Structural requirement of casein peptides for transcytosis through the caco-2 cell monolayer: hydrophobicity and charge property affect the transport pathway and efficiency. **J. Agric. Food Chem.**, Washington, v. 67, p. 11778-11787, 2019.

WANG, Y., FU, L. Effect of ultrasound treatment on allergenicity reduction of milk casein via colloid formation. **J. Agric. Food Chem.**, Washington, v. 68, p. 4678-4686, 2020.

WANG, B., LI, B. Charge and hydrophobicity of casein peptides influence transepithelial transport and bioavailability. **Food Chem.**, Oxford, v. 245, p. 646-652, 2018.

Appendix

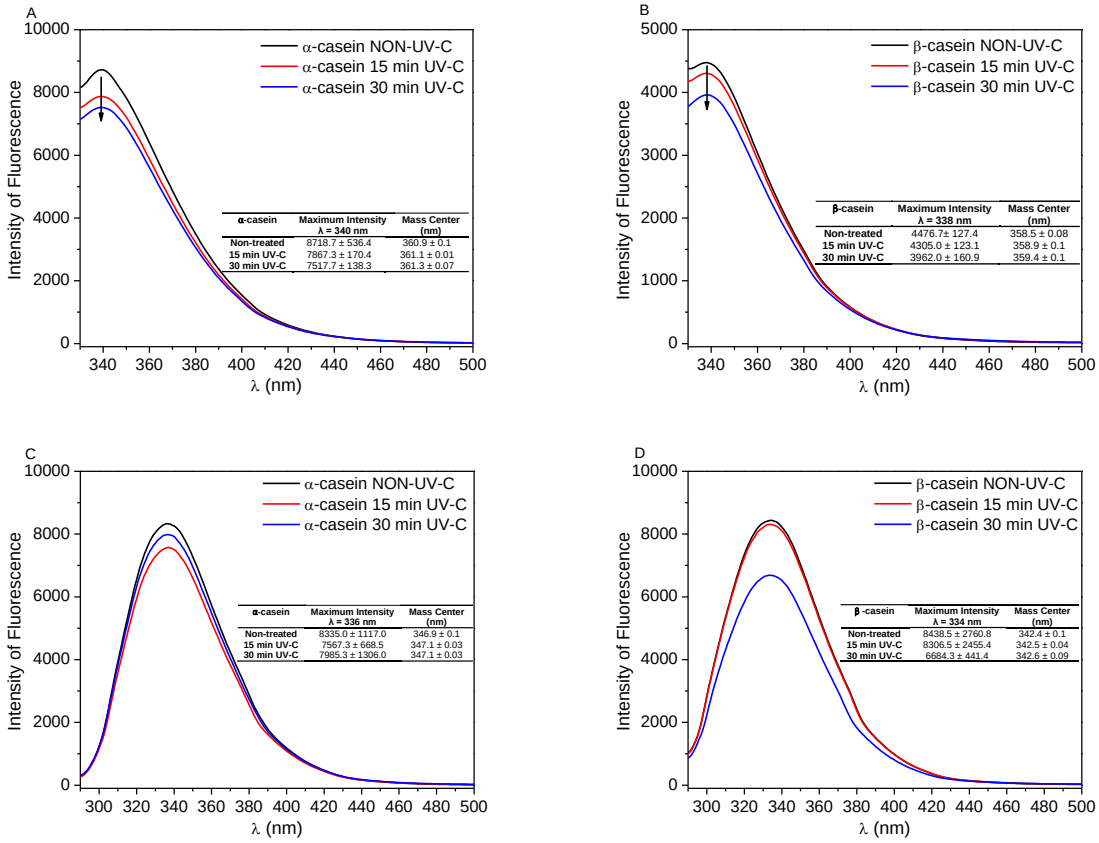

Fluorescence emission of tryptophan (A and B), and tyrosine (C and D) for α and β-casein obtained for untreated, ultraviolet light irradiated (UV-C; dose of 3 W m^{-2} for 15 and 30 min) in phosphate buffer, pH 6.5.

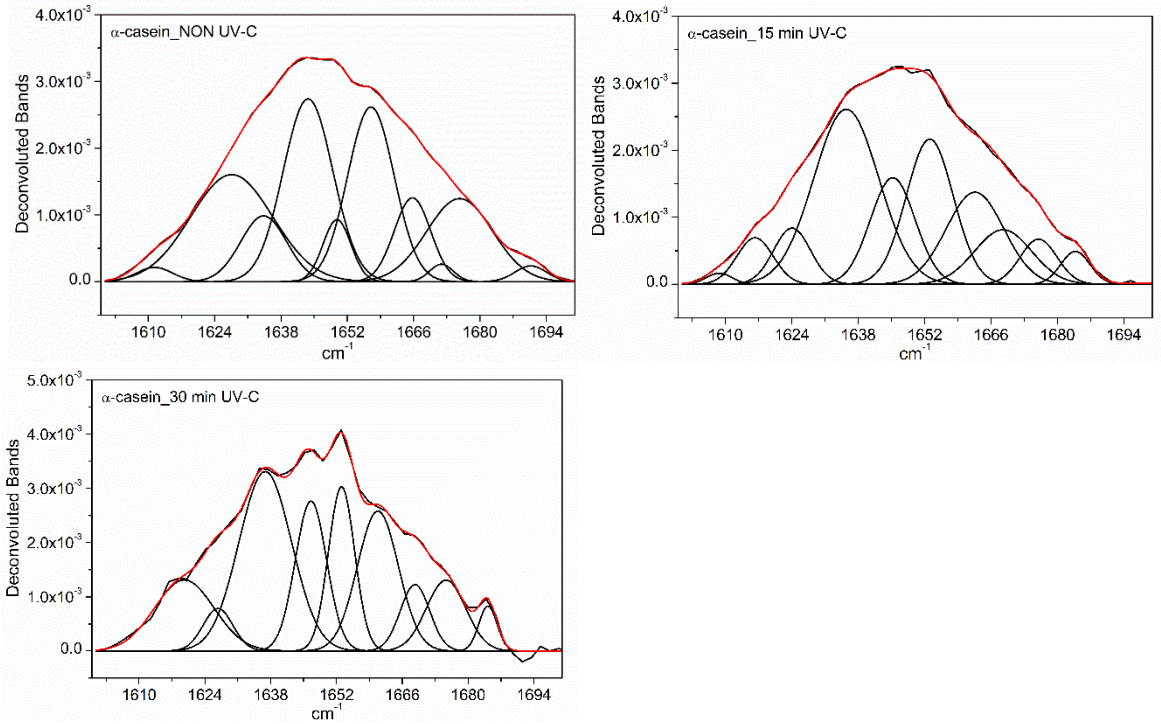

Spectra of ATR-FTIR for α-casein untreated, ultraviolet light irradiated (UV-C; dose of 3 W m^{-2} for 15 and 30 min) in phosphate buffer pD 6.8, I = 160 mM.

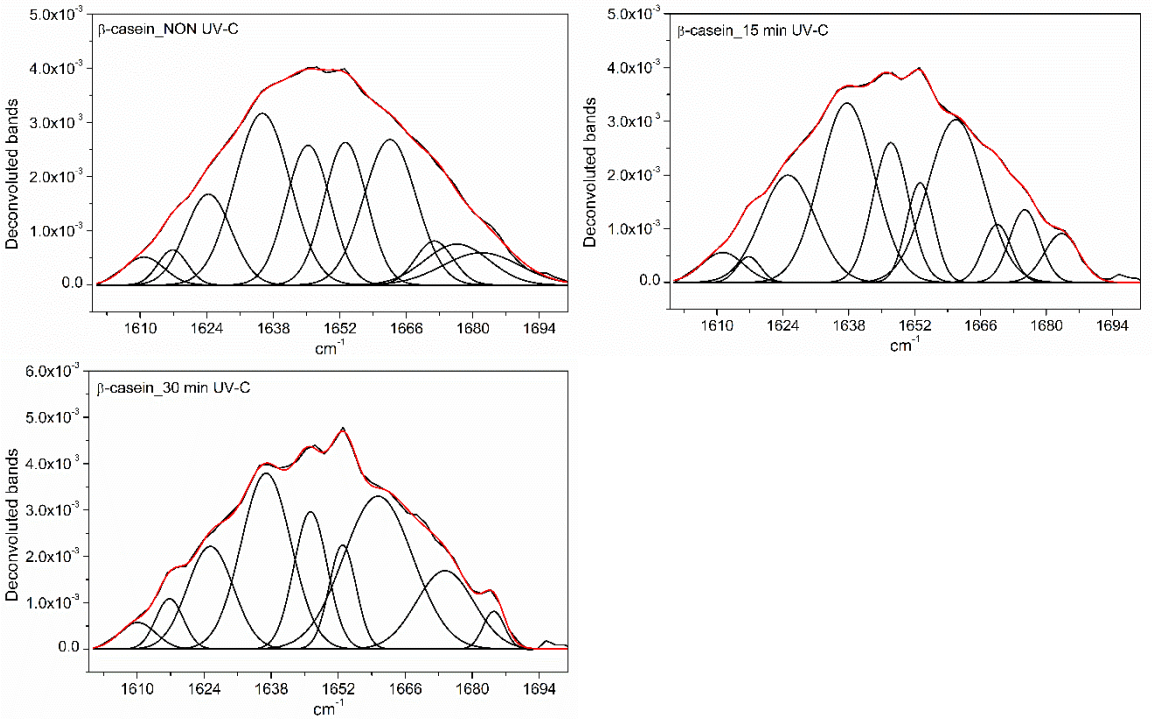

Figure S2B – Spectra of ATR-FTIR for β -casein untreated, ultraviolet light irradiated (UV-C; dose of 3 W m^{-2} for 15 and 30 min) in phosphate buffer pD 6.8, I = 160 mM.

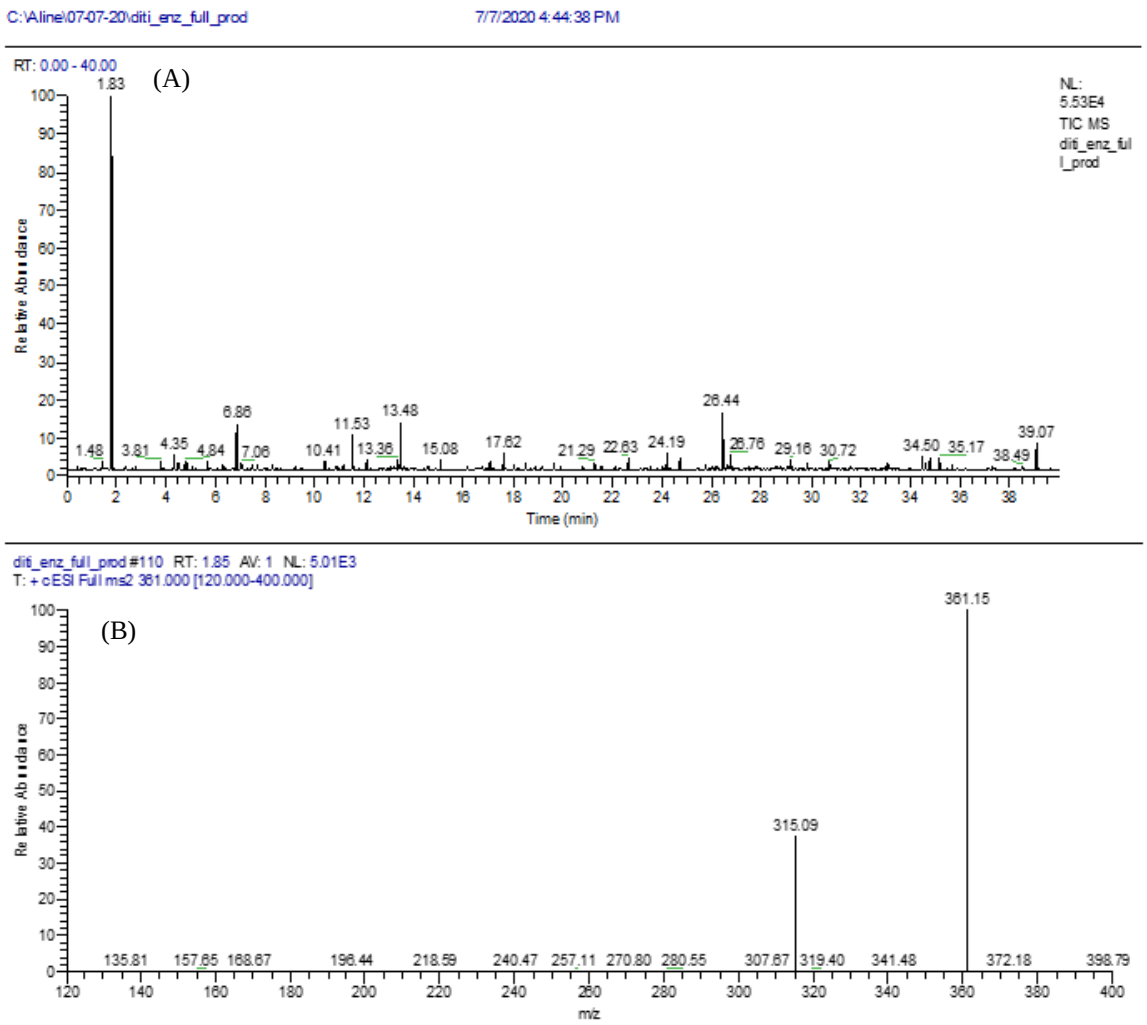

Total ion chromatogram (TIC) (A) and mass spectra (B) of di-tyrosine acquired as product ion scan mode.

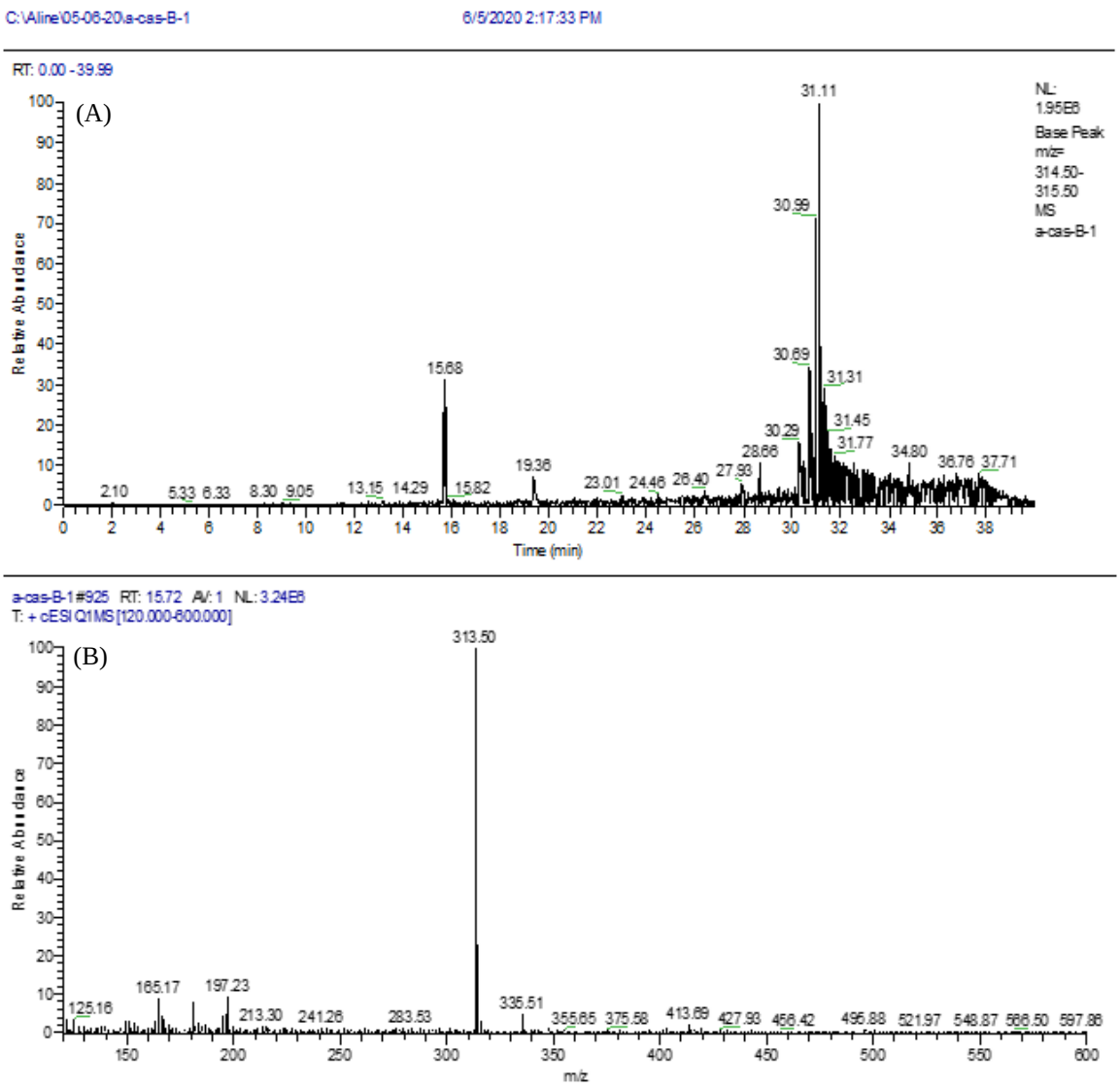

Extracted ion chromatogram (EIC) (A- α-casein non-irradiated) and mass spectra (B - α-casein non-irradiated) from m/z 315 acquired as product ion scan mode.

UV-C pretreatment

Peptides released from gastric digestion of the pretreated α-casein (dose of 3 W m^{-2} for 15 min of exposure to UV-C light) and detected after 15 min of transport across caco-2 cell monolayer.

m/z	Range	Sequence	Papp (cm s^{-1}) NON UV-C	Range	Sequence	Papp (cm s^{-1}) UV-C
546.201	88 - 92	PNSVE	2.22E-01	88 - 92	PNSVE	4.83E-01
	195 - 199	SDIPN		195 - 199	SDIPN	
597.284				187 - 191	QYTDA	1.73E+00
635.18	160 - 163	FYPE 2: Phospho (STY)	2.85E-01			
671.27	105 - 109	RYLGY *	8.10E-02	105 - 109	RYLGY *	3.62E-01
741.325	143 - 148	HAQQKE	3.58E-02	143 - 148	HAQQKE	1.06E-01
770.317	75 - 81	MEAESIS	1.51E-01	155 - 160	QELAYF	6.41E-01
780	N.D.	N.D.	N.D.	209 - 214	TTMPLW* 3: Oxidation (M) 6: Oxidation (HW)	1.06E+00
				209 - 214	TTMPLW 6: Oxidation O2 (W)	
784.368	105 - 110	RYLGYL *	9.57E-02	105 - 110	RYLGYL *	5.70E-01
796.293	156 - 161	ELAYFY	1.26E-01	156 - 161	ELAYFY	4.57E-01
	209 - 214	TTMPLW * 3: Oxidation (M) 6: Oxidation O2 (W)		209 - 214	TTMPLW * 3: Oxidation (M) 6: Oxidation O2 (W)	
925.522	N.D.	N.D.	N.D.	208 - 214	KTTMPLW 4: Oxidation (M) 7: Oxidation O2 (W)	1.30E-01
930.459	N.D.	N.D.	N.D.	180 - 187	YYVPLGTQ	1.61E-01
	N.D.	N.D.	N.D.	181 - 188	YVPLGTQY	
952.386	43 - 50	FPEVFGKE	2.74E-01	43 - 50	FPEVFGKE	1.09E+00
968.381				165 - 170	FRQFYQ 5: Phospho (STY)	3.85E-01
973.388	131 - 138	AEERLHSM	8.83E-02	131 - 138	AEERLHSM	2.09E-01
978.384	n.d.			67 - 74	QAMEDIKQ 3: Oxidation (M)	1.01E+00

995.37	99 - 106	EDVPSERY	1.08E+00	N.D.	N.D.	
1009.509	N.D.	N.D.	N.D.	136 - 144	HSMKEGIHA	1.38E-02
1011.351	144 - 152	AQQKEPMIG 7: Oxidation (M)	1.93E-01	144 - 152	AQQKEPMIG 7: Oxidation (M)	7.55E-01
1037.556	33 - 40	ENLLRFFV	5.79E-02	33 - 40	ENLLRFFV	3.86E-01
1041.598	N.D.	N.D.	N.D.	196 - 205	DIPNPIGSEN	5.16E-02
1125.58	148 - 157	EPMIGVNQEL	3.38E-01	148 - 157	EPMIGVNQEL	1.80E+00
1272.75	203 - 213	SENSEKTTMPL 9: Oxidation (M)	1.96E-02	203 - 213	SENSEKTTMPL 9: Oxidation (M)	1.45E-01
	09-20	LVAVALARPK HP		09-20	LVAVALARPKHP	
	10-21	VAVALARPKHP I		10-21	VAVALARPKHPI	
1279.521	53 - 64	NELSKDIGSEST	2.43E-01	53 - 64	NELSKDIGSEST	2.24E+00
1310.755	N.D.	N.D.	N.D.	16 - 26	RPKHPIKHQGL	2.61E-02
1336.496	204 - 214	ENSEKTTMPLW	1.68E-01	204 - 214	ENSEKTTMPLW	1.96E+00
1385.835	157 - 166	LAYFYPELFR 3: Phospho (STY)	2.65E-02	157 - 166	LAYFYPELFR 3: Phospho (STY)	1.71E-02
	157 - 166	LAYFYPELFR 5: Phospho (STY)		157 - 166	LAYFYPELFR 5: Phospho (STY)	
1637.805	07-21	TCLVAVALARP KHPI 2: Sulfonic Acid (SO3H)	3.03E-02	07-21	TCLVAVALARPK HPI 2: Sulfonic Acid (SO3H)	6.92E-02
	07-20	LTCLVAVALAR PKHP 3: Sulfonic Acid (SO3H)		07-20	LTCLVAVALARP KHP 3: Sulfonic Acid (SO3H)	
1664.933	16 - 29	RPKHPIKHQGL PQE	3.53E-02	16 - 29	RPKHPIKHQGLPQ E	9.08E-02
1687.003	N.D.	N.D.	N.D.	63 - 76	STEDQAMEDIKQ ME 7: Oxidation (M) 13: Oxidation (M)	9.14E-01
				62 - 75	ESTEDQAMEDIK QM 8: Oxidation (M) 14: Oxidation (M)	
1702.938	99 - 112	EDVPSERYLGY LEQ	1.42E-01	99 - 112	EDVPSERYLGYL EQ	2.10E-01

				151 - 163	IGVNQELAYFYPE 9: Phospho (STY) 11: Phospho (STY)	
1877.129	N.D.	N.D.	N.D.	16 - 31	RPKHPIKHQGLPQ EVL	1.93E-02

*Bioactive peptide; N.D.: Non detected.

Peptides released from gastric digestion of the pretreated α-casein (dose of 3 W m^{-2} for 15 min of exposure to UV-C light) and detected after 90 min of transport across caco-2 cell monolayer.

m/z	**Range**	**Sequence**	**Papp (cm s^{-1})_NON UV-C**	**Range**	**Sequence**	**Papp (cm s^{-1}) UV-C**
546.265	88 - 92	PNSVE	3.17E-02	99 - 103	PNSVE	7.81E-02
	195 - 199	SDIPN		100 - 104	SDIPN	
597.299				187 - 191	QYTDA	3.77E-01
635.259	160 - 163	FYPE 2: Phospho (STY)	3.87E-02	160 - 163	FYPE 2: Phospho (STY)	3.84E-01
657.531	09-15	LVAVALA	7.78E-02			
671.417	105 - 109	RYLGY *	9.39E-03	105 - 109	RYLGY *	5.84E-02
741.462	143 - 148	HAQQKE	5.75E-03	143 - 148	HAQQKE	1.89E-02
770.397	N.D.	N.D.	N.D.	155 - 160	QELAYF	9.79E-02
780.406	N.D.	N.D.	N.D.	209 - 214	TTMPLW * 3: Oxidation (M) 6: Oxidation (HW)	2.15E-01
				209 - 214	TTMPLW * 6: Oxidation O2 (W)	
784.508	105 - 110	RYLGYL *	1.63E-02	105 - 110	RYLGYL *	9.10E-02
796.452	156 - 161	ELAYFY	2.42E-02	156 - 161	ELAYFY	9.65E-02
	209 - 214	TTMPLW* 3: Oxidation (M) 6: Oxidation O2 (W)		209 - 214	TTMPLW * 3: Oxidation (M) 6: Oxidation O2 (W)	
925.614	208 - 214	KTTMPLW 4: Oxidation (M) 7: Oxidation O2 (W)	3.04E-03	208 - 214	KTTMPLW 4: Oxidation (M) 7: Oxidation O2 (W)	2.16E-02
930.573	180 - 187	YYVPLGTQ	6.21E-03	180 - 187	YYVPLGTQ	3.68E-02

	181 - 188	YVPLGTQY		181 - 188	YVPLGTQY	
952.47	43 - 50	FPEVFGKE	4.61E-02	43 - 50	FPEVFGKE	2.25E-01
973.487	131 - 138	AEERLHSM	1.44E-02	131 - 138	AEERLHSM	5.93E-02
978.478	N.D.	N.D.	N.D.	67 - 74	QAMEDIKQ 3: Oxidation (M)	2.01E-01
995.464	99 - 106	EDVPSERY	1.26E-01	N.D.		
1003.717	116 - 123	LKKYKVPQ	2.30E-03	N.D.		
	117 - 124	KKYKVPQL				
1009.61	136 - 144	HSMKEGIHA	1.11E-02	N.D.		
1011.555	144 - 152	AQQKEPMIG 7: Oxidation (M)	3.06E-02	N.D.		
1037.637	33 - 40	ENLLRFFV	1.58E-02	N.D.		
1041.691	196 - 205	DIPNPIGSEN	5.93E-03	N.D.		
1125.788	148 - 157	EPMIGVNQEL	4.84E-02	148 - 157	EPMIGVNQEL	3.16E-01
1272.904	203 - 213	SENSEKTTMPL 9: Oxidation (M)	4.80E-03			
	09-20	LVAVALARPKH P				
	10-21	VAVALARPKHPI				
1279.747	53 - 64	NELSKDIGSEST	4.62E-02	53 - 64	NELSKDIGSEST	4.44E-01
1336.68	204 - 214	ENSEKTTMPLW	4.18E-02	204 - 214	ENSEKTTMPLW	3.30E-01
1385.94	157 - 166	LAYFYPELFR 3: Phospho (STY)	5.30E-03	N.D.		
	157 - 166	LAYFYPELFR 5: Phospho (STY)		N.D.		
1597.739	168 - 180	FYQLDAYPSGA WY 12: Oxidation (HW)	9.13E-03	N.D.		

	169 - 181	YQLDAYPSGAWYY		N.D.		
1637.943	07-21	TCLVAVALARPKHPI 2: Sulfonic Acid (SO3H)	6.94E-03	07-21	TCLVAVALARPKHPI 2: Sulfonic Acid (SO3H)	2.46E-02
	06-20	LTCLVAVALARPKHP 3: Sulfonic Acid (SO3H)		07-20	LTCLVAVALARPKHP 3: Sulfonic Acid (SO3H)	
1665.066	16 - 29	RPKHPIKHQGLPQE	8.88E-03	16 - 29	RPKHPIKHQGLPQE	2.86E-02
1686.944	N.D.	N.D.	N.D.	63 - 76	STEDQAMEDIKQME 7: Oxidation (M) 13: Oxidation (M)	2.27E-01
				62 - 75	ESTEDQAMEDIKQM 8: Oxidation (M) 14: Oxidation (M)	
1703.069	99 - 112	EDVPSERYLGYLEQ	2.66E-02	99 - 112	EDVPSERYLGYLEQ	4.56E-02

*Bioactive peptide; N.D.: Non detected.

Peptides released from gastric digestion of the pretreated β-casein (dose of 3 W m^{-2} for 15 min of exposure to UV-C light) and detected after 15 min of transport across caco-2 cell monolayer.

m/z	**Range**	**Sequence**	**Papp (cm s^{-1})_NON UV-C**	**Range**	**Sequence**	**Papp (cm s^{-1}) UV-C**
640.325	61 - 65	QDKIH	6.40E-02	61 - 65	QDKIH	3.69E-02
656.318	82 - 87	PNSLPQ	2.53E-02	n.d.		
657.315	121 - 125	HKEMP 4: Oxidation (M)	1.93E-02	121 - 125	HKEMP 4: Oxidation (M)	1.93E-02
672.344	83 - 88	NSLPQN	1.04E-01			
729.374				214 - 220	GPVRGPF	4.74E-02
772.335				07-14	ACLVALAL 2: Oxidized (SS)	2.13E-02

				08-15	CLVALALA 1: Oxidized (SS)	
				06-13	LACLVALA 3: Oxidized (SS)	
787.406	172 - 178	FPPQSVL	5.88E-02	172 - 178	FPPQSVL	4.33E-02
802.503	201 - 207	PIQAFLL	2.10E-02	201 - 207	PIQAFLL	1.11E-02
809.372	154 - 159	LLQSWM 5: Oxidation (HW) 6: Oxidation (M)	8.56E-02	154 - 159	LLQSWM 5: Oxidation (HW) 6: Oxidation (M)	8.19E-02
	154 - 159	LLQSWM 5: Oxidation O2 (W)		154 - 159	LLQSWM 5: Oxidation O2 (W)	
825.354	N.D.			195 - 200	YPQRDM 6: Oxidation (M)	4.69E-02
915.562	N.D.			12-19	LALARELE	7.92E-03
941.514	64 - 71	IHPFAQTQ *	2.89E-02	64 - 71	IHPFAQTQ *	1.67E-02
946.528	105 - 113	PEVMGVSKV	4.61E-02	105 - 113	PEVMGVSKV	3.47E-02
964.472	137 - 145	SQSLTLTDV	3.11E-02	137 - 145	SQSLTLTDV	2.86E-02
995.585	209 - 217	QEPVLGPVR	2.89E-02	209 - 217	QEPVLGPVR	3.10E-02
1033.514	N.D.			170 - 178	VMFPPQSVL 2: Oxidation (M)	4.37E-02
1038.567				76 - 85	PFPGPIPNSL	4.02E-02
				77 - 86	FPGPIPNSLP	
1052.591	N.D.			209 - 218	QEPVLGPVRG	2.91E-02
				01-9	MKVLILACL 8: Sulfonic Acid (SO3H)	
1094.658	215 - 224	PVRGPFPIIV	1.40E-02	215 - 224	PVRGPFPIIV	1.60E-02
1108.595	70 - 79	TQSLVYPFPG	1.39E-01	70 - 79	TQSLVYPFPG	1.06E-01
1130.578	100 - 109	PPFLQPEVMG 9: Oxidation (M)	3.60E-01	100 - 109	PPFLQPEVMG 9: Oxidation (M)	2.35E-01
1146.547	N.D.			144 - 153	DVENLHLPLP	9.54E-02
1151.69	01-10	MKVLILACLV 8: Sulfonic Acid (SO3H)	1.61E-02	01-10	MKVLILACLV 8: Sulfonic Acid (SO3H)	1.75E-02
1184.617	71 - 80	QSLVYPFPGP 5: Phospho (STY)	3.38E-02	71 - 80	QSLVYPFPGP 5: Phospho (STY)	4.10E-02

1198.626	159 - 168	MHQPHQPLPP 1: Oxidation (M)	1.33E-02	159 - 168	MHQPHQPLPP 1: Oxidation (M)	1.28E-02
1206.617	158 - 166	WMHQPHQPL 1: Oxidation O2 (W)	1.41E-01	158 - 166	WMHQPHQPL 1: Oxidation O2 (W)	1.46E-01
	158 - 166	WMHQPHQPL 1: Oxidation (HW) 2: Oxidation (M)		158 - 166	WMHQPHQPL 1: Oxidation (HW) 2: Oxidation (M)	
1222.565				32 - 42	SSSEESITRIN	7.06E-02
1300.74				100 - 111	PPFLQPEVMGVS	8.64E-03
1322.675	135 - 146	TESQSLTLTDVE	3.28E-02	135 - 146	TESQSLTLTDVE	5.67E-02
1338.662	N.D.			133 - 144	PFTESQSLTLTD	2.58E-02
1343.705	N.D.			193 - 203	VPYPQRDMPIQ	7.97E-02
1381.715	27 - 39	IVESLSSSEESIT	9.69E-03	N.D.		
1399.72	158 - 168	WMHQPHQPLPP 1: Oxidation O2 (W)	1.18E-02	158 - 168	WMHQPHQPLPP 1: Oxidation O2 (W)	1.72E-02
	158 - 168	WMHQPHQPLPP 1: Oxidation (HW) 2: Oxidation (M)		158 - 168	WMHQPHQPLPP 1: Oxidation (HW) 2: Oxidation (M)	
1414.732	69 - 80	QTQSLVYPFPGP 7: Phospho (STY)	4.17E-02	N.D.		
1512.766	113 - 125	VKEAMAPKHKEMP 5: Oxidation (M)	1.04E-02	N.D.		
	113 - 125	VKEAMAPKHKEMP 12: Oxidation (M)				
1674.88	n.d.			113 - 126	VKEAMAPKHKEMPF 5: Oxidation (M) 12: Oxidation (M)	1.82E-02
1698.835	158 - 171	WMHQPHQPLPPTVM	5.32E-03	158 - 171	WMHQPHQPLPPTVM	6.27E-03
1712.838	N.D.			192 - 205	AVPYPQRDMPIQAF 4: Phospho (STY)	2.43E-02

1720.845	198 - 210	RDMPIQAFLL YQE 3: Oxidation (M) 11: Phospho (STY)	1.62E-02	198 - 210	RDMPIQAFLLYQE 3: Oxidation (M) 11: Phospho (STY)	6.02E-02
1736.813	N.D.			198 - 211	RDMPIQAFLLYQEP 3: Oxidation (M)	2.73E-02
2137.151	153 - 170	PLLQSWMHQP HQPLPPTV 6: Oxidation O2 (W)	9.65E-02	153 - 170	PLLQSWMHQPHQPLPPT V 6: Oxidation O2 (W)	1.24E-02
	153 - 170	PLLQSWMHQP HQPLPPTV 6: Oxidation (HW) 7: Oxidation (M)		153 - 170	PLLQSWMHQPHQPLPPT V 6: Oxidation (HW) 7: Oxidation (M)	
2159.264				07-26	ACLVALALARELEELNV PGE 2: Sulfonic Acid (SO3H)	4.21E-03
2337.313				103 - 123	LQPEVMGVSKVKEAMA PKHKE	1.04E-02
2807.7	179 - 203	SLSQSKVLPVP QKAVPYPQRD MPIQ	1.89E-03	N.D.		
	180 - 204	LSQSKVLPVP QKAVPYPQRD MPIQA 21: Oxidation (M)				
2877.789	97 - 122	VVVPPFLQPE VMGVSKVKE AMAPKHK 12: Oxidation (M) 21: Oxidation (M)	2.30E-03	97 - 122	VVVPPFLQPEVMGVSKV KEAMAPKHK 12: Oxidation (M) 21: Oxidation (M)	2.44E-03

*Bioactive peptide; N.D.: Non detected.

Peptides released from gastric digestion of the pretreated β-casein (dose of 3 W m^{-2} for 15 min of exposure to UV-C light) and detected after 90 min of transport across caco-2 cell monolayer.

m/z	Range	Sequence	Papp (cm s^{-1})_NON UV-C	Range	Sequence	Papp (cm s^{-1}) UV-C
640.327	61 - 65	QDKIH	3.08E-02	61 - 65	QDKIH	1.13E-01
657.324				121 - 125	HKEMP 4: Oxidation (M)	5.00E-02
672.362	83-88	NSLPQN	4.21E-02			
675.286				16 - 20	RELEE	5.31E-02
729.345				214 - 220	GPVRGPF	1.15E-01
787.404	172 - 178	FPPQSVL	2.35E-02	172 - 178	FPPQSVL	2.75E-01
802.511	201 - 207	PIQAFLL	7.57E-03	N.D.		
809.403	154 - 159	LLQSWM 5: Oxidation (HW) 6: Oxidation (M)	4.84E-02	154 - 159	LLQSWM 5: Oxidation (HW) 6: Oxidation (M)	4.06E-01
	154 - 159	LLQSWM 5: Oxidation O2 (W)		154 - 159	LLQSWM 5: Oxidation O2 (W)	
825.396	N.D.			195 - 200	YPQRDM 6: Oxidation (M)	1.09E-01
941.524	64 - 71	IHPFAQTQ *	7.24E-03	64 - 71	IHPFAQTQ *	3.66E-02
946.514	105 - 113	PEVMGVSKV	1.83E-02	105 - 113	PEVMGVSKV	8.35E-02
964.502	137 - 145	SQSLTLTDV	8.06E-03	137 - 145	SQSLTLTDV	2.83E-02
995.591	209 - 217	QEPVLGPVR	1.44E-02	209 - 217	QEPVLGPVR	9.34E-02
1011.597	113 - 121	VKEAMAPKH	9.04E-02	N.D.		
1033.49				170 - 178	VMFPPQSVL 2: Oxidation (M)	1.31E-01
1038.585	76 - 85	PFPGPIPNSL	1.39E-02	76 - 85	PFPGPIPNSL	9.43E-02
	77 - 86	FPGPIPNSLP		77 - 86	FPGPIPNSLP	
1052.604	209 - 218	QEPVLGPVRG	1.06E-02	209 - 218	QEPVLGPVRG	5.81E-02

	01-9	MKVLILACL 8: Sulfonic Acid (SO3H)		01-9	MKVLILACL 8: Sulfonic Acid (SO3H)	
1056.524	122 - 129	KEMPFPKY 3: Oxidation (M)	4.49E-02	N.D.		
1094.66	215 - 224	PVRGPFPIIV	7.38E-03	215 - 224	PVRGPFPIIV	3.26E-02
1108.613	70 - 79	TQSLVYPFP G	6.79E-02	70 - 79	TQSLVYPFPG	4.73E-01
1130.586	100 - 109	PPFLQPEVM G 9: Oxidation (M)	2.32E-01	100 - 109	PPFLQPEVMG 9: Oxidation (M)	1.41E+00
1146.543	N.D.			144 - 153	DVENLHLPLP	1.42E-01
1151.683	01-10	MKVLILACL V 8: Sulfonic Acid (SO3H)	7.67E-03	01-10	MKVLILACLV 8: Sulfonic Acid (SO3H)	5.33E-02
1184.604	71 - 80	QSLVYPFPG P 5: Phospho (STY)	1.28E-02	71 - 80	QSLVYPFPGP 5: Phospho (STY)	1.36E-01
1198.643	159 - 168	MHQPHQPLP P 1: Oxidation (M)	4.36E-03	159 - 168	MHQPHQPLPP 1: Oxidation (M)	1.34E-02
1206.608	158 - 166	WMHQPHQP L 1: Oxidation O2 (W)	5.86E-02	158 - 166	WMHQPHQPL 1: Oxidation O2 (W)	5.81E-01
	158 - 166	WMHQPHQP L 1: Oxidation (HW) 2: Oxidation (M)		158 - 166	WMHQPHQPL 1: Oxidation (HW) 2: Oxidation (M)	
1222.541				32 - 42	SSSEESITRIN	1.63E-01
1300.743				100 - 111	PPFLQPEVMGVS	3.03E-02
1322.705	135 - 146	TESQSLTLT DVE	2.45E-02	135 - 146	TESQSLTLTDVE	2.55E-01
1338.612				133 - 144	PFTESQSLTLTD	5.80E-02
1343.672				193 - 203	VPYPQRDMPIQ	3.98E-01
1399.709	158 - 168	WMHQPHQP LPP 1:	5.27E-03	158 - 168	WMHQPHQPLPP 1: Oxidation O2 (W)	6.02E-02

		Oxidation O2 (W)				
	158 - 168	WMHQPHQP LPP 1: Oxidation (HW) 2: Oxidation (M)		158 - 168	WMHQPHQPLPP 1: Oxidation (HW) 2: Oxidation (M)	
1414.712	69 - 80	QTQSLVYPF PGP 7: Phospho (STY)	2.93E-02	69 - 80	QTQSLVYPFPGP 7: Phospho (STY)	3.86E-01
1512.756	113 - 125	VKEAMAPK HKEMP 5: Oxidation (M)	4.05E-03	113 - 125	VKEAMAPKHKEM P 5: Oxidation (M)	2.10E-02
	113 - 125	VKEAMAPK HKEMP 12: Oxidation (M)		113 - 125	VKEAMAPKHKEM P 12: Oxidation (M)	
1674.873				113 - 126	VKEAMAPKHKEM PF 5: Oxidation (M) 12: Oxidation (M)	1.82E-02
1698.845	158 - 171	WMHQPHQP LPPTVM	2.06E-03			
1720.702				198 - 210	RDMPIQAFLLYQE 3: Oxidation (M) 11: Phospho (STY)	7.69E-02
2337.381	103 - 123	LQPEVMGVS KVKEAMAP KHKE	4.62E-03	103 - 123	LQPEVMGVSKVK EAMAPKHKE	2.64E-02
2877.712	97 - 122	VVVPPFLQP EVMGVSKV KEAMAPKH K 12: Oxidation (M) 21: Oxidation (M)	1.73E-03	N.D.		

*Bioactive peptide; N.D.: Non detected.

Peptides released from gastric digestion of the pretreated micellar casein (dose of 3 W m^{-2} for 15 min of exposure to UV-C light and low-temperature long-time pasteurized (62-64 ° C for 30 min)) and detected after 15 min of transport across caco-2 cell monolayer.

m/z	Range	Sequence	Papp (cm s^{-1}) NON UV-C	Range	Sequence	Papp (cm s^{-1}) UV-C	Papp (cm s^{-1}) LTLT 30 min	Protein
597.275	N.D.			187 - 191	QYTDA	3.01E-02	9.92E-04	α-casein
640.385	61 - 65	QDKIH	3.52E-02	61 - 65	QDKIH	1.04E-02		β-casein
657.403	09-15	LVAVALA	1.86E-02	121 - 125	HKEMP 4: Oxidation (M)	4.66E-03		α / β-casein
671.384	105 - 109	RYLGY *	1.51E-02	105 - 109	RYLGY *	2.36E-03		α-casein
672.405	83 - 88	NSLPQN	2.60E-02	83 - 88	NSLPQN	9.21E-03	2.01E-03	β-casein
675.361	02-6	MKSFF 1: Oxidation (M)	2.04E-02	16 - 20	RELEE	3.71E-03		κ / β-casein
729.442	131 - 136	PKKNQD	2.75E-02	214 - 220	GPVRGPF	6.21E-03	1.12E-03 (κ-casein)	κ / β-casein
741.458	143 - 148	HAQQKE	3.96E-03	143 - 148	HAQQKE	3.62E-03		α-casein
748.453	181 - 187	NTVQVTS	2.23E-02	163 - 169	TVATLED	9.26E-03	3.98E-03	κ-casein
770.444	155 - 160	QELAYF	6.37E-02	155 - 160	QELAYF	7.95E-03	2.98E-03	α-casein
772.426	54 - 59	SRYPSY *	1.57E-02					κ-casein
784.48	105 - 110	RYLGYL *	8.65E-03	105 - 110	RYLGYL *	3.16E-03		α-casein
787.476	172 - 178	FPPQSVL	4.91E-02	172 - 178	FPPQSVL	1.92E-02	3.57E-03	β-casein

802.548	201 - 207	PIQAFLL	6.26E-03				3.61E-03	β-casein
809.46	154 - 159	LLQSWM 5: Oxidation (HW) 6: Oxidation (M)	1.78E-01	154 - 159	LLQSWM 5: Oxidation (HW) 6: Oxidation (M)	5.47E-02	1.38E-02	β-casein
	154 - 159	LLQSWM 5: Oxidation O2 (W)		154 - 159	LLQSWM 5: Oxidation O2 (W)			β / κ-casein
825.431	84 - 91	KPAAVRSP	7.96E-02	195 - 200	YPQRDM 6: Oxidation (M)	2.91E-02	3.93E-03 (κ-casein)	κ / β -casein
827.471	38 - 44	FFSDKIA	5.45E-02	38 - 44	FFSDKIA	8.38E-03		κ-casein
867.534	202-208	IQAFLLY	5.69E-02	89 - 96	IPPLTQTP	-	4.45E-03	β -casein
874.436	96 - 102	QWQVLSN	6.18E-02					κ-casein
883.514	173 - 180	VIESPPEI	6.63E-02					κ-casein
905.542	95 - 101	LQWQVLS 3: Oxidation O2 (W)	7.98E-02	39 - 46	FVAPFPEV	7.92E-02	4.15E-03	κ / α-casein
				40 - 47	VAPFPEVF			α-casein
915.699	12-19	LALARELE	1.12E-02					β -casein
925.634	208 - 214	KTTMPLW 4: Oxidation (M) 7: Oxidation O2 (W)	4.45E-03	N.D.				α-casein
930.535	180 - 187	YYVPLGTQ	2.55E-02	N.D.				α-casein
	181 - 188	YVPLGTQY						α-casein

941.552	64 - 71	IHPFAQTQ*	5.97E-03	142 - 149	LTDVENLH	-	1.74E-03	β -casein
946.564	105 - 113	PEVMGVSKV	2.37E-02	105 - 113	PEVMGVSKV	1.41E-02		β -casein
964.535	N.D.			137 - 145	SQSLTLTDV	5.75E-03	8.72E-04	β -casein
968.474	165 - 170	FRQFYQ 5: Phospho (STY)	4.28E-02					α-casein
973.544	131 - 138	AEERLHSM	3.81E-02	83 - 91	SEEIVPNSV	1.60E-02	3.39E-03	α-casein
995.624	99 - 106	EDVPSERY	4.41E-02	209 - 217	QEPVLGPVR	8.49E-03	1.86E-03 (α-casein)	α/ β-casein
1009.515				136 - 144	HSMKEGIHA	1.19E-02		α-casein
1018.572	94 - 101	ILQWQVLS 4: Oxidation O2 (W)	9.67E-02					κ-casein
1033.622	180 - 189	INTVQVTSTA	9.02E-02	170 - 178	VMFPPQSVL 2: Oxidation (M)	5.56E-02		κ/ β-casein
1037.627	33 - 40	ENLLRFFV	4.12E-03			6.09E-03		α-casein
1038.646	76 - 85	PFPGPIPNSL	2.29E-02	132 - 140	EPFTESQSL	--	1.11E-03	β-casein
1052.651	209 - 218	QEPVLGPVR G	2.29E-02	209 - 218	QEPVLGPVRG	5.37E-03	6.80E-04	β-casein
	01-9	MKVLILACL 8: Sulfonic Acid (SO3H)		01-9	MKVLILACL 8: Sulfonic Acid (SO3H)			β-casein
1094.757	215 - 224	PVRGPFPIIV	2.29E-02					β-casein
1108.66	70 - 79	TQSLVYPFPG	7.93E-02	70 - 79	TQSLVYPFPG	1.86E-02	1.35E-03	β-casein

1120.621	95 - 103	LQWQVLSNT 3: Oxidation O2 (W)	4.03E-02			1.03E-02		κ-casein
1125.712	148 - 157	EPMIGVNQEL	3.48E-02	148 - 157	EPMIGVNQEL	8.84E-03		α-casein
1130.617	100 - 109	PPFLQPEVMG 9: Oxidation (M)	6.40E-01	100 - 109	PPFLQPEVMG 9: Oxidation (M)	3.45E-02	5.46E-03	β-casein
1142.582	N.D.			145 - 154	QQKEPMIGVN	1.65E-02		α-casein
				146 - 155	QKEPMIGVNQ			α-casein
1146.601	100 - 110	LSNTVPAKSC Q 10: Oxidized (SS)	2.14E-01	144 - 153	DVENLHLPLP	1.29E-02	1.59E-03 (β-casein)	κ/ β-casein
1167.684	58 - 65	SYGLNYYQ 2: Phospho (STY) 7: Phospho (STY)	9.91E-02					κ-casein
	58 - 65	SYGLNYYQ 6: Phospho (STY) 7: Phospho (STY)						κ-casein
	58 - 65	SYGLNYYQ 2: Phospho (STY) 6: Phospho (STY)						κ-casein
1184.638	71 - 80	QSLVYPFPGP 5: Phospho (STY)	1.48E-02	71 - 80	QSLVYPFPGP 5: Phospho (STY)	8.30E-03	1.74E-03	β-casein

1198.636	159 – 168	MHQPHQPLPP 1: Oxidation (M)	1.33E-02	159 – 168	MHQPHQPLPP 1: Oxidation (M)	4.20E-03	7.92E-04	β-casein
1206.646	158 – 166	WMHQPHQPL 1: Oxidation O2 (W)	1.19E-01	158 – 166	WMHQPHQPL 1: Oxidation O2 (W)	3.62E-02	6.95E-02	β-casein
	158 - 166	WMHQPHQPL 1: Oxidation (HW) 2: Oxidation (M)		158 - 166	WMHQPHQPL 1: Oxidation (HW) 2: Oxidation (M)			β-casein
1222.629	79 - 88	YPYYAKPAAV 1: Phospho (STY)	5.13E-02	32 - 42	SSSEESITRIN	1.35E-02	2.68E-03 (β-casein)	κ-casein
	79 - 88	YPYYAKPAAV 3: Phospho (STY)						κ-casein
	79 - 88	YPYYAKPAAV 4: Phospho (STY)						κ-casein
1279.669	53 - 64	NELSKDIGSEST	2.33E-02	53 - 64	NELSKDIGSEST	6.69E-03		α-casein
1336.666	204 - 214	ENSEKTTMPLW	7.99E-02	133 - 143	ERLHSMKEGIH	1.00E-02		α-casein
1340.825	21 - 31	AQEQNQEQPIR	1.76E-02					κ-casein
1343.728	111 - 122	AQPTTMARHPHP	2.08E-01	193 - 203	VPYPQRDMPIQ	1.86E-02		κ-casein
	120 - 131	PHPHLSFMAIPP						κ-casein

1414.766	69 - 80	QTQSLVYPFP GP 7: Phospho (STY)	1.86E-01	69 - 80	QTQSLVYPFP GP 7: Phospho (STY)	2.57E-02		β-casein
1664.976	16 - 29	RPKHPIKHQG LPQE	1.60E-02	16 - 29	RPKHPIKHQG LPQE	8.81E-03	2.50E-03	α-casein
1674.897	N.D.			113 - 126	VKEAMAPKH KEMPF 5: Oxidation (M) 12: Oxidation (M)	2.49E-03		β-casein
1686.927				16 - 29	RPKHPIKHQG LPQE		2.43E-03	α-casein
1698.815				158 - 171	WMHQPHQPL PPTVM	5.08E-03		β-casein

*Bioactive peptide; N.D.: Non detected.

Peptides released from gastric digestion of the pretreated micellar casein (dose of 3 W m^{-2} for 15 min of exposure to UV-C light and low-temperature long-time pasteurized (62-64 ° C for 30 min)) and detected after 90 min of transport across caco-2 cell monolayer.

m/z	**Range**	**Sequence**	**Papp (cm s^{-1}) NON UV-C / LTLT**	**Range**	**Sequence**	**Papp (cm s^{-1}) UV-C**	**Papp (cm s^{-1}) LTLT**	**Protein**
546.25	88 - 92	PNSVE	4.71E-02					α-casein
	195 - 199	SDIPN						α-casein
597.265				187 - 191	QYTDA	3.51E-02		α-casein
635.2	-			160 - 163	FYPE 2: Phospho (STY)		2.93E-03	α-casein

640.314	61 - 65	QDKIH	7.19E-02	61 - 65	QDKIH	2.92E-02		β-casein
657.368	09-15	LVAVALA	6.38E-02					α-casein
671.324	105 - 109	RYLGY *	1.11E-02					α-casein
672.382	83 - 88	NSLPQN	5.07E-02	83 - 88	NSLPQN	1.59E-02	1.11E-03	β-casein
675.303	02-6	MKSFF 1: Oxidation (M)	6.47E-02					κ-casein
729.376	131 - 136	PKKNQD	3.75E-02	214 - 220	GPVRGPF	1.03E-02	5.77E-04	κ / β-casein
741.376	143 - 148	HAQQKE	3.44E-03					α-casein
748.357	181 - 187	NTVQVTS	2.44E-02	163 - 169	TVATLED	1.66E-02	2.31E-03	κ-casein
770.421	155 - 160	QELAYF	1.41E-01	155 - 160	QELAYF	2.27E-02	1.48E-03	α-casein
772.366	54 - 59	SRYPSY *	3.83E-02					κ-casein
784.44	105 - 110	RYLGYL *	6.39E-03					α-casein
787.455	172 - 178	FPPQSVL	5.17E-02	172 - 178	FPPQSVL	2.66E-02	1.93E-03	β-casein
802.423			-	201 - 207	PIQAFLL	-	3.11E-03	β-casein
809.44	154 - 159	LLQSWM 5: Oxidation (HW) 6: Oxidation (M)	3.20E-01	154 - 159	LLQSWM 5: Oxidation (HW) 6: Oxidation (M)	6.76E-02	6.70E-03	β-casein
	154 - 159	LLQSWM 5: Oxidation O2 (W)		154 - 159	LLQSWM 5: Oxidation O2 (W)			β-casein
825.416	84 - 91	KPAAVRS P	9.04E-02	195 - 200	YPQRDM 6: Oxidation (M)	2.13E-02	2.68E-03	κ/ β-casein

							(κ-casein)	
827.439	38 - 44	FFSDKIA	1.19E-01	38 - 44	FFSDKIA	9.93E-03	5.70E-03	κ-casein
867.575	89 - 96	IPPLTQTP	2.81E-02				2.45E-03	β-casein
874.469	96 - 102	QWQVLSN	1.17E-01	96 - 102	QWQVLSN	2.16E-02		κ-casein
883.556	173 - 180	VIESPPEI	1.53E-01	108 - 115	SCQAQPTT 2: Sulfonic Acid (SO3H)	7.54E-03		κ-casein
905.47	95 - 101	LQWQVLS 3: Oxidation O2 (W)	6.73E-02	39 - 46	FVAPFPEV	1.72E-02	2.45E-03	κ/α-casein
930.441	180 - 187	YYVPLGTQ	3.14E-02					α-casein
	181 - 188	YVPLGTQY						α-casein
940.506	143 - 150	TDVENLHL	5.45E-03					β-casein
941.467	64 - 71	IHPFAQTQ	2.76E-03	64 - 71	IHPFAQTQ	-	1.74E-03	β-casein
946.571	142 - 149	LTDVENLH	4.86E-02	154 - 160	LLQSWMH 5: Oxidation (HW) 6: Oxidation (M)	1.77E-02		β-casein
	105 - 113	PEVMGVSKV		154 - 160	LLQSWMH 5: Oxidation O2 (W)			β-casein
964.468	137 - 145	SQSLTLTDV	8.04E-04	137 - 145	SQSLTLTDV	-	7.42E-04	β-casein

968.539	165 - 170	FRQFYQ 5: Phospho (STY)	1.04E-01	165 - 170	FRQFYQ 5: Phospho (STY)	8.47E-03		α-casein
973.529	131 - 138	AEERLHSM	2.90E-02	131 - 138	AEERLHSM	2.19E-02	2.23E-03	α-casein
995.601	99 - 106	EDVPSERY	4.44E-02	202 - 209	IQAFLLYQ	1.73E-02	1.08E-03 (α-casein)	α/β-casein
1033.577	180 - 189	INTVQVTSTA	7.85E-02	170 - 178	VMFPPQSVL 2: Oxidation (M)		1.95E-03	κ/β-casein
1037.594	33 - 40	ENLLRFFV	1.65E-03					α-casein
1038.642	76 - 85	PFPGPIPNSL	1.83E-02	76 - 85	PFPGPIPNSL	1.06E-02	5.79E-04	β-casein
1052.645	209 - 218	QEPVLGPVRG	1.83E-02	209 - 218	QEPVLGPVRG	9.95E-03	5.84E-04	β-casein
1056.541	122 - 129	KEMPFPKY 3: Oxidation (M)	4.23E-02					β-casein
1094.678	215 - 224	PVRGPFPIIV	8.70E-03					β-casein
1108.644	70 - 79	TQSLVYPFPG	1.34E-01	70 - 79	TQSLVYPFPG	3.62E-02	7.92E-04	β-casein
1120.594	95 - 103	LQWQVLSNT 3: Oxidation O2 (W)	5.83E-02					κ-casein

1125.689	148 - 157	EPMIGVNQEL	6.38E-02	148 - 157	EPMIGVNQEL	1.03E-02		α-casein
1130.622	100 - 109	PPFLQPEVMG 9: Oxidation (M)	1.52E+00	100 - 109	PPFLQPEVMG 9: Oxidation (M)	1.21E-01	2.60E-03	β-casein
1142.574				145 - 154	QQKEPMIGVN	5.29E-02		α-casein
				146 - 155	QKEPMIGVNQ			α-casein
1146.589	100 - 110	LSNTVPAKSCQ 10: Oxidized (SS)	3.99E-01	144 - 153	DVENLHLPLP	2.83E-02	1.04E-03 (β-casein)	κ/β-casein
1167.631	58 - 65	SYGLNYYQ 6: Phospho (STY) 7: Phospho (STY)	1.19E-01					κ-casein
	58 - 65	SYGLNYYQ 2: Phospho (STY) 6: Phospho (STY)						κ-casein
1184.63	71 - 80	QSLVYPFPGP 5: Phospho (STY)	1.06E-02	71 - 80	QSLVYPFPGP 5: Phospho (STY)	1.41E-02	1.29E-03	β-casein

1198.638	159 – 168	MHQPHQPLPP 1: Oxidation (M)	4.16E-03	159 – 168	MHQPHQPLPP 1: Oxidation (M)	2.26E-03	6.23E-04	β-casein
1206.624	158 – 166	WMHQPHQPL 1: Oxidation O2 (W)	1.50E-01	158 – 166	WMHQPHQPL 1: Oxidation O2 (W)	1.35E-01	1.34E-02	β-casein
	158 - 166	WMHQPHQPL 1: Oxidation (HW) 2: Oxidation (M)		158 - 166	WMHQPHQPL 1: Oxidation (HW) 2: Oxidation (M)			β-casein
1222.601	79 - 88	YPYYAKPAAV 1: Phospho (STY)	4.17E-02	32 - 42	SSSEESITRIN	2.30E-02	2.24E-03 (β-casein)	κ/β-casein
	79 - 88	YPYYAKPAAV 3: Phospho (STY)						κ-casein
	79 - 88	YPYYAKPAAV 4: Phospho (STY)						κ-casein
1253.689	77 - 87	LPYPYYAKPAA	3.41E-02					κ-casein
1279.666	53 - 64	NELSKDIGSEST	4.56E-02	53 - 64	NELSKDIGSEST	1.01E-02		α-casein

1324.747	171 - 182	PEVIESPPEINT	5.31E-03					κ-casein
1336.637	204 - 214	ENSEKTTMPLW	4.34E-02	204 - 214	ENSEKTTMPLW	2.61E-02		α-casein
1343.712	111 - 122	AQPTTMARHPHP	2.61E-01	193 - 203	VPYPQRDMPIQ	1.99E-01	1.59E-03 (β-casein)	κ/β-casein
	120 - 131	PHPHLSFMAIPP						κ-casein
1399.627	70 - 81	TQSLVYPFPGPI 6: Phospho (STY)	2.75E-03	158 - 168	WMHQPHQPLPP 1: Oxidation (HW) 2: Oxidation (M)	-	3.78E-03	β-casein
1414.74	69 - 80	QTQSLVYPFPGP 7: Phospho (STY)	1.52E-01	69 - 80	QTQSLVYPFPGP 7: Phospho (STY)	2.51E-01	2.52E-03	β-casein
1512.733	113 - 125	VKEAMAPKHKEMP 12: Oxidation (M)	3.18E-03	115 - 127	EAMAPKHKEMPFP	-	2.70E-03	β-casein
1597.65				171 - 183	LDAYPSGAWYYVP 9: Oxidation (HW) 10: Phospho (STY)	-	9.21E-04	α-casein
1664.987	16 - 29	RPKHPIKHQGLPQE	7.44E-03	16 - 29	RPKHPIKHQGLPQE	2.46E-03	1.46E-03	α-casein

1698.841		1.55E-03	113 - 126	VKEAMAPK HKEMPF 5: Oxidation (M) 12: Oxidation (M)	6.46E-04	β-casein
1707.056			158 - 171	WMHQPHQP LPPTVM	1.20E-03	β-casein

*Bioactive peptide; N.D.: Non detected.

PEF pretreatment – Cold Temperature ± 4.5 °C, for 31 and 6 µs of residence time at 1 and 5 L h^{-1} corresponding to 100 and 92 kJ L^{-1}

Peptides released from gastric digestion of the micellar casein PEF treated (16 kV cm^{-1}) and detected after 90 min of transport across caco-2 cell monolayer.

m/z calculated	m/z	Protein	Sequence	Range	Permeability Coefficient (10^{-6} cm s^{-1})					
					CT_NON_PEF		CT_1 L h^{-1}		CT_5 L h^{-1}	
					30 min	90 min	30 min	90 min	30 min	90 min
597.314	597.204	α-casein	FRQF	165 - 168		15.1	14.1	19.9	10.9	10.3
672.383	672.302	β-casein	PVRGPF	215 - 220	20.9	19.6	14.0	21.6	14.9	14.2
672.383	672.302	β-casein	VRGPFP	216 - 221	20.9	19.6	14.0	21.6	14.9	14.2
675.183	675.199	α-casein	YLGY- 1: Phospho (STY) 4: Phospho (STY)*	106-109		109	161.5	111.2	160.2	99.2
728.405	729.337	κ-casein	AVRSPAQ	87 - 93	11.7	11.5	7.24E	12.5	9.22	8.31
748.300	748.311	β-casein	EDELQD	57 – 62				46.8		
770.379	770.350	α-casein	AEERLH- 6: Oxidation (HW)	131 - 136		13.9		14.8		11.1

787.453	787.371	κ-casein	TEIPTIN	138 - 144	56.7	43.4	37.7	39.7	38.0	30.1
787.453	787.371	κ-casein	EIPTINT	139-145	56.7	43.4	37.7	39.7	38.0	30.1
802.498	802.404	α -casein	KLLILTC -7: Oxized (SS)	02-08		27.9		34.2	56.9	52.7
808.456	809.358	κ-casein	FSDKIAK*	39 - 45	57.3	54.4	41.5	62.5	42.4	37.9
825.347	825.334	β-casein	SLSSSES	30 - 37	35.1	39.3		37.1	24.1	25.9
827.406	827.328	α-casein	YKVPQL*	119 - 124				47.8		
867.456	867.455	α-casein	LLILTCL- 5: Phospho (STY) 6: Oxized (SS)	3 - 9		20.4				
905.484	905.419	α-casein	NENLLRF	32 - 38		18.8		21.7		20.8
941.457	941.451	κ-casein	KKNQDKT- 7: Phospho (STY)	132 - 138	17.0	16.3	22.0	29.5	15.2	14.2
944.468	945.406	κ-casein	NQDKTEIP	134 - 141		7.76				
955.525	956.441	κ-casein	FFSDKIAK	38 - 45				13.6		5.81
964.381	964.417	α-casein	QFYQLDA- 3: Phospho (STY)	167 – 173		6.70		13.6		12.4
964.381	964.417	α-casein	NQELAYF- 6: Phospho (STY)	154 - 160				13.6		12.4
973.402	973.382	α-casein	GVNQELAY- 8: Phospho (STY)	152 - 159					40.6	36.5
995.556	995.507	κ-casein	AKYIPIQY	44 - 51	13.9	13.9	10.2	13.6	11.5	10.0
1011.403	1011.485	α-casein	QKEDVPSE- 7: Phospho (STY)	97 - 104		8.09			5.30	5.75
1033.502	1033.465	β-casein	PFLQPEVMG- 8: Oxidation (M)	101 - 109		15.4		17.2		16.5
1038.569	1038.521	α-casein	KEGIHAQQK	139 - 147	9.01	9.2	7.29	9.29	8.44	6.85
1042.406	1042.448	β-casein	LLQSWMH- 4: Phospho (STY) 5: Oxidation (HW) 6: Oxidation (M) 7: Oxidation (HW)	154 - 160				36.6		33.8
1051.553	1051.515	α-casein	PNSVEQKHI	88 - 96		12.2		26.5	13.0	13.3
1108.615	1108.503	α-casein	ENLLRFFVA	33 – 41	22.4	24.0	16.6	21.2	18.0	16.7
1130.464	1130.498	α-casein	QYTDAPSFSD	187 - 196	21.4	25.3	15.5	25.9	17.4	17.9
1146.438	1146.470	α-casein	DIKQMEAES	71 - 79	11.6	16.3	72.7	15.6	8.4	10.5
1184.511	1184.608	α-casein	LGYLEQLLR	107 – 115	160	158	23.0	34.3	32.5	30.8
1184.511	1184.608	α-casein	GYLEQLLRL	108 - 116	160		23.0	34.3	32.5	30.8
1198.506	1198.506	κ-casein	YYAKPAAVR- 1: Phospho (STY) 2: Phospho (STY)	81 - 89				15.6		16.2
1206.703	1206.758	α-casein	LLRFFVAPFP	35 - 44	155	92.2		24.7		66.0
1222.598	1222.484	α-casein	IKQMEAESISS	72 - 82		16.6				18.6

1300.568	1300.566	β-casein	MPFPKYPVEP- 1: Oxidation (M) 6: Phospho (STY)*	124 - 133						59.8
1318.606	1318.578	α-casein	AEERLHSMKEG- 6: Oxidation (HW) 8: Oxidation (M)	131 - 141	554.5	289.8	529.8	304.7	445.9	232.3
1322.522	1322.610	α-casein	LAYFYPELF- 3: Phospho (STY) 5: Phospho (STY)	157 – 165		26.8		24.9		
1334.582	1334.557	α-casein	GAWYYVPLGTQ- 5: Phospho (STY)	177 - 187	711	408.6				
1338.726	1338.619	α-casein	GLPQEVLNENLL- 6: Oxidation (HW) 8: Oxidation (M)	25 - 36	14.1	13.7	8.29	11.7		11.7
1340.626	1340.604	κ-casein	PIRCEKDERF- 4: Sulfonic acid (SOH3)	29 - 38	36.6	29.4	28.2	23.2	37.5	26.2
1362.620	1362.592	β-casein	HQPHQPLPPTV- 1: Oxidation (HW) 4: Oxidation (HW) 10: Phospho (STY)	160 - 170	40.6	32.1	31.3	30.0		
1377.65	1378.538	κ-casein	VPAKSCQAQPTTM- 13: Oxidation (M)	104 - 116		20.9	20.6	21.6	21.3	16.7
1399.7	1399.613	α-casein	AEERLHSMKEGI	131 - 142	41.3	41.1	24.0	31.4	35.9	33.1
1414.744	1414.631	α-casein	HPIKHQGLPQEV- 1: Oxidation (HW) 5: Oxidation (HW)	19 - 30		8.10		6.64	5.76	5.82
1437.679	1437.568	β-casein	NIPPLTQTPVVV - 6: Phospho (STY) 8: Phospho (STY)	88 - 99				18.3		
1485.697	1485.657	κ-casein	PFLGAQEQNQEQP	17 – 29		7.66			5.06	5.25
1512.506	1512.678	α-casein	PNPIGSENSEKT- 6: Phospho (STY) 9: Phospho (STY) 12: Phospho (STY)	198 - 209		17.0	13.3	17.3	16.6	15.7
1550.716	1550.598	α-casein	GAWYYVPLGTQYT- 3: Oxidation O2 (W)	177 - 189				19.4		
1664.810	1664.866	β-casein	PPLTQTPVVVPPFL- 4: Phospho (STY) 6: Phospho (STY)	90 – 103	18.6	24.5	16.5	24.7	34.8	35.3
1664.810	1664.866	β-casein	IPPLTQTPVVVPPF- 5: Phospho (STY) 7: Phospho (STY)	89 - 102	18.6	24.5	16.5	24.7	34.8	35.3
1674.790	1674.773	α-casein	KYKVPQLEIVPNS- 2: Phospho (STY) 13: Phospho (STY)	118 - 130		14.5		15.8		17.3
1698.756	1698.789	α-casein	YPELFRQFYQLD- 1: Phospho (STY)	161 - 172		4.80		5.73		4.29
1698.756	1698.789	α-casein	YPELFRQFYQLD- 9: Phospho (STY)	161 - 172		4.80		5.73		4.29
1702.809	1702.796	α-casein	FPEVFGKEKVNELS- 14: Phospho (STY)	43 - 56				23.5		

1705.858	1706.909	κ-casein	LQWQVLSNTVPAKSC- 3: Oxidation O2 (W)	95 - 109	7.65		6.07		5.25
1736.78	1736.709	α-casein	SGAWYYVPLGTQYTD- 4: Oxidation (HW)	176 - 190			9.71		
1736.78	1736.709	α-casein	GAWYYVPLGTQYTDA- 3: Oxidation O2 (W)	177 - 191					
1988.932	1989.041	α-casein	EIVPNSVEQKHIQKED- 6: Phospho (STY) 11: Oxidation (HW)	85 - 100	20.3		16.1		
2138.180	2138.314	α-casein	NLLRFFVAPFPEVFGKEK	34 - 51	13.4				
2337.248	2337.398	α-casein	ARPKHPIKHQGLPQEVLNEN	15 - 34	6.04	7.74	9.59		5.11

*Bioactive Peptide

PEF pretreatment – Room Temperature ± 22.5 °C, for 31 and 6 μs of residence time at 1 and 5 L h^{-1} corresponding to 84 and 24 kJ L^{-1}

Peptides released from gastric digestion of the micellar casein PEF treated (16 kV cm^{-1}) and detected after 90 min of transport across caco-2 cell monolayer.

					Permeability Coefficient (10^{-6} cm s^{-1})					
					RT_NON_PEF		RT_1 L h^{-1}		RT_5 L h^{-1}	
m/z calculated	m/z	Protein	Sequence	Range	30 min	90 min	30 min	90 min	30 min	90 min
522.241	522.450	α-casein	ISSSE	80 - 84	142.1	83.0	892.6	455.7		
	528.748	Not found			45.1	28.4	51.5	31.2		
	530.754	Not found					62.7	36.3	40.0	37.0
550.251	550.505	β-casein	EVMGV	106 - 110			696.8	435.7		
563.250	563.165	α-casein	AYFY	158 - 161						14.3
597.251	597.198	α-casein	QYTDA	187 - 191		9.97			16.0	18.1

672.356	672.329	κ-casein	PEINTV	178 - 183	26.8	22.3	12.5	12.8	23.6	29.1
675.283	675.226	α-casein	EDVPSE	99 - 104	349.5	181.2	270.8	155.5	218.4	112.6
729.389	729.367	κ-casein	PKKNQD	131 - 136	31.6	18.2	15.3	11.7	14.7	20.6
769.409	769.370	κ-casein	PPEINTV	177 - 183						13.6
770.404	770.371	α-casein	QGLPQEV	24 - 30		8.55				15.3
787.423	787.418	α-casein	RELEEL*	16-21			43.0	29.7	66.0	47.9
788.415	788.405	β-casein	RLKKY- 5: Phospho (STY)	115-119	50.8	32.1				
802.414	802.429	α-casein	QKEPMIG	146 - 152		20.5	31.3	35.8	36.9	40.8
809.371	809.373	α-casein	SEKTTMP- 6: Oxidation (M)	206 - 212				26.4		
825.530	825.356	α-casein	AVALARPK	11-18				38.3		35.4
826.431	826.379	α-casein	IPNPIGSE	197 - 204		11.9				15.5
830.425	830.410	α-casein	EVLNENL	29 - 35			5.44	4.50		
867.534	867.494	β-casein	PVVVPPFL	96 - 103		20.1				
889.441	889.436	κ-casein	PFLGAQEQ	17 - 24						41.7
905.460	905.440	κ-casein	KPAAVRSP- 7: Phospho (STY)	84 - 91		15.7				27.9
956.449	956.466	α-casein	YKVPQLE- 1: Phospho (STY)	119 - 125		6.21				13.5
964.458	964.459	α-casein	IGSENSEKT	201 - 209				12.7		22.6
973.442	973.438	β-casein	MGVSKVKE- 1: Oxidation (M) 4: Phospho (STY)	108 - 115	29.4	29.5			40.9	46.9
995.516	995.523	β-casein	ELQDKIHP- 7: Oxidation (HW)	59 - 66		19.3		13.5	17.1	19.6
1011.589	1011.505	α-casein	CLVAVALARP- 1: Oxidized (SS)	8 - 17					8.79	11.1
1033.502	1033.464	κ-casein	PTTEAVESTV	155 - 164						22.0
1037.559	1037.556	α-casein	LLILTCLVA- 5: Phospho (STY) 7: Oxidized (SS)	3 - 11		9.08				10.8
1038.569	1038.552	α-casein	KEGIHAQQK	139 - 147	12.1	9.42	12.4	11.3	11.4	14.5
1042.520	1042.491	α-casein	ERYLGYLE	104 - 111				17.9	30.3	42.2
1052.552	1052.527	α-casein	NENLLRFF	32 - 39						11.8
1108.483	1108.521	α-casein	EDIKQMEAE- 6: Oxidation (M)	70 - 78		17.3	16.1	14.3	14.6	19.8
1130.563	1130.488	α-casein	ELFRQFYQ	163 - 170						28.9

1146.547	1146.482	α-casein	VNQELAYFY	153 - 161				8.54		20.8
1279.601	1279.532	α-casein	NELSKDIGSEST	53 - 64						8.28
1318.646	1318.609	κ-casein	TILALTLPFLG- 1: Phospho (STY) 6: Phospho (STY)	10 - 20	619.5	292.5				
1324.722	1.324,667	α-casein	PQEVLNENLLR	27 - 37		8.36				-
1334.582	1334.588	α-casein	GAWYYVPLGTQ	177 - 187	513.1	253.4	497.1	261.7	517. 3	380.9
1340.700	1340.645	α-casein	PELFRQFYQL	162 - 171			41.7	27.1	3.98	38.0
1362.484	1362,646	α-casein	YPSGAWYYVP	174 - 183			49.6	8.27		
1378.582	1378.561	α-casein	LHSMKEGIHAQ- 2: Oxidation (HW) 3: Phospho (STY) 4: Oxidation (M) 9: Oxidation (HW)	135 - 145						33.9
1512.853	1512.687	κ-casein	QQKPVALINNQFL	65 – 77				15.9	18.6	22.3
1664.879	1664.896	α-casein	KEGIHAQQKEPMIGV	139 - 153	37.2	29.4	23.2	3.03	36.7	45.0
1674.790	1674.828	α-casein	KYKVPQLEIVPNS	118 - 130		14.2				24.9
1698.782	1698.789	α-casein	YPELFRQFYQLD- 1: Phospho (STY)	161 - 172				8.28		
1702.811	1702.858	α-casein	PSGAWYYVPLGTQYT	175 - 189				25.6		32.7
1988.932	1989.082	α-casein	EIVPNSVEQKHIQKED- 6: Phospho (STY) 11: Oxidation (HW)	85 - 100					40.5	33.4

*Bioactive Peptide